

OFFICIAL DOCUMENT

DO NOT REMOVE FROM
THE RESEARCH OFFICE

Seismic Zonation for Highway Bridge Design

WA-RD 172.1

Final Report
December 1988



Washington State Department of Transportation
Planning, Research and Public Transportation

in cooperation with the
United States Department of Transportation
Federal Highway Administration

WASHINGTON STATE DEPARTMENT OF TRANSPORTATION
TECHNICAL REPORT STANDARD TITLE PAGE

| | | | |
|--|--------------------------------------|---|-----------|
| 1. REPORT NO WA-RD 172.1 | 2. GOVERNMENT ACCESSION NO. | 3. RECIPIENT'S CATALOG NO. | |
| 4. TITLE AND SUBTITLE SEISMIC ZONATION FOR HIGHWAY BRIDGE DESIGN | | 5. REPORT DATE December 1988 | |
| | | 6. PERFORMING ORGANIZATION CODE | |
| 7. AUTHOR(S) Dr. J.D. Higgins Dr. R.J. Fragaszy Mr. L.D. Beard | | 8. PERFORMING ORGANIZATION REPORT NO. | |
| 9. PERFORMING ORGANIZATION NAME AND ADDRESS Washington State Transportation Center Washington State University Pullman, WA 99164-2910 | | 10. WORK UNIT NO. | |
| | | 11. CONTRACT OR GRANT NO. Y-3400, T2 | |
| 12. SPONSORING AGENCY NAME AND ADDRESS Washington State Department of Transportation Olympia, WA 98504 | | 13. TYPE OF REPORT AND PERIOD COVERED Final Report | |
| | | 14. SPONSORING AGENCY CODE | |
| 15. SUPPLEMENTARY NOTES This study was conducted in cooperation with the U.S. Dept. of Transportation, Federal Highway Administration. | | | |
| 16. ABSTRACT This report includes a state-of-the-art review of seismicity, attenuation characteristics, and seismic zonation in Washington and the Pacific Northwest. Based on this information, a map of velocity-related acceleration coefficients for Washington was developed. The map is in a format suitable for use in the AASHTO highway bridge design procedure. Also, it is based on more detailed seismic and geologic data than the present AASHTO map and was developed specifically for Washington rather than the entire United States. Therefore, the map is suggested as a potential replacement for the present AASHTO map for seismic bridge design in Washington. | | | |
| 17. KEY WORDS Seismic Zonation | | 18. DISTRIBUTION STATEMENT | |
| 19. SECURITY CLASSIF. (of this report) | 20. SECURITY CLASSIF. (of this page) | 21. NO. OF PAGES | 22. PRICE |

SEISMIC ZONATION FOR HIGHWAY BRIDGE DESIGN

by

Jerry D. Higgins, Principal Investigator*
Richard J. Fragaszy, Co-investigator**
Lawrence D. Beard, Research Assistant

*Department of Geological Engineering
Colorado School of Mines
Golden, CO 80401

Washington State Transportation Center (TRAC)
**Department of Civil Engineering
Washington State University
Pullman, WA 99164-2910

WSDOT Technical Monitor
Alan P. Kilian
Chief Geotechnical Engineer
Materials Laboratory

Final Report

Research Project Y-3400
Task 2

Prepared for

Washington State Transportation Commission
Department of Transportation
and in cooperation with
U.S. Department of Transportation
Federal Highway Administration

December 1988

CREDIT REFERENCE

The work upon which this report is based was supported by the Washington State Department of Transportation and the U.S. Department of Transportation, Federal Highway Administration.

The contents of this report reflect the views of the authors who are responsible for the facts and the accuracy of the data presented herein. The contents do not necessarily reflect the official views or policies of the Washington State Department of Transportation or the Federal Highway Administration. This report does not constitute a standard, specification, or regulation.

TABLE OF CONTENTS

| | |
|---|-----|
| CREDIT REFERENCE | ii |
| DISCLAIMER | iii |
| LIST OF ILLUSTRATIONS | vi |
| SUMMARY | 1 |
| CONCLUSIONS | 3 |
| RECOMMENDATIONS | 5 |
| I. INTRODUCTION | 6 |
| II. LITERATURE REVIEW | 9 |
| Geology of Washington State | 9 |
| Olympic Mountains | 9 |
| Coast Range | 11 |
| Puget Lowland | 11 |
| North Cascades | 12 |
| South Cascades | 13 |
| Columbia Plateau | 13 |
| Okanogan-Selkirk Highlands | 14 |
| Tectonics | 14 |
| Seismicity | 20 |
| Seismicity of the Puget Sound Area | 20 |
| Seismicity of Washington, Excluding the Puget Sound | 24 |
| Historic Earthquakes Effecting Washington State | 25 |
| December 14, 1872 North Cascades..... | 25 |
| July 16, 1936 Milton-Freewater, OR... | 25 |
| February 15, 1946 Puget Sound..... | 26 |
| April 13, 1949 Olympia, WA..... | 26 |
| April 29, 1965 Puget Sound, WA..... | 26 |
| Ground Motions Under Earthquake Loading | 29 |
| Measurement of Earthquake "Size" | 29 |
| Ground Motion Measurement | 33 |
| Seismic Analysis of Structures | 36 |
| Attenuation of Ground Motion with Distance from the Source | 39 |
| Effects of Local Soil Conditions on Ground Shaking | 42 |

| | | |
|------|---|-----|
| III. | SEISMIC ZONATION MAPPING | 49 |
| | History of Seismic Zoning--National Maps . . . | 49 |
| | Seismic Zonation--Theory and Methodology . . . | 53 |
| | Seismic Zonation Maps Applicable to Washington State | 59 |
| | Rasmussen & others (1975) | 65 |
| | U.S.G.S. Open-File Report 75-375 (1975) . . | 69 |
| | Algermissen and Perkins, 1976 (76) | 75 |
| | ATC Tentative Guidelines for the Seismic Design of Buildings, 1978 (13) | 79 |
| | Selection of Ground Motion Parameters. | 79 |
| | Design Elastic Response Spectra | 86 |
| | ATC-6, Seismic Design Specifications for Bridges (1) | 90 |
| | Evaluation of ATC Guidelines | 92 |
| | Perkins, D.M. et al., 1980 (70) | 93 |
| | Innen and Hadley, 1984 (72) | 97 |
| | Innen and Hadley, 1986 (102) | 110 |
| IV. | RECOMMENDATIONS FOR THE MODIFICATION OF WSDOT SEISMIC DESIGN PROCEDURES | 120 |
| | Selection of Seismic Design Coefficients . . . | 120 |
| | Development of a Velocity-Related Acceleration Map Based on Acceleration and Velocity Maps . | 133 |
| | Evaluation of Model Soil Profiles | 137 |
| V. | REFERENCES | 143 |
| VI. | GLOSSARY | 155 |

LIST OF FIGURES

| | | |
|-----|--|----|
| 1. | Geologic provinces of the Pacific Northwest | 10 |
| 2. | Schematic model of plate interactions | 15 |
| 3. | Juan de Fuca plate map | 17 |
| 4. | Artist's drawing of how the subduction process might be occurring | 21 |
| 5. | Earthquake hypocenters for events occurring between 1970 and 1978 | 23 |
| 6. | Isoseismal map for the 1936 earthquake | 27 |
| 7. | Area affected by the earthquake of 1949 | 28 |
| 8. | Intensity map of the Puget Sound earthquake of 1965 | 30 |
| 9. | Relation between moment magnitude and various magnitude scales | 34 |
| 10. | A typical accelerogram and associated velocity and displacement time-history | 35 |
| 11. | Example of response spectra plotted on tripartate log paper | 38 |
| 12. | Approximate relationship between maximum accelerations on rock and other local site conditions | 43 |
| 13. | Average acceleration spectra for different soil conditions | 45 |
| 14. | Idealized undamped velocity spectrum curves | 47 |
| 15. | Seismic risk map of the U.S. | 52 |
| 16. | Elements of the hazard calculation | 55 |
| 17. | Attenuation curve development for the Puget Sound region | 63 |
| 18. | Intensity attenuation curves for earthquakes approximately 40-60 km deep | 66 |
| 19. | Attenuation of intensity with epicentral distance ... | 70 |
| 20. | Map of MMI distribution in the Puget Sound region ... | 72 |
| 21. | Map of MMI distribution in Seattle | 73 |

| | | |
|-----|---|-----|
| 22. | Map of MMI distribution in Tacoma | 74 |
| 23. | Seismic source areas for the western U.S. | 77 |
| 24. | Preliminary map of horizontal acceleration in rock .. | 78 |
| 25. | Schematic representation showing how EPA amd EPV are obtained from a response spectrum | 81 |
| 26. | Contour map for EPA | 84 |
| 27. | Contour map for EPV-related acceleration coefficient | 85 |
| 28. | Normalized response spectra recommended for use in building code | 88 |
| 29. | Examples showing variation of ground motion spectra in different tectonic regions | 89 |
| 30. | Comparison of free field ground motion spectra and lateral design force coefficients | 91 |
| 31. | Seismogenic zones for the Pacific Northwest | 94 |
| 32. | 500-yr return period acceleration on rock | 98 |
| 33. | Map of 500-year return period velocity on rock | 99 |
| 34. | Vertical cross section through velocity model | 102 |
| 35. | Contoured peak horizontal accelerations, 1965 earthquake | 104 |
| 36. | Contoured peak horizontal acceleration for the case of uniform bedrock at surface | 105 |
| 37. | Contoured peak horizontal acceleration for a layer of laterally varying velocity | 106 |
| 38. | Plot of log of peak ground acceleration vs. epicentral distance | 108 |
| 39. | Perspective plot of the Puget Sound area and the subducted Juan De Fuca plate | 112 |
| 40. | Base risk map for Puget Sound earthquakes | 113 |
| 41. | Amplification of PGA as a function of site shear-wave velocity | 115 |
| 42. | Seismic risk map for Puget Sound | 116 |

| | | |
|-----|--|-----|
| 43. | Map of risk from seismic ground motion in Puget Sound, WA | 118 |
| 44. | Locations of cross sections A and B | 130 |
| 45. | Variation of a , v , and v/a for cross section A-A'... | 131 |
| 46. | Variation of a , v , and v/a for cross section B-B'... | 132 |
| 47. | Velocity-related acceleration coefficient map of Washington | 135 |
| 48. | Model soil profiles for Washington | 139 |

LIST OF TABLES

1. Peak accelerations and epicentral distances for three Puget Sound strong motion recorders during the 1965 earthquake61
2. Annual earthquake occurrence rates of the Pacific Northwest96
3. Comparison of recorded and predicted peak acceleration values for the 1965 Seattle earthquake .109
4. Variation of a , v , and v/a at distance from the source128
5. Comparison of normalized response spectra for model soil profiles and AASHTO soil types I, II, III141

SUMMARY

Since the basic data for the AASHTO Guide Specifications for Seismic Design of Highway Bridges were developed, new data on seismicity and ground motion in the Puget Sound region and the Pacific Northwest have been published. Also, a number of seismic risk studies have been made for nuclear power plants and dams in Washington. Since the AASHTO guide suggests improvements on its method when adequate data become available, this study was initiated to review and evaluate the applicability of existing data. The ultimate objective of this study was to develop a zonation map of design ground motion (acceleration coefficients) for bridge design in Washington using new available data on the unique seismicity and geology of the region.

An extensive review of seismic studies for dams and nuclear power plants in Washington was accomplished as well as a review of recent seismic zonation research in the area. Methodologies of zonations found in the literature review were evaluated on the basis of two criteria: 1) The zonation must be consistent with AASHTO design procedures or must be easily modified to be consistent, and 2) The new zonation must provide design coefficients of greater accuracy than those presently being used in the AASHTO guide.

Most of the studies reviewed were eliminated on the basis of 1 or 2 listed above. An alternative to the AASHTO zonation map was constructed based on acceleration and velocity maps developed by Perkins and others [56] for the Pacific Northwest. This work is an improvement over the zonation study that the AASHTO

acceleration coefficient map was based upon and meets the objectives of this study. The proposed map of velocity-related acceleration coefficients is based upon a seismic zonation that incorporates additional Washington geology into the delineation of seismic source zones and eliminates some of the simplified assumptions used in the construction of the 1983 AASHTO map.

The map of velocity-related acceleration coefficients constructed in this study is suggested for use by WSDOT in place of figure 3 in the AASHTO guide.

CONCLUSIONS

A review of seismic studies of dams and nuclear power plants in the Pacific Northwest shows that no new methods have been proposed (or used) that would contribute significant data for the improvement of the AASHTO method for seismic design of highway bridges.

A review of the literature concerning seismic zonation of Washington and the Pacific Northwest revealed significant recent work. A number of methods were reviewed; however, the writers conclude that two approaches are the most significant for the purpose of this report.

The recent zonation research applied to the Puget Sound region using raytracing and focusing was reviewed for its potential for modification of the AASHTO map now in use. It was concluded that this method is in the research stages and presently is not readily applicable to the AASHTO guide specifications. However, the research shows potential for future applications and should be reviewed after further work.

The work of Perkins and others [56] is an improvement over the zonation study that the AASHTO map of acceleration coefficients was based upon and meets the objectives of this study. The Perkins work incorporates additional Washington geology into the delineation of seismic source zones, and it expresses ground motion in terms of velocity and acceleration. Velocity data expressed in the same probabilistic terms as acceleration was used to develop an improved velocity-related

acceleration coefficient map recommended for use in the AASHTO design procedure. The construction of this map is not dependent upon simplified assumptions (construction of smoothed response spectra and simplified velocity attenuation relationships) used to construct the AASHTO maps.

Considering the limitations of detailed geological and seismological data in the Pacific Northwest, the writers believe that the proposed map of acceleration coefficients is based on the most detailed seismic zonation practical with regard to peak ground motions on rock.

RECOMMENDATIONS

The map of velocity-related acceleration coefficients constructed in this study is recommended as an alternative source of the acceleration coefficient, A , for the AASHTO design procedure (an alternative to AASHTO Figure 3).

Further research is recommended to investigate possible methods to develop complete response spectra for model soil profiles so that the AASHTO "site coefficient" may be chosen for the period of the specific structure being designed rather than an average value over a range of periods that is used presently. The TRAC/WSU research that is presently in progress shows promise in this area.

I. INTRODUCTION

The Puget Sound region ranks as one of the most seismically active areas in the contiguous United States. Major earthquakes in recent history include the 1949 magnitude 7.1 event and the 1965 magnitude 6.5 event. Both caused significant ground motions and structural damage over a large area.

The high seismic hazard over much of the state necessitates the consideration of seismic forces when designing highway bridges and related structures. At present Washington State Department of Transportation (WSDOT) is utilizing design guidelines set forth by AASHTO [6]. These guidelines were developed by the Applied Technology Council (ATC). The design procedure is essentially a simplified version of the ATC seismic design guidelines for Buildings (ATC-3-06) [9].

The ASSHTO guidelines represent a "first cut" attempt at developing standardized seismic design procedures for bridges and set forth a relatively uncomplicated design approach. However, the guidelines consider seismicity over the entire United States, resulting in a lack of detail for many areas, including Washington State. Ground motion data are presented in the form of acceleration coefficients contoured on a small scale map of the United States.

Additionally, the three "soil type" acceleration modification factors are based on average conditions so they can be applied nationally. These modification factors have not been validated for seismic source mechanisms or soil conditions in the northwest United States. Even if complete revision of the

present modification factors is not warranted, additional factors may be developed for specific profiles encountered within the state.

Since the basic data for the AASHTO guide were developed, new data on seismicity and seismic zonation for the Pacific Northwest has been published. Also, a number of site specific seismic studies on major engineering structures have been completed. These data might be used to modify and improve the data base for the AASHTO approach, thus improving its accuracy and applicability for Washington State.

The AASHTO design guidelines suggest improvement on their methods when adequate data become available. They suggest the inclusion of specific consideration of (1) earthquake magnitude, (2) source mechanism of the earthquake, (3) distance of the earthquake from the proposed site and the geology of the travel path, and (4) characteristics of the soil deposits at the site. The following pages will address the factors listed above to whatever extent allowed by the present state of knowledge.

The ultimate objective of this research program was to develop an updated zonation map of design ground motion (acceleration coefficients) for bridge design in Washington using new available data on the unique seismicity and geology of the region. This work would be aimed at improving the AASHTO guide specifications [6] rather than developing a new design procedure.

Contained herein is a review of the present state of knowledge regarding the geology, tectonics, seismicity, seismic zonation, and surficial conditions for the State of Washington.

Due to the higher seismicity and population density of the Puget Sound area, a large portion of the time and effort dedicated to this report was spent on analysis of this area.

In order to understand both the advantages and shortcomings of various seismic design approaches a basic understanding of earthquake induced ground motions, how they effect structures, and how those motions are modified by local geology and site conditions is required. Thus, a portion of the literature review is spent addressing these issues.

Finally, recommendations are made regarding modifications to the present AASHTO guide specifications as they apply to Washington and the present seismic coefficient map and soil modification factors. These proposed changes should not be viewed as changes to the design procedure itself, but improvement of the ground response input data.

II. LITERATURE REVIEW

A number of contributing factors must be considered when examining the seismic activity and associated ground motions for a particular region. Major considerations include geology, tectonics, seismicity, and ground response characteristics. Each subject will be discussed with sufficient detail to provide the reader with a basic understanding of the important concepts and the general state of knowledge.

Geology of Washington State

The state of Washington can be divided into a number of geologic provinces, such as those shown in Figure 1. While boundaries may vary somewhat from investigator to investigator, the basic province divisions are widely accepted.

Olympic Mountains

Although the Olympic mountains may be considered part of the Coast Range, structurally they are quite separate. The eastern extreme may be the remnant of an ancient seamount structure similar to that hypothesized for the Coast Range. A fragment of oceanic crust and associated sediments was rafted against the continental margin in the late Tertiary. Overthrusting followed by underthrusting produced the horseshoe shaped geometry found today.

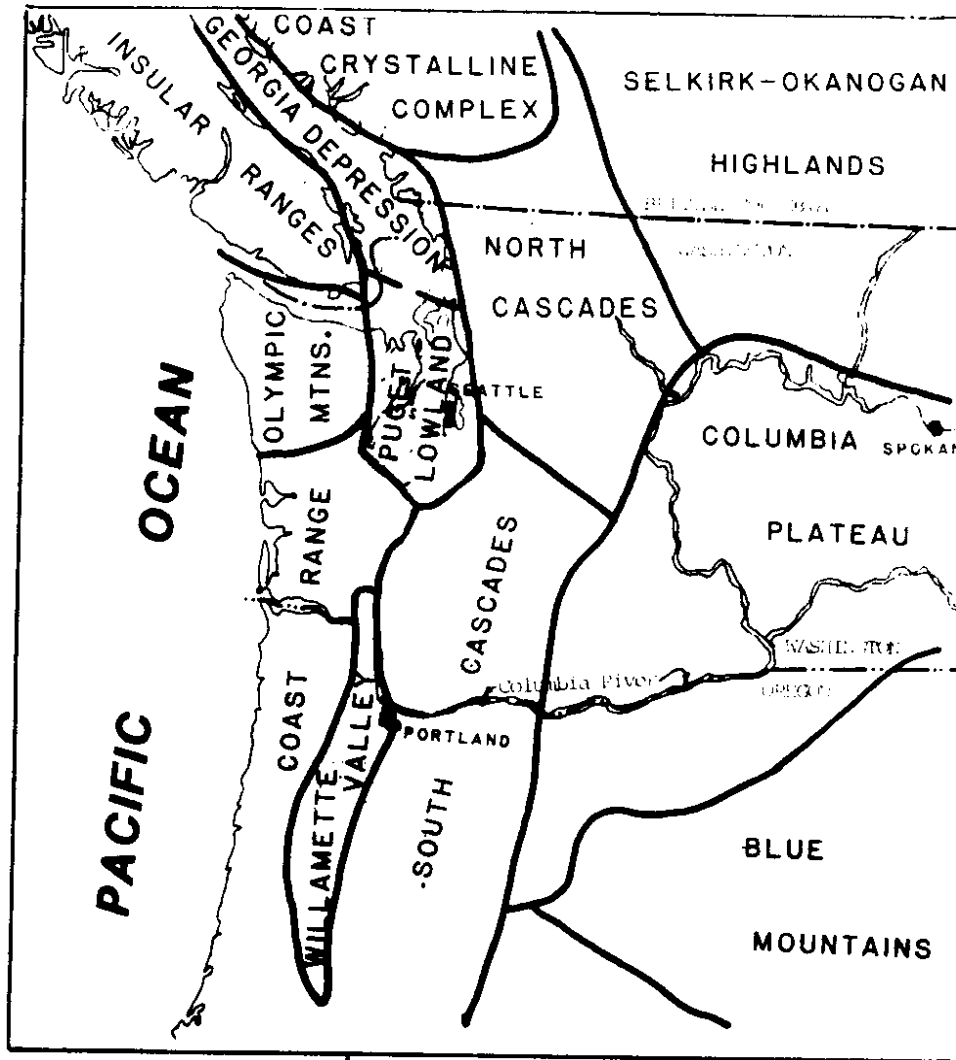


Figure 1. Geologic provinces of the Pacific Northwest.(74)

Coast Range

The coast range consists of early Tertiary submarine volcanics and tuffs overlain by volcanic and sedimentary rocks of mid-Tertiary age [74]. The older volcanics may be an ancient seamount sequence that rafted against the continental margin along with overlying sediments during Tertiary time. The whole sequence was then uplifted to its present elevation during the late Tertiary.

Puget Lowland

The Puget lowland is a structural and topographic low bounded on the west by the Olympic and Coast mountains and on the east by the Cascade range. The north-south trending trough has been subjected to repeated continental glaciation during the Pleistocene Epoch resulting in extensive modification to the landforms then present [25]. Modification was the result of scour during glacial advancement from the north and deposition of glacial sediments during subsequent recessions. Due to repeated glaciation, the majority of the sediments are highly overconsolidated.

Estimates of maximum sediment thickness range over a full order of magnitude. The area of greatest sediment thickness is beneath the city of Seattle. Early investigations estimated maximum thickness as high as 6.2 mi [22]. More recent studies have reduced the estimate to approximately 0.7 mi [26,82].

Following retreat of the most recent glacial event, the Vashon Stage of the Fraser Glaciation, erosion has been the most

active geomorphologic agent. The erosion process has primarily been acting in the upland areas with deposition taking place in the lowlands. Consequently, fluvial and estuary deposits of sands, silts, clays and peat are often found overlying the denser glacial deposits. Additionally, artificial hydraulic fills of primarily sandy material may be found in many locations adjacent to the Sound as a result of port development.

Due to the overlying sediments deposited in the Puget Lowlands, the bedrock geology is not well understood. At present, depth to bedrock is thought to be controlled by a horst-graben structure. The grabens form sedimentary basins beneath the Seattle and Tacoma areas with an intervening horst [22,26,82]. The underlying bedrock geology is thought to consist of Paleozoic and Mesozoic sedimentary and pre-Devonian crystalline rocks in the northern parts with Tertiary continental and marine sedimentary, and volcanic rocks to the south [17].

North Cascades

The North Cascades consist primarily of a late Mesozoic to early Tertiary crystalline and metamorphic province flanked by Tertiary sedimentary and volcanic rocks. The North Cascades are part of the still active Cascade Volcanic Arc [74]. The North and South Cascade geologic provinces are separated by the Olympic-Wallowa Lineament (OWL), located near Snoqualmie Pass. The OWL passes through the range in a northwesterly trend and defines a distinct structural and lithologic boundary.

South Cascades

The South Cascades consist primarily of a Cenozoic volcanic sequence. The sequence can be separated into the Western Cascade Group (Eocene to early Pliocene) and the younger High Cascade Group (Pliocene to Holocene). The western Cascade Group consists of lava flows, pyroclastic flows, mudflows, and volcanoclastic elements. The High Cascade Group overlies the Western Cascade Group in many locations and largely consists of basalts, basaltic andesites, with lesser quantities of andesite and dacite [75]. Mount St. Helens is located within this province.

Columbia Plateau

The Columbia plateau is composed of a thick sequence of flood basalts extruded through fissure eruptions in the Miocene [73]. The plateau surface slopes gently to the southwest, from an elevation of about 2,500 ft in the northeast to 1,000 ft along the Columbia and Snake Rivers. Surficially exposed tectonic structures consist of a series of northwest to east-west trending anticlines and associated faults located on the western and southern sectors of the plateau as well as along the margins. The combined effects of the basalt group dipping away from the surrounding mountains due to uplift and subsidence within the plateau has produced a number of structural basins in the south-central portion of the plateau [73].

Okanogan-Selkirk Highlands

The core of the Okanogan-Selkirk Highlands (OSH) consists of granites and crystalline metamorphic rocks flanked by structurally complex metamorphic rocks on either side [72]. The OSH is the southern most expression of an extensive belt of crystalline rocks that trend northerly into Canada. On the west it is bounded by the Methow Graben. To the south Columbia River Basalts interfinger with locally derived sediments from the Highlands.

Tectonics

The source of contemporary tectonics in the Pacific Northwest is the subduction of the Juan de Fuca (JDF) plate beneath the western edge of North America. Although many general aspects of the genesis of the JDF plate are understood, much controversy still exists regarding its degree of activity and the driving mechanism behind this activity.

The JDF plate is a remnant of the larger Farallon plate [10]. Approximately 30 million years (m.y.) ago the North American plate, moving relatively westward, overrode the southern edge of the Farallon plate, including the leading edge of the Pacific Rise spreading center (Fig. 2A). This overriding action extinguished that portion of the spreading center and created a triple junction between the North American, Pacific, and Farallon plates. The north-south trending San Andreas megashear zone was then formed to the south of the triple junction. The relative movements of the Pacific and North American Plates resulted in

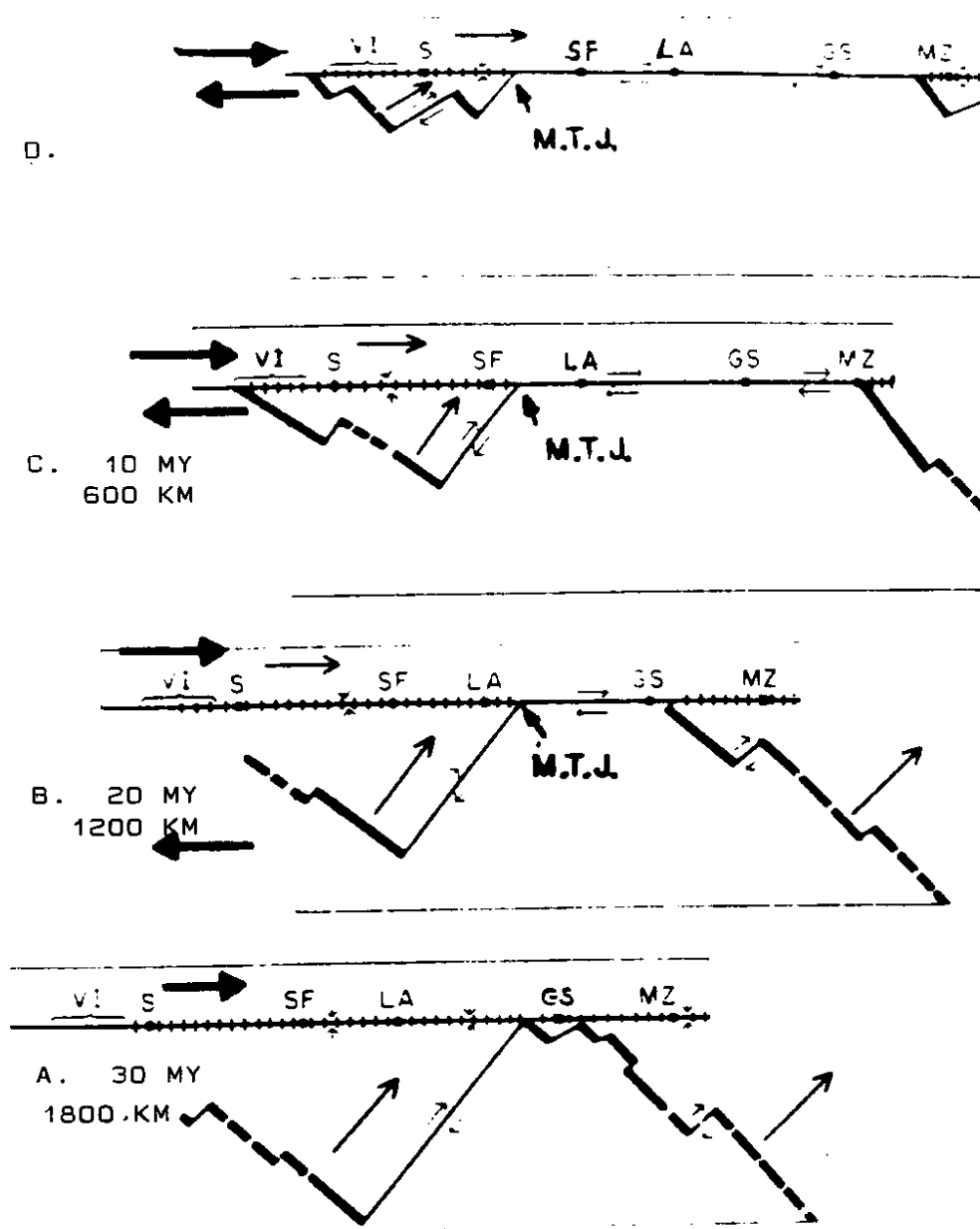


Figure 2. Schematic model of plate interactions. VI-Vancouver Island, S-Seattle, SF-San Francisco, LA-Los Angeles, GS-Guaymas, MZ-Matatlan. East Pacific Rise in dark lines. M.T.J. is Mendocino Triple Junction. Large arrows denote relative plate motions. (10)

right lateral shear, causing the Pacific and Farallon plates to migrate northward (Fig. 2B). In conjunction with the lateral shear to the south, the Farallon Plate continued to subduct beneath the North American plate, causing it to get progressively smaller (Fig. 2C), with the relative movement continuing until present (Fig. 2D).

As the Farallon plate became smaller it apparently fragmented due to the stresses induced by the Pacific and North American plates. These fragmented sections acted independently, with different spreading rates and directions. Three of these remnant fragments are recognized today, the Gorda, Juan de Fuca, and Explorer plates. The JDF plate is the largest of the three (Figure 3).

There is much debate presently regarding the relative activity of the JDF plate. Controversy exists as to how actively the JDF plate is subducting, the rate of subduction, the degree of coupling between the North American and JDF plates, and the shape of the subducted portion.

Although there is some debate regarding how actively the JDF plate is subducting, there is general agreement that the JDF plate is moving 1-1.5 in/yr to the northwest, relative to the North American plate [78]. It is still debated whether the JDF plate is actively subducting. While the preponderance of evidence supports active subduction, a great deal of controversy exists as to whether the subduction is coupled or aseismic. Coupling between the JDF and North American plates would result in large stresses accumulating at the margin due to the lack of

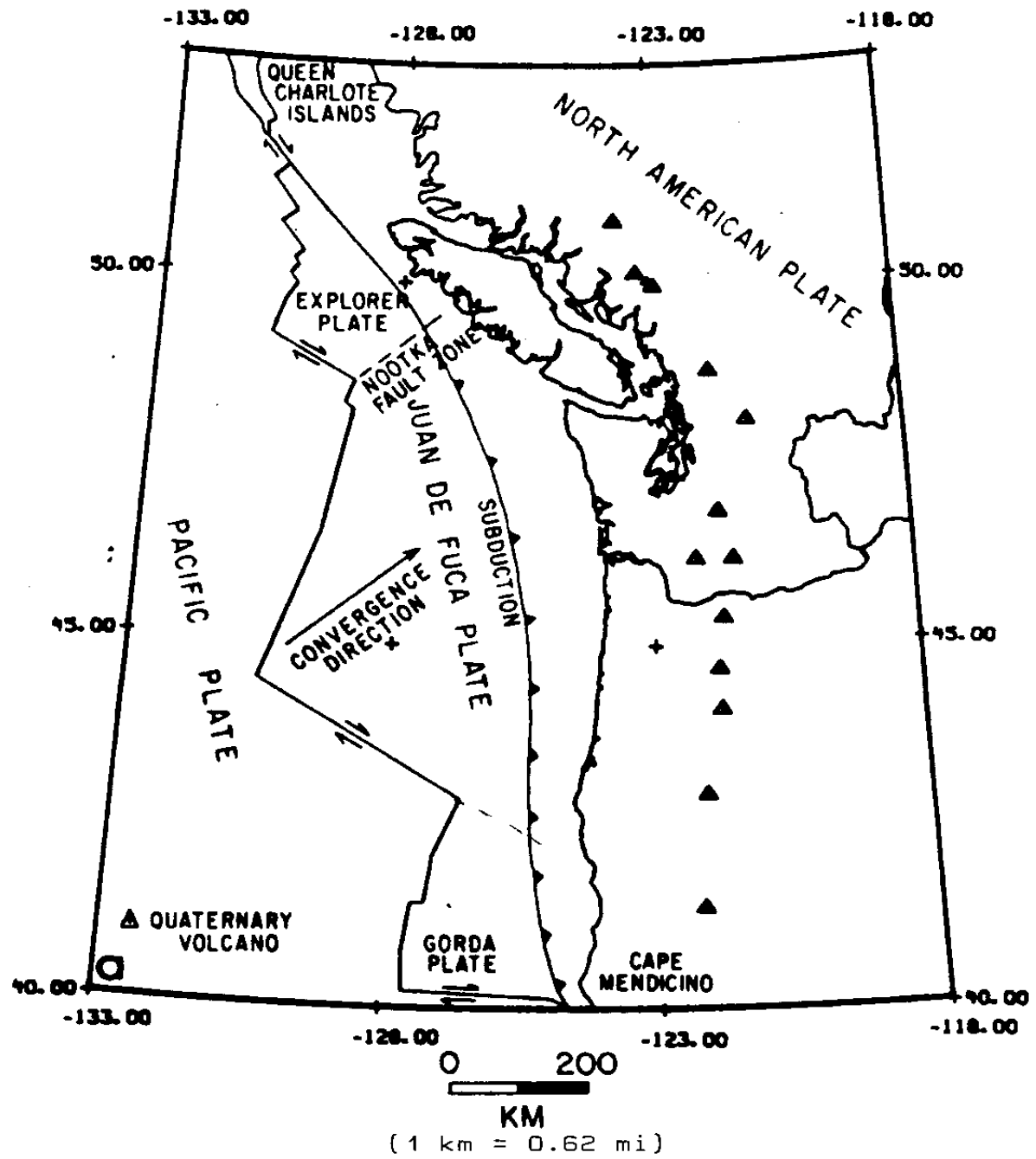


Figure 3. Juan de Fuca plate map. (68)

slippage. This implies a large, shallow focus earthquake is likely to occur sometime in the future, something that is not evidenced by the existing earthquake record. The evidence supporting this theory [30,60,68,78] is far from conclusive, but cannot be discounted.

Features supporting coupling include:

- rate of convergence
- young age of JDF plate
- absence of back-arc basin
- shallow oceanic trench
- NE horizontal compression of continental margin

Features supporting aseismic subduction include:

- no extensive, growing coastal mountain range [76]
- relative earthquake quiescent along margin
- no well defined Benioff zone to depths of 124-186 mi
- crustal uplift of continental margin [7]
- no record of previous shallow focus subduction zone earthquakes.

As indicated above, there is supporting evidence for both hypotheses. A great deal of additional study is necessary before any conclusions may be drawn in favor of either theory.

The shape of the subducted portion of the plate is also subject to a certain amount of debate. A number of recent studies conclude the plate initially dips approximately 6-11 degrees below the continental margin, then steepens to a dip of approximately 40-55 degrees beneath the Puget Sound Region [41,59,67,68]. All of the estimates to date are based on the

development of velocity models of the subsurface combined with interpretation of geophysical data. Consequently, a great deal of approximation and interpretation is required and a unique solution is not possible. As more data becomes available the models should start converging. More recently, a model requiring an initial 25 degrees dip of the subducting plate instead of 10 degrees has been proposed [21]. This would place the subducting plate below the maximum depth of recorded seismicity, implying the deeper focus earthquakes recorded in the past occurred above the subducting plate, possibly in a remnant plate. This is supported by the lack of agreement between the principal stress axis calculated from past events and that expected for the subducting plate. Nothing has been published on this theory to date, so a rigorous evaluation is not possible. However, it does illustrate the diversity of interpretations possible based on the available data.

In summary, the tectonic setting of western Washington is unique and not completely understood. The Juan de Fuca Plate is probably still subducting beneath the west coast, although the rate of subduction, the degree of coupling and the shape of the subducting plate are all still a matter of debate. Since the JDF plate is bounded on the north and south by north trending strike-slip faults, the stress field and associated movement is highly complex and difficult to interpret. The inability to define the geometry of the subducting plate is caused by the difficulty in producing a unique solution based on the available data. It may not be possible to answer these questions with confidence until

another large earthquake occurs. Figure 4 is an artist's conceptualization of how the subduction process might be occurring.

Seismicity

The vast majority of historic seismicity within the State of Washington is the result of activity in the Puget Sound region. This is not surprising, when the area's proximity to an active tectonic margin is considered. Due to its relatively high rate of seismic activity compared to other areas in Washington, a majority of the discussion on seismicity will be directed towards the Puget Sound area.

Seismicity of the Puget Sound Area

Earthquakes originating within the Puget Sound region can be divided into two suites based on focal depth [20,68]. The shallow zone extends to a depth of approximately 12-19 mi. The deeper zone ranges in depth between 24 and 44 mi, coincident with the subducting JDF plate, as presented in the previous section.

There is little surface expression of faulting within the Puget Sound region. Additionally, there appears to be little correlation between mapped faults and shallow seismicity [68]. The lack of surface expression may be the result of low angle thrust faults at moderate depth [27], although substantive evidence does not exist to support such a supposition. Epicentral locations for shallow focus events are diffuse,

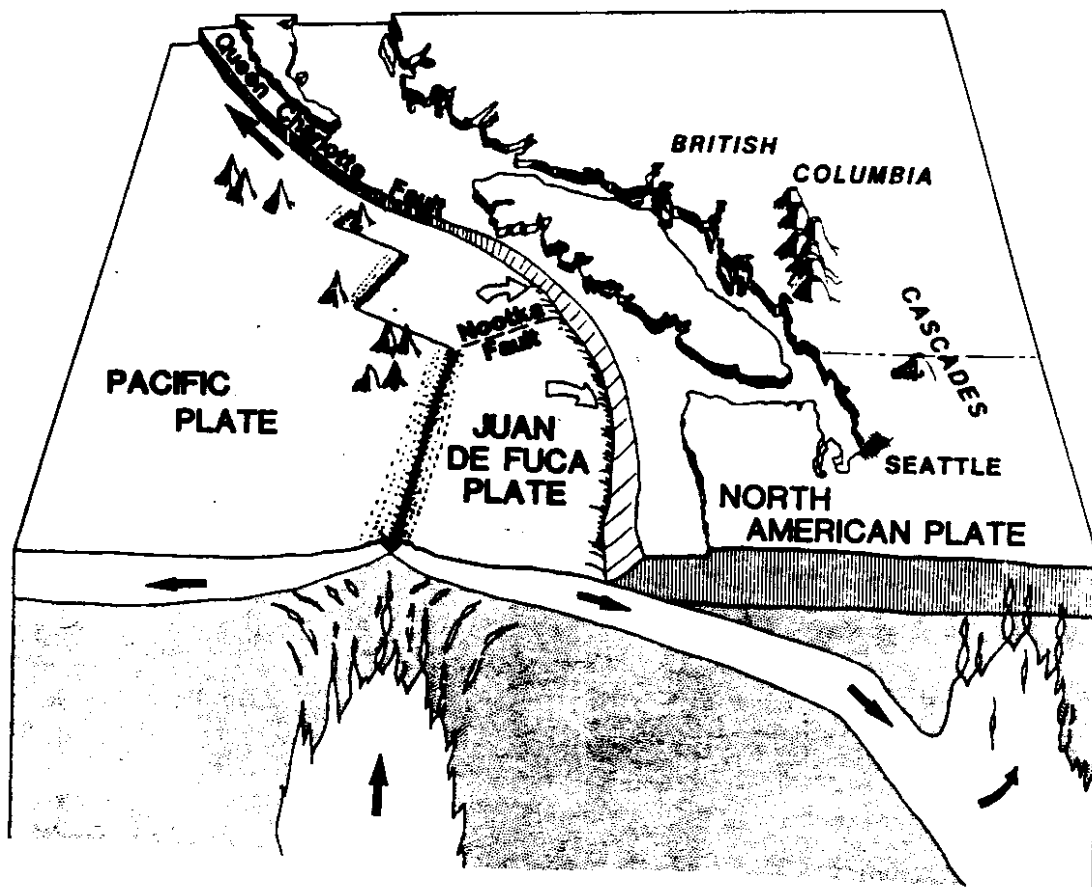


Figure 4. Artist's drawing of how the subduction process might be occurring. (77)

indicating they are not related to any large scale faulting [19,68].

Composite fault plane solutions suggest N-S compression for crustal earthquakes [19]. This implies that the regional stress field is more strongly affected by the interaction between the Pacific and North American Plates, rather than between the JDF and North American Plates.

The deep suite accounts for all the large earthquakes of record, at least for those hypocenters that have been determined with accuracy. The most widely accepted hypothesis regarding the location of the deep focus earthquakes is that they are occurring in the upper portion of the subducting plate [67,68]. Fault plane solutions indicate normal faulting parallel to the axis of bending in the slab [5,68]. This may be due to increased tensional stresses as the slab dips more steeply beneath the Puget Sound.

Until recently it has been predicted that all large magnitude earthquakes are likely to originate in the deeper suite. However, recent investigators have indicated the possibility of a large magnitude, shallow focus, subduction zone earthquake ($M > 8.0$) [30,60,78]. The argument for such an event is based on a coupled plate boundary, as previously discussed. Although the hypothesis has merit, it is considered too speculative at present to be considered for design purposes. Figure 5 displays earthquake hypocenters for events occurring between 1970 and 1978. Although this represents a fairly short

X - SECTION, ALL QUAKES .DE. MAG 2.0, APERTURE 300 KM
 AZIMUTH OF PROJECTION = 60 DEGREES
 (USGS Open File Report 83-19)

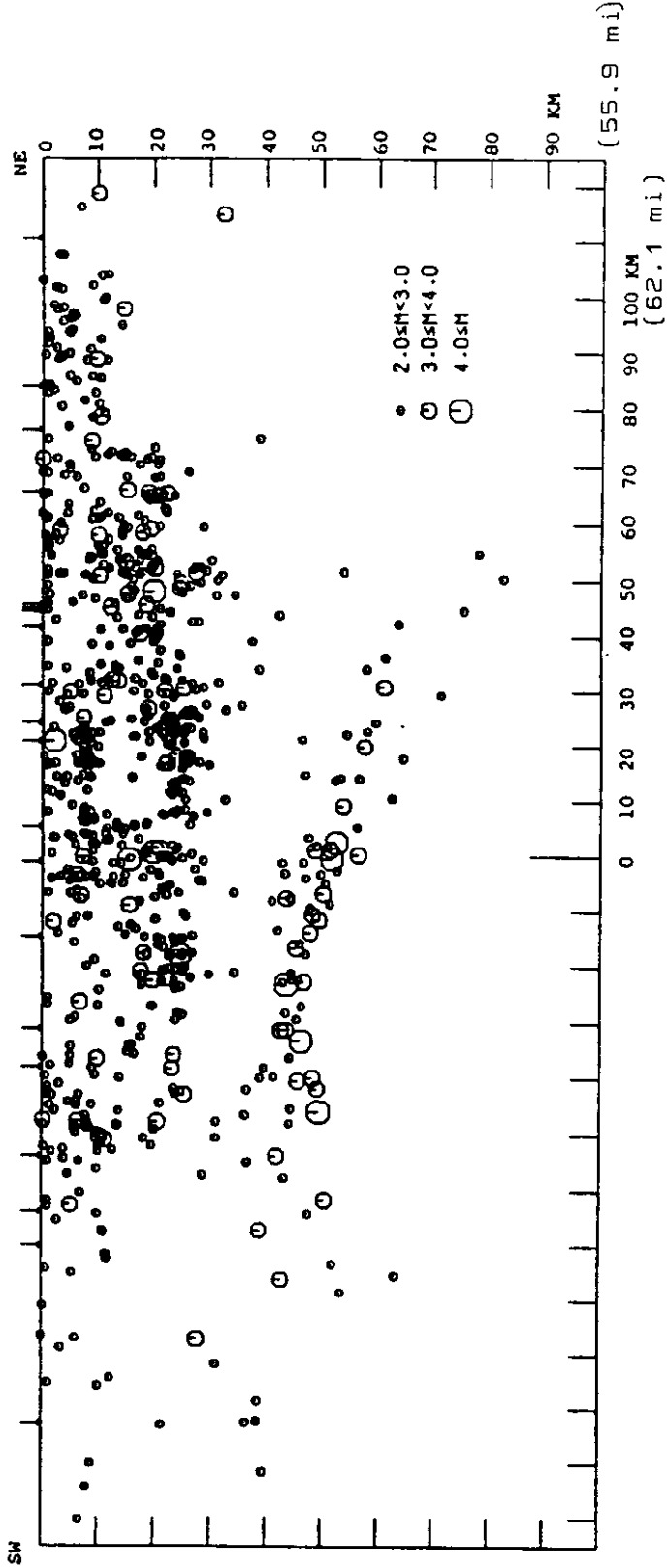


Figure 5. Earthquake hypocenters for events occurring between 1970 and 1978 in Washington. Cross-section projecting all hypocenters onto a plane which strikes at an azimuth of 60 degrees. Total aperture width for projection is 186 mi (300 km). The center of the projection is at 47° 30' N and 122° 30' W. Includes earthquakes with magnitudes 2.0 or greater.

time interval, it is a good indication of the spacial distribution of events between the two seismic zones.

Seismicity of Washington, Excluding
the Puget Sound

Seismicity within the state outside the Puget Sound Region has consisted of smaller magnitude events with a lower frequency of occurrence. In many cases it is not possible to associate an earthquake event with a specific tectonic structure or seismic zone. This lack of correlation requires discussing the majority of seismic events in terms of single events rather than the characteristics of seismotectonic zones. Two source zones outside the Puget Sound Region were considered sufficiently well defined to discuss as zones rather than single events. Specific earthquakes considered important to the seismicity of Washington State will be discussed in the next section.

The Willamette Lowland, considered a southern extension of the Puget Lowland, may be classified as a seismotectonic zone based on historic seismicity and association with the subducted JDF plate. Although similar to the Puget Lowland in source mechanism, historic seismicity has occurred at a slower rate, and has produced a lower maximum historic magnitude of 5.5 [56].

The Chelan area in North-Central Washington is the possible location of perhaps the largest earthquake in Washington's history. The earthquake of 1872 had a maximum Modified Mercalli Intensity (MMI) of VII-VIII [18,81], with an estimated magnitude of 7.0-7.5. Due to low population density, the exact epicentral

location is hard to pinpoint, but probably was somewhere between Lake Chelan and the Canadian border to the NNW.

Since the exact location of the 1872 earthquake is unknown, the Lake Chelan area cannot be designated a seismic source zone solely based on that event. In addition to the 1872 earthquake, a number of smaller events, generally with magnitudes less than 5.0, have been reported for the Lake Chelan area. Based on existing data the maximum magnitude for the area has been estimated to be approximately 5.8 [14].

Historic Earthquakes Affecting

Washington State

A number of relatively large earthquakes have occurred either in or near Washington State over its rather short recorded history. The following are considered to be some of the more important events.

December 14, 1872 North Cascades.--As previously noted, the 1872 earthquake is not well defined in terms of location, depth, or magnitude. It is perhaps the largest event reported within the state with a magnitude possibly as high as 7.5 [42,52]. Although the hypocentral location is highly speculative, it is assumed to be deeper than 6 mi, possibly explaining the lack of surface expression [18]. In contrast to major Puget Sound events, the 1872 earthquake had numerous aftershocks.

July 16, 1936 Milton-Freewater, OR.--The 1936 Milton-Freewater event was instrumentally recorded and had a magnitude of approximately 5.8 with an associated epicentral intensity of

VII+ [57]. Although a definite connection between event and causative fault has not been found, field evidence suggests the earthquake occurred along the Wallula fault system [72]. Numerous aftershocks were felt with a maximum intensity of V [57]. Although Milton-Freewater is located in Oregon, Walla Walla, WA is in close proximity to the north. Figure 6 is an isoseismal intensity map of the event.

February 15, 1946 Puget Sound.--The February 15, 1946 earthquake was located in the southern portion of the Puget Sound region, between Olympia and Tacoma. A magnitude of 6.3 was recorded with an associated epicentral intensity of VII. The event was felt over an area of 70,000 square miles [57].

April 13, 1949 Olympia, WA.--This was the first large earthquake located within the Puget Sound region to be instrumentally recorded locally. With a magnitude of 7.1, it is also the largest Puget Sound event recorded. A maximum intensity of VIII and felt area of 150,000 square miles has been estimated [57]. The 1949 earthquake is typical of the large deep focus events that have occurred within the region. No after shocks were recorded and it had a deep focal depth of approximately 44 mi [57]. Figure 7 indicates the epicentral location, maximum intensity, and felt area for the event.

April 29, 1965 Puget Sound, WA.--Located between Seattle and Tacoma, the 1965 Puget Sound earthquake was a magnitude 6.5 event with a maximum intensity of VIII. The earthquake had an estimated focal depth of 35 mi and was felt over a 130,000 square

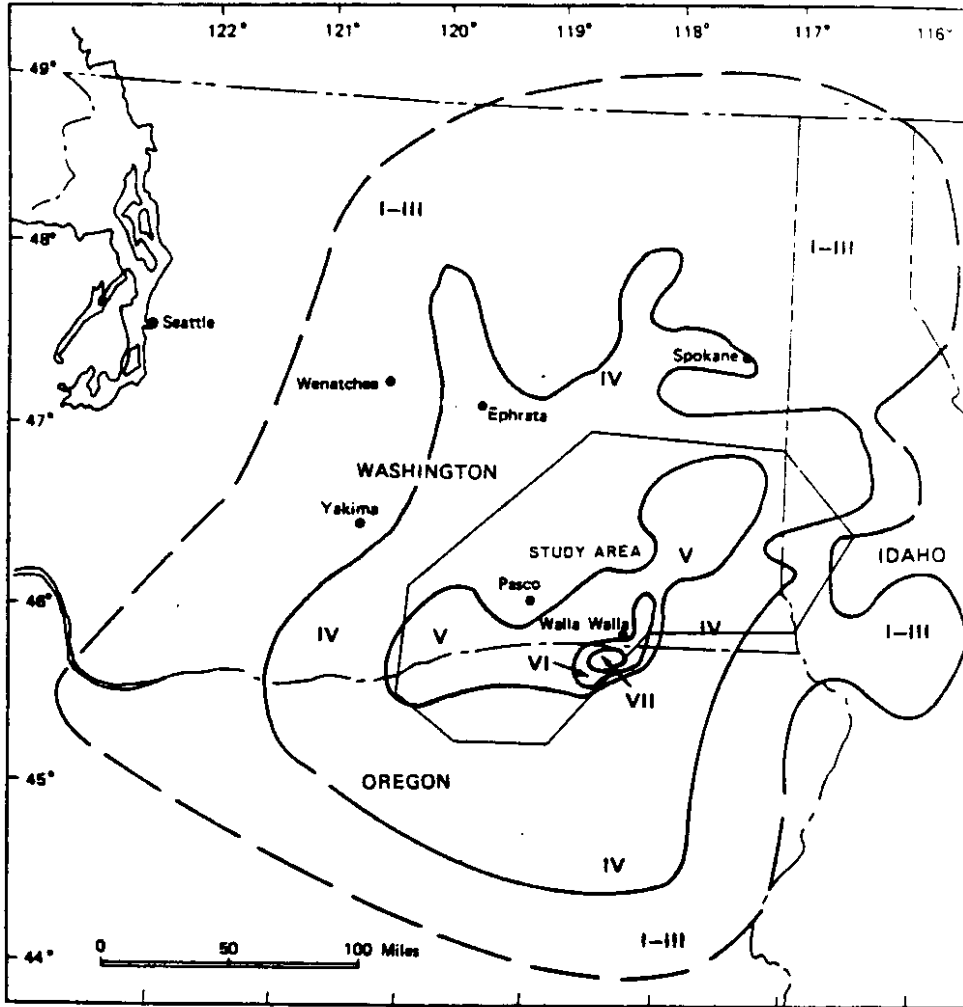


Figure 6. Isoseismal map for the July 16, 1936 earthquake. (72)

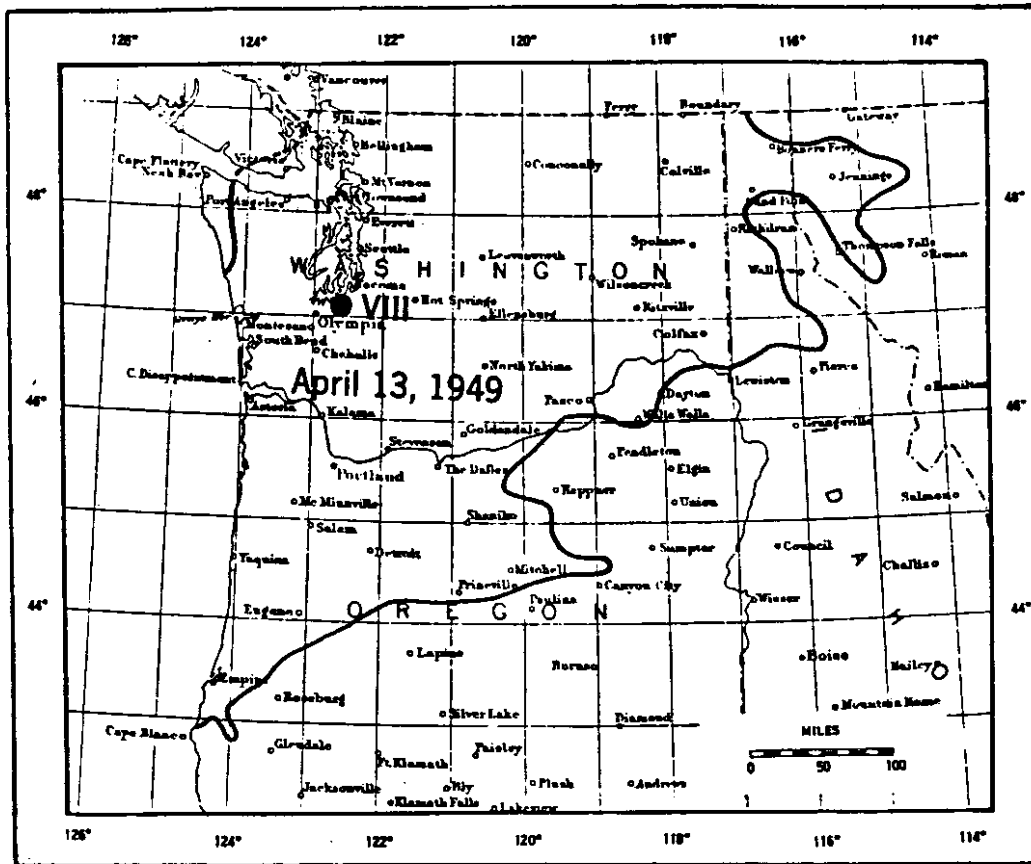


Figure 7. Area affected by the earthquake of April 13, 1949. (45)

mile area. As with the 1949 event, no after shocks were recorded. Figure 8 is an intensity map of the event.

Ground Motions Under Earthquake Loading

Ground motions generated by an earthquake are the result of an extremely complex physical event. The surface motions are due to several factors, including the source mechanism, local and regional geology, and the attenuation characteristics of the subsurface and surficial materials, just to name a few. From an engineering perspective it is necessary to describe the damage potential of an earthquake based on one or more ground motion parameters, or some empirical relationship between the ground shaking severity and damage potential. Over the years a number of methods have been developed to describe the relationship between the "size" of the event and its subsequent effect on man made structures. These relationships range from purely observational to relatively complex mathematical formulations. This section will discuss some of the more widely used methods of analysis, and some of the physical factors that effect ground motions.

Measurement of Earthquake "Size"

The measurement of the "size" of an earthquake event is usually described in terms of either intensity or magnitude. Intensity scales were employed as a measure of earthquake ground shaking prior to the development of strong motion recording devices. Although a number of intensity scales have been

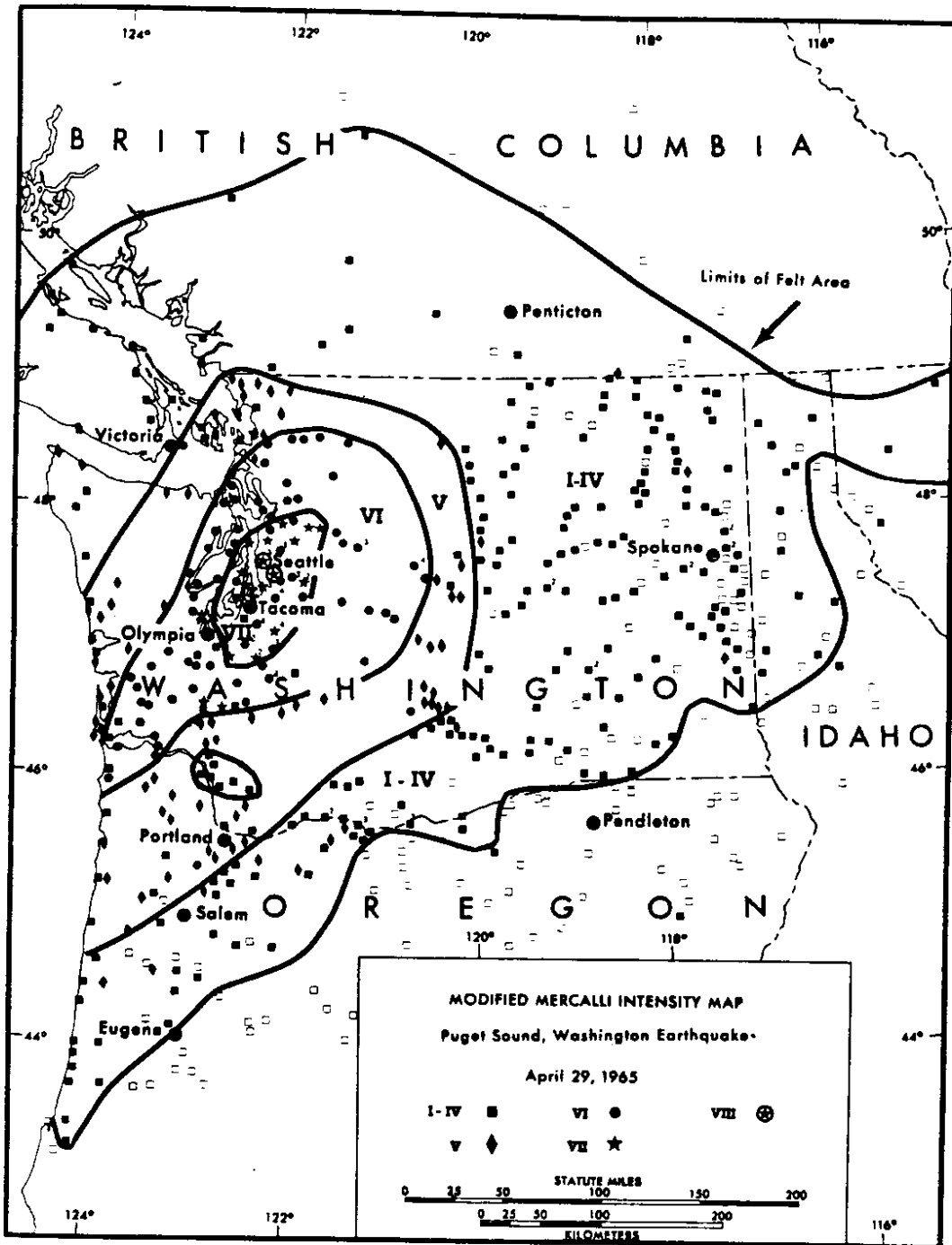


Figure 8. Intensity map of the Puget Sound, Washington earthquake of April 29, 1965. (2)

developed, from as early as 1735, the Modified Mercalli Intensity (MMI) Scale is most commonly used today. As with all intensity scales a numerical value is assigned to the earthquake based on human perception of ground motion and damage to man-made structures. The Modified Mercalli Intensity Scale ranges from a value of I for ground motion barely felt under ideal conditions up to XII for total destruction of all structures.

Since the MMI scale is primarily based on building damage, construction methods and building type play a large role in determining intensity. Thus, a variation in intensity may be indicated for a given area if structural variation exists; even if the ground motions are identical. At best, the use of intensity may be considered a convenient, although crude, method of describing the damage caused by an earthquake. The fact that MMI provides a number and correlations between intensity and ground motion parameters have been developed, have resulted in its use for earthquake engineering design. When intensity is used for design the inherent imprecision of the method must be kept in mind.

This is not to say that MMI is not a useful parameter. The length of time earthquakes have been instrumentally recorded is extremely short. Consequently, MMI from historic earthquakes are often used to supplement instrumented records when developing recurrence relationships and maximum magnitudes for statistical analysis. Additionally, MMI may provide a better estimation of ground response than magnitude when soil amplification or focusing occurs.

Earthquake magnitude is probably the most misunderstood and improperly used concept of earthquake engineering. The four most common measurements of magnitude being used today are: 1) local magnitude M_L ; 2) surface wave magnitude, M_S ; 3) body wave magnitude, M_b ; and 4) moment magnitude, M_o . Each magnitude scale is a measure of the source spectral amplitude at a discrete frequency. M_L is a measure of the high frequency component between 1 and 3 Hz. M_b is proportional to the 1 Hz amplitude. M_S corresponds to 0.05Hz. M_o corresponds to very low frequency spectral amplitude [52].

The inconsistency is primarily due to the ambiguity of the Richter magnitude scale. Richter magnitude is usually defined by M_L for small California events and M_S for larger earthquakes. For earthquakes in other areas it is defined by either M_b or M_S , or both in some cases, even though the values are usually different [52].

This lack of consistency in definition of magnitude is one reason why different magnitude values are sometimes reported for the same event. In other cases, the mixing of magnitude scales has resulted in excessive data scatter when investigators have attempted to develop magnitude dependent attenuation relationships. Regardless of the magnitude scale used, it is extremely important to clearly state which scale is being used and apply it consistently. In order to prevent confusion in this report, Richter magnitude will be applied using the definition proposed by Nuttli [51]:

$$M_R = M_L \text{ if } M \leq 6 \text{ or } = M_S \text{ if } M > 6.$$

There is a tendency for all magnitude scales except moment magnitude to reach a limiting value (saturation) as the size of earthquake increases [12]. This tendency is illustrated in Figure 9 and has resulted in an increased use of M_0 since it does not exhibit saturation at large magnitudes.

Ground Motion Measurement

The primary data for earthquake engineering are time-history records of acceleration recorded by strong motion accelerographs. A knowledge of these data and how they relate to building damage is essential in understanding the response of structures to seismic loading.

The fundamental ground motion parameters that can be obtained from an accelerogram are acceleration, velocity, and displacement. Acceleration is obtained directly from the accelerogram recording. Velocity is obtained by integrating the acceleration over time, e.g.,

$$v = \int_{t_1}^{t_2} a(t) dt$$

while displacement is obtained by double integration of acceleration, or integration of velocity, e.g.,

$$D = \int_{t_1}^{t_2} v(t) dt$$

An example of a typical accelerogram and associated velocity and displacement time-histories are presented in Figure 10. As can be seen from the figure, acceleration has the highest frequency

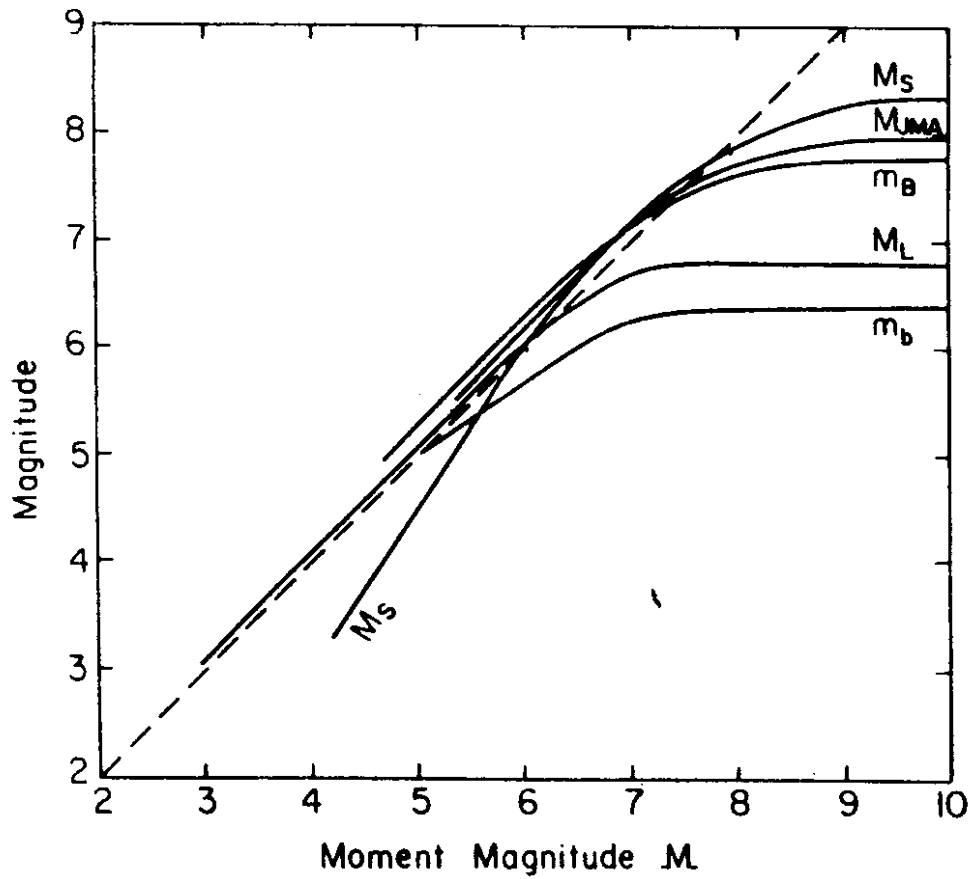


Figure 9. Relation between moment magnitude and various magnitude scales. M_s -surface wave, m_b -short-period body wave, M_B -long-period body wave, M_L -local, and M_{JMA} -Japan. Dashed line shows a 1:1 relation for reference. (12)

PUGET SOUND, WASH.. EARTHQUAKE APR 29, 1965 - 0729 PST
110310 65.003.0 FEDERAL OFFICE BUILDING, SEATTLE, WASHINGTON COMP S32E
PEAK VALUES : ACCEL = -52.2 CM/SEC/SEC VELOCITY = 5.6 CM/SEC DISPL = -2.5 CM

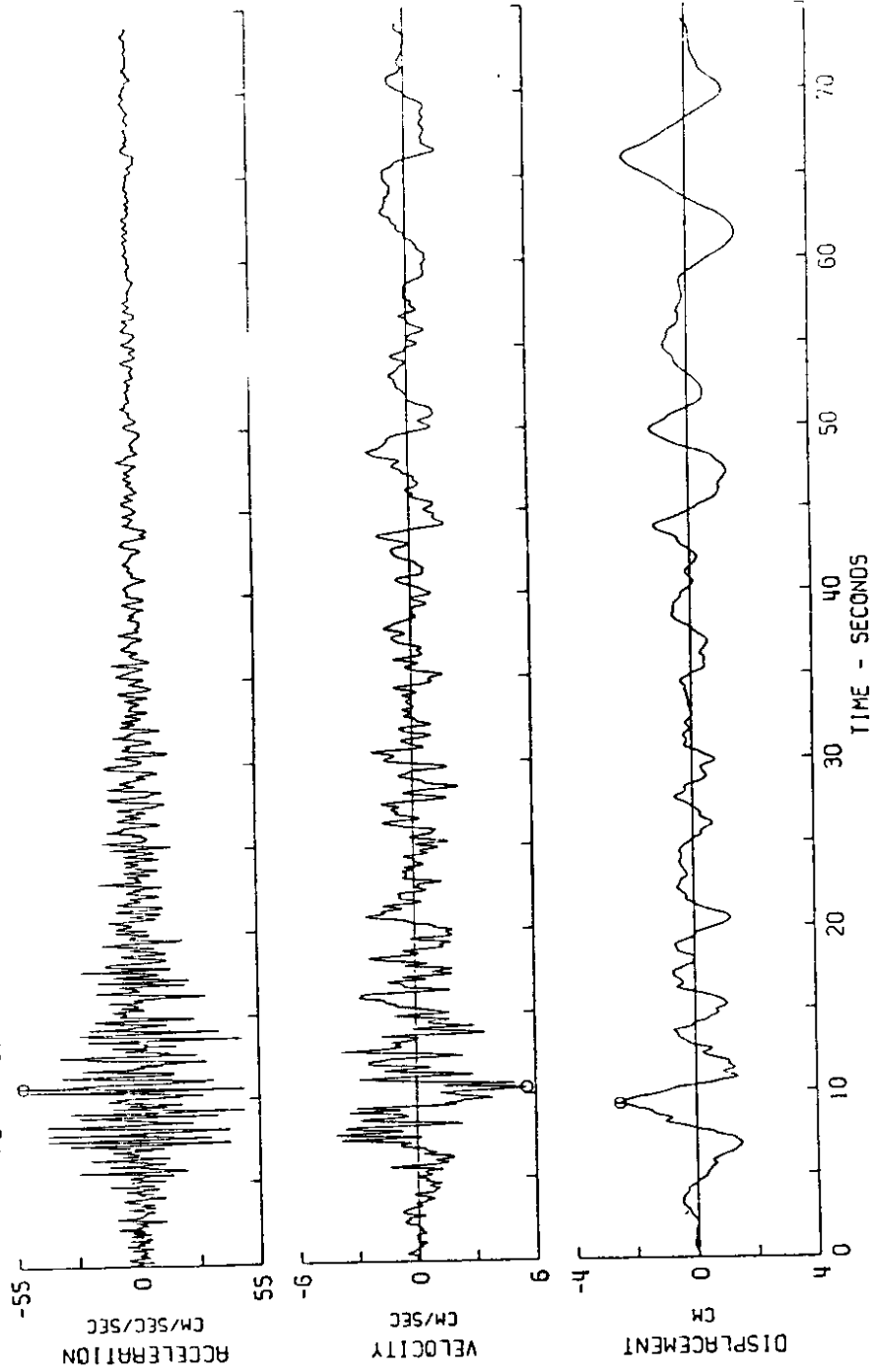


Figure 10. A typical accelerogram and associated velocity and displacement time-history.

components and displacement the lowest. The importance of this observation will become apparent when the relationship between ground motion and building damage is discussed.

Most accelerograph sites record three components of ground motion, two orthogonal horizontal recordings, and one vertical. Although the relationship between horizontal and vertical acceleration are not consistent, a general rule of thumb is that $a_v \approx 2/3 a_h$.

Seismic Analysis of Structures

There are two basic approaches to the seismic analysis of structures: pseudostatic and dynamic. Pseudostatic analysis establishes the earthquake loading as an inertial force, then applies the force statically to the structure or structural component at the center of mass [36]. The structure is then analyzed to determine its ability to sustain the additional load. Since an earthquake produces both vertical and horizontal forces, both vertical and horizontal loadings may be analyzed. However, the horizontal loading is usually the critical factor, so in many cases the vertical component is ignored. The magnitude of the load is the product of the mass of the structure and a seismic coefficient.

In its crudest form a seismic coefficient is a peak (or percentage of peak) acceleration based on a design earthquake. In its more refined form a seismic coefficient accounts for spectral amplification in the period range of interest and the influence of local soil conditions.

A true dynamic analysis simulates earthquake motion by applying a cyclical load similar to the design earthquake. This approach, often termed time-history analysis, is a time consuming, complicated procedure that is not considered necessary for most structures. However, it does have the advantage of being able to incorporate earthquake duration into the analysis, something that most other forms of analysis are forced to ignore. Time history analysis is usually employed when non-linear structural response is a major consideration.

When inelastic effects are not considered extremely important, a simplified form of dynamic analysis is often used. This method is typically non-site-specific and utilizes smoothed response spectra for analysis. The natural periods of vibration of the structure are determined. In most cases the first 3 to 6 modes suffice [50]. The smoothed response spectra is then entered at the appropriate periods to obtain the associated spectral accelerations. The modal responses are then combined to determine the total response.

Response spectra may be presented in various ways. A common technique is to plot or construct the response spectra on tripartate log paper as illustrated in Figure 11. This method has the advantage of displaying spectral acceleration, velocity, and displacement on the same plot. Additionally, empirical methods have been developed to construct smoothed response spectra from peak ground motion values plotted on tripartate paper [48,49,50]. This type of plot also provides a convenient

PUGET SOUND, WASHINGTON EARTHQUAKE APR 29, 1965 - 0729 PST

1118032 65.001.0 OLYMPIA, WASHINGTON HWY TEST LAB COMP 5864

DAMPING VALUES ARE 0, 2, 5, 10 AND 20 PERCENT OF CRITICAL

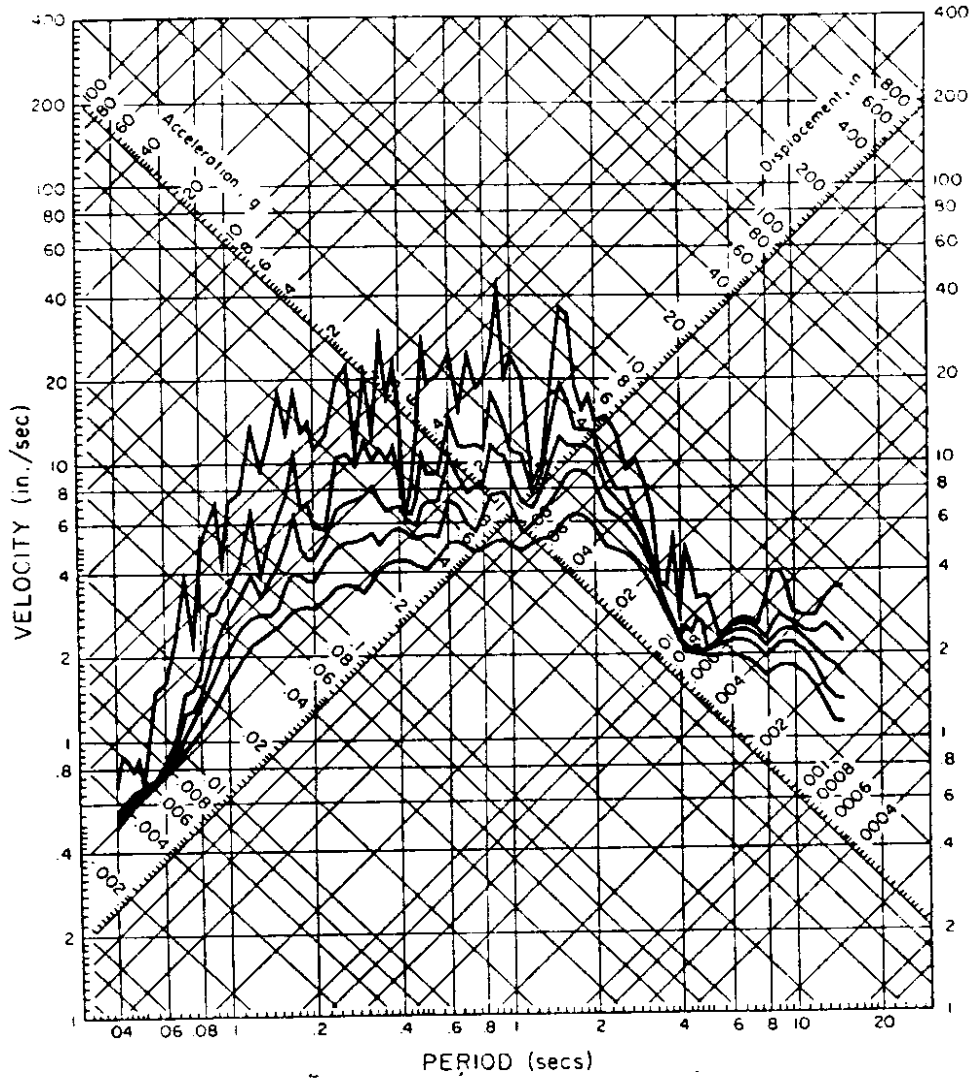


Figure 11. Example of response spectra plotted on tripartate log paper.

format when modifying the elastic response spectra for inelastic response using ductility factors.

The ATC guidelines [6,9] utilize an "Elastic Seismic Response Coefficient" to approximate the design spectra and is defined as:

$$C_{s_m} = \frac{1.2 AS}{T_m^{2/3}}$$

where

A = acceleration coefficient (g)

S = soil modification factor

T_m = period for mode m (sec)

C_{s_m} = seismic response coefficient for mode m

It must be remembered that a number of simplifying assumptions were required to develop this equation. In cases where unusual design constraints must be considered, this approach should only be used for preliminary design. A more site specific approach should then be used to either validate or modify the original design.

Attenuation of Ground Motion with

Distance from the Source

Attenuation of ground motion is influenced by a number of factors including geometric spreading, internal damping, geologic inhomogeneities, and phase conversions of body waves to surface waves, to name a few. Presently only attenuation resulting from geometric spreading and internal damping are considered in most

empirical expressions of attenuation with distance from the source. General agreement does not exist among investigators regarding the mathematical description of attenuation, or which factors are the most influential.

Most relationships incorporate a magnitude and a distance term and are of the form:

$$\log y = A + F(M) + F'(R)$$

where y is the ground motion (a, v or d), A is a constant, M is magnitude, and R is distance. An expression of this form assumes y is log-normally distributed. It further assumes that the magnitude and distance functions can be separated and arithmetically combined [32].

The definition of magnitude and distance vary with the investigator. In a number of early investigations the type of magnitude used (M_L, M_A, M_S , etc) was not defined. Thus, it was not known whether a consistent measure of magnitude was utilized, and if so, which scale was used. In cases where magnitude was not standardized, excessive scatter was exhibited or erroneous relationships developed.

Distance has been defined a number of ways:

1. Epicentral Distance
2. Hypocentral Distance
3. Distance to the causative fault
4. Distance to energy center
5. Distance to surface projection of energy center.

The measure of distance is not necessarily a limiting factor, but must be taken into consideration. For instance, in

one investigation distance is based on distance to the causative fault [61]. The data for this investigation is from California earthquakes which have a typical focal depth of 3-9 mi. If such a relationship was used for the Puget Sound area, where major earthquake focal depths are typically 25-44 mi, an adjustment would have to be made to account for the difference in focal depth. A few examples of recent investigations of attenuation of a , v , and d are references 13, 16, 23, 35, 53, 54.

The relationship between a , v and d tends to vary with magnitude and distance from the source; i.e., they tend to attenuate at different rates. Newmark [47] found that for most practical instances $ad/v^2 = 5$ to 15. High frequency ground motions tend to attenuate the most rapidly. Therefore, acceleration should attenuate more rapidly than velocity and velocity more rapidly than displacement. At great distance an earthquake vibration is similar to a sinusoidal wave, where $ad/v^2 = 1$.

This provides a fairly easy method of checking the validity of a set of a , v , and d attenuation relationships. The values of a , v and d can be calculated for different distances from the source. The ratio v/a should increase with distance, while ad/v^2 should decrease [32]. Additionally, ad/v^2 should fall between 5 and 15.

A large portion of the research effort presently being expended is focused on near-field attenuation. Although this is an important consideration in areas of shallow faulting, the depth of focus for large earthquakes in the Puget Sound area is

such that ground motion, even at the epicenter, can probably be considered outside the influence of near-field effects. Thus, near-field attenuation will not be specifically addressed.

Effects of Local Soil Conditions on Ground Motions

When discussing the effects of local soil conditions on ground motion two aspects should be considered (1) the actual ground motion amplification, and (2) effects on the response spectra. A number of investigations have been made over the last 10-15 years regarding both aspects and will be briefly discussed.

Most researchers have concluded that acceleration is the least affected by local soil conditions, while displacement exhibits the greatest amplification [13,32,69,70]. In some cases acceleration may be lower on soil sites than on rock, while velocity and displacement values are consistently higher on soil sites.

The amplification effects of soil on acceleration appears to be limited by the strength properties of the soil. At higher accelerations relatively large shear strains are induced in the soil profile, resulting in damping and thus, dissipation of energy. It has been found that the greatest acceleration soil amplification may be expected for weaker rock motions [63]. Figure 12 illustrates the relationship between acceleration in rock and acceleration for other local site conditions.

As can be seen from the figure, the degree of amplification (or damping) is related to the type of soil. Soft soils tend to

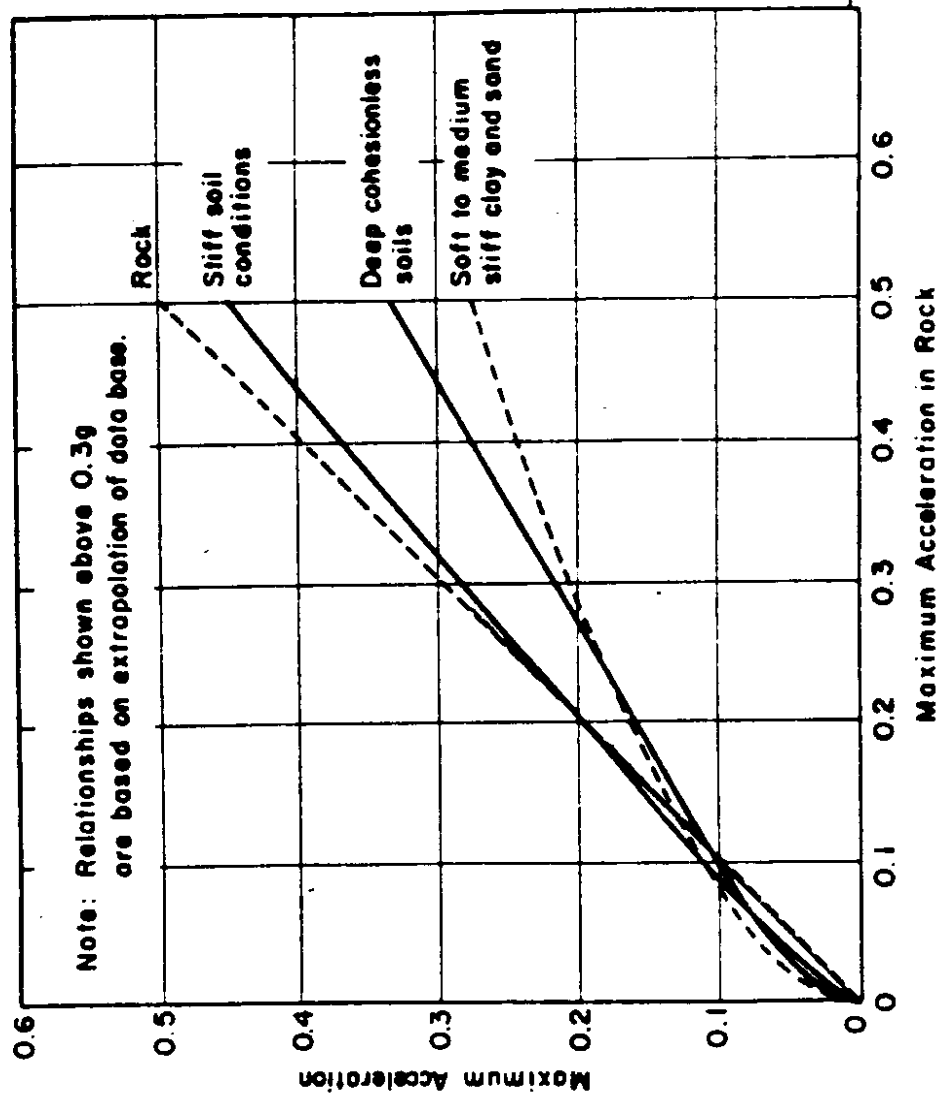


Figure 12. Approximate relationships between maximum accelerations on rock and other local site conditions. (64)

exhibit greater amplification at low accelerations and greater damping at high accelerations. Conversely, stiff soil sites produce lower amplifications at low acceleration, but less damping at higher accelerations. This same tendency of greater amplification at lower values of ground motion can also be observed in velocity and displacement, although the degree of amplification is not directly related.

When examining the increased damage potential resulting from site conditions, spectral amplification must be considered at least as important as ground motion amplification, if not more so. As previously discussed, the response spectra reflects the actual motions induced in a single-degree-of-freedom structure over a range of periods. Consequently, it is more indicative of the actual motions induced in a structure by an earthquake than is ground motion. While the modification of spectral response due to soil conditions is partially due to site amplification, it is largely the result of significant differences in the v/a and ad/v^2 ratios for different local site conditions [43].

Soil deposits tend to damp out ground motions at some frequencies and amplify in other frequency ranges. Typically soft soils damp out high frequency motions and amplify lower frequency motions. Stiff, shallow soils exhibit spectral envelopes similar to rock; peak spectral values at fairly high frequency (>5Hz), then a fairly rapid decay.

Figure 13 [64] presents typical acceleration spectral amplification curves for different site conditions. The spectral characteristics of the rock and stiff soil curves may be

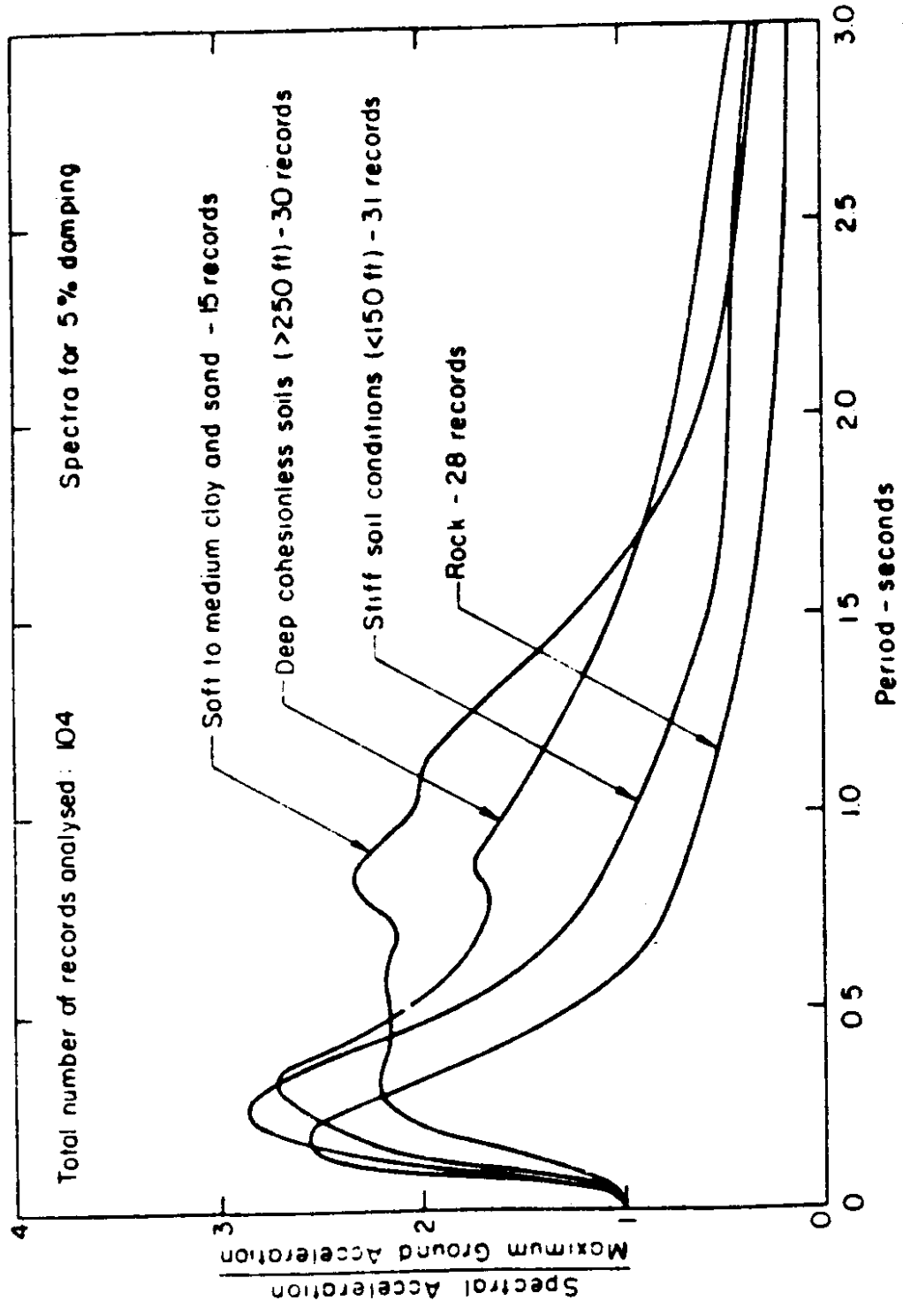


Figure 13. Average acceleration spectra for different site conditions. (64)

sufficiently similar to be represented by one curve. Such a decision was made for the ATC seismic design guides [6,9].

The frequencies at which spectral amplification occur is highly dependent on the resonant frequencies of the soil deposit. The natural period of a soil deposit is a function of the dynamic strength properties of the soil(s) and thickness of the deposit. The fundamental period of a deposit tends to increase with thickness and decrease with increasing shear modulus (G). Thus, a thick, soft soil will have a long natural period and a shallow, stiff deposit a short natural period. This concept is reflected in the previous figure.

The spectral shape is also dependent on the magnitude of the earthquake. For a given peak ground motion, the spectral response will be substantially different for a small, local earthquake than for a large, distant earthquake. In general, the local event will produce a short period peak with a fairly rapid decay. The more distant event will result in a longer period peak and slower decay. This relationship is idealized in Figure 14 and is largely the result of high frequency components of ground motion being damped out with distance from the source.

The worst case scenario of amplification results when the fundamental periods of the bedrock motion, soil deposit, and building all coincide. Such was the case in the September 19, 1985 Mexico City earthquake. Bedrock motions in Mexico City, 350 Km from the epicenter, was only ~ 0.04 g, but had an anomalous spectral peak at a period of 2 seconds. The natural period of the overlying clay deposit also has a fundamental period of

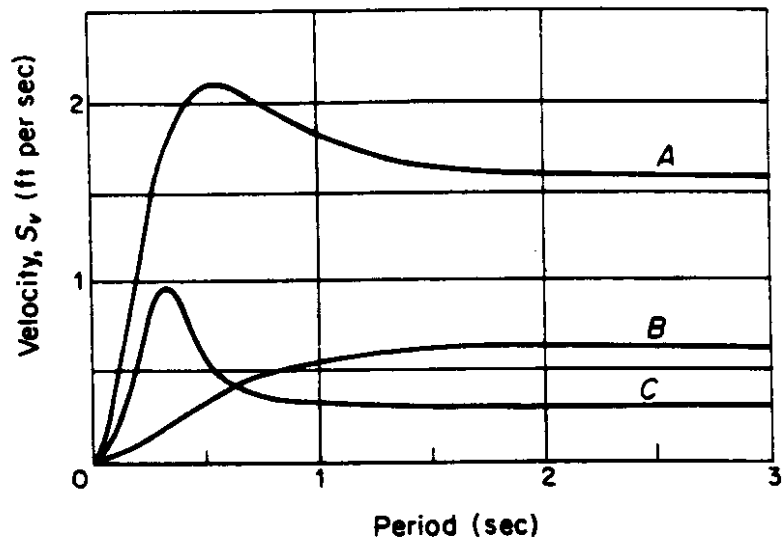


Figure 14. Idealized undamped velocity spectrum curves that illustrate the effect of magnitude and distance. Curve A, 25 mi from center of large earthquake; curve B, 70 mi from center of large shock; curve C, 8 mi from center of small ($M = 5.3$) shock.

(ref: Housner, G.W., 1970, Strong ground motion. In Wiegel, R.L. (editor), Earthquake Engineering: Prentice Hall, pp. 75-91.)

approximately 2 seconds. This produced a surface acceleration of 0.16 g, an amplification of 4X. A number of buildings in this section of the city had natural periods of approximately 2 seconds. Response spectra produced from an accelerograph located in one such building revealed a peak spectral acceleration of approximately 1 g at a period of 2 seconds. This translates to a total amplification of bedrock acceleration of approximately 25X [62].

III. SEISMIC ZONATION MAPPING

A seismic zonation map displays the spatial variation of some ground motion parameter, typically peak horizontal acceleration or intensity. The zonation process divides a region into areas or zones of similar ground-shaking potential. It is usually assumed that peak ground motions are equally likely to occur at any location within a given source zone [27].

Seismic source zones are defined based on the best available information regarding: (1) seismicity; (2) relation of seismicity to geology and tectonics; (3) the physical and temporal characteristics of the earthquake source zones; (4) ground motion attenuation; and (5) influence of local site conditions. There are two basic types of seismic source zones, line sources and point sources. A line source is used to represent an individual fault. It is usually assumed that an earthquake has an equal probability of occurrence at any location along the fault. A point source is often used in areas of more diffuse seismicity, or areas where historic seismicity cannot be associated with a specific tectonic structure.

History of Seismic Zoning--National Maps

Seismic zonation mapping may be considered in its infancy, with a history of only 50 years. The progress of seismic zonation mapping is closely related to the progress being made in understanding the physical processes resulting from an earthquake

event. It has only been within the last 10-15 years that a sufficient data base of strong motion records have been available for statistical analysis.

Even though substantial progress has been made, a great deal of controversy still exists in the characterization of ground motion resulting from an earthquake event. Important considerations such as attenuation (particularly in the near-field), local site conditions, source characteristics and, the temporal distribution of events, defy simple quantification. Consequently, a great deal of disagreement still exists concerning the specification of ground motion for engineering design and the validity of seismic zonation in general.

As more ground motion data are collected and more insight is gained into the parameters governing the seismic response for a given source-path-site it may be expected that the concepts utilized in seismic zonation will also change or evolve. This evolution will probably not be restricted to methodology, but should include changes in the ground motion parameters specified. It is well accepted that spectral response is more indicative of potential earthquake damage than peak acceleration. Thus, seismic zonation maps displaying spectral acceleration or velocity for a range of building periods, with consideration given to local site conditions, may be expected in the future [27].

The first national earthquake zonation map was published in 1948 [71]. It divided the United States into zones numbered 0 to 3 with 3 indicating the greatest damage potential. The map was

incorporated into the Uniform Building Code (UBC) in 1949 and remained in use until 1970. In 1970 an improved map (Figure 15) using the same general divisions (0 to 3), but based on additional data, was substituted into the UBC [1]. In 1976 portions of zone 3 were redefined as zone 4, indicating greater damage potential for some areas in California. The increased risk was based on greater frequency of occurrence and greater maximum magnitude [27].

In 1976 Algermissen and Perkins [3] published a national seismic zonation map that was a large step forward in both concept and detail. Previous maps were based on maximum intensity for some intensity scale, primarily Modified Mercalli, while Algermissen and Perkins' map presented peak acceleration values with a 90 percent probability of nonexceedence in a 50 year period. The map defined 71 seismic source zones, providing a much improved basis for engineering design than previous attempts.

In 1978 the Applied Technology Council (ATC) produced two new ground-shaking maps [9]. These maps were largely based on the map developed by Algermissen and Perkins, but the ground motion parameters were defined differently. Two separate ground motion parameters, Effective Peak Acceleration (EPA) and Effective Peak Velocity (EPV), were defined based on spectral acceleration and spectral velocity rather than actual peak accelerations and velocities. Even so, ground motion contours appear similar to those developed by Algermissen and Perkins with the exception of lower maximum accelerations in California in the

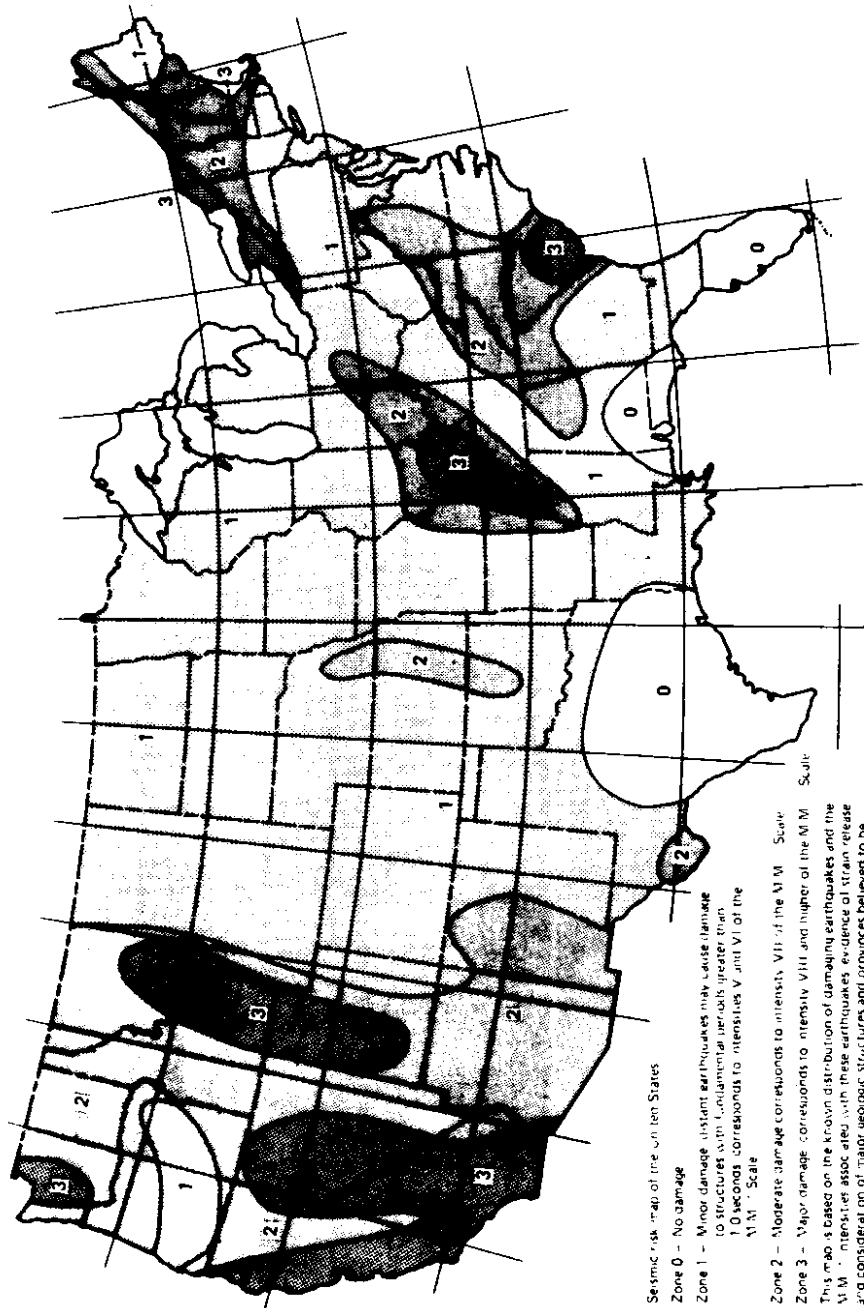


Figure 15. Seismic risk map of the United States. (1)

ATC report. The ATC report will be discussed in greater detail in a subsequent section.

Although the 1976 Algermissen and Perkins map was a great improvement over previous attempts, it was perceived to have three major shortcomings [5]: 1) limited incorporation of geologic information in the generalization of the seismic history, 2) ground motions defined for only one level of probability, and 3) ground motion defined only in terms of acceleration. In 1982, Algermissen and others [5] published a new set of maps in response to these criticisms. The new maps display peak values of acceleration and velocity on rock for exposure periods of 10, 50, and 250 years, with a 90% probability of nonexceedence. Additionally, improved information with respect to geologic information and earthquake records provided greater consistency and detail in the zonation process. The total number of zones were more than doubled, from 71 to 174. Although there is still room for improvement, this is by far the best national zonation map presently in print.

Seismic Zonation--Theory and Methodology

Over the history of seismic zonation mapping two types of maps have been constructed. The first type relies on the history of past earthquake effects, typically in terms of intensity. It is then assumed that future earthquakes will produce similar effects. Most of the early zonation maps used this approach. The second type utilizes probabilistic concepts, extrapolating ground motions from past earthquakes and potential earthquake

sources [27]. Although the first method still has applicability, particularly in areas lacking sufficient earthquake records to provide a valid statistical sampling, most recent zonation work has concentrated on the probabilistic approach. Consequently, only the probabilistic approach will be discussed herein.

Although the methods used for the probabilistic approach to seismic zonation differ slightly with the investigator, the basic methodology is similar. The concepts presented below are based on the work of Algermissen and others [5] and may differ slightly from other investigators.

A basic assumption of probabilistic hazard mapping is that earthquakes are exponentially distributed with respect to magnitude and randomly distributed in time. The time distribution is assumed to be Poissonian, which has been found to be fairly accurate for larger shocks. Since small shocks are not of particular interest for engineering purposes, the assumption of a Poisson distribution is considered a good approximation.

There are three primary steps involved in the development of a probabilistic ground motion map: 1) delineation of seismic source zones; 2) development of statistical relationships from the historic earthquake record in each zone; and 3) calculation and mapping of the extreme cumulative probability, F_{\max} , $t(a)$, of ground motion, a , for time, t . This procedure is illustrated in Figure 16, and discussed in the following paragraphs.

Earthquakes within a given seismic source zone can be modeled in three different ways: (Figure 16A) 1) point sources in areas, used to represent earthquakes resulting from short

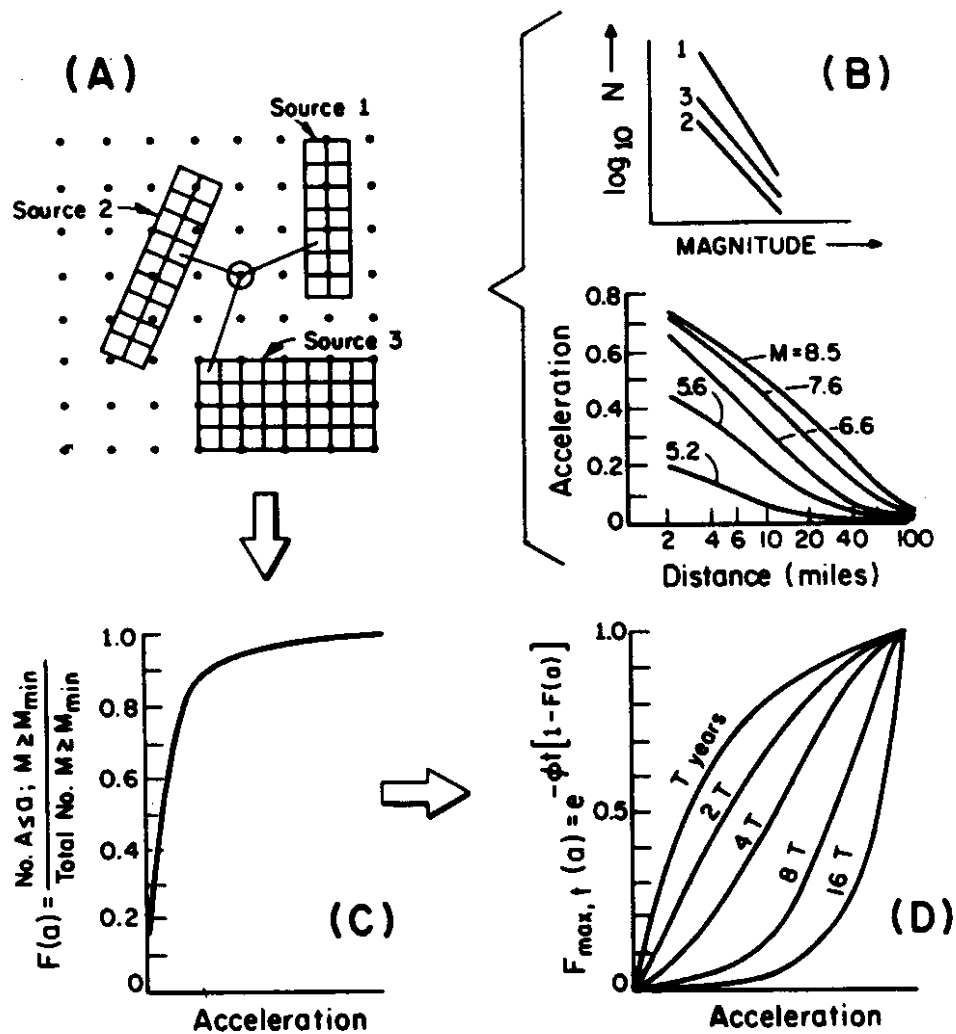


Figure 16. (5)
Elements of the hazard calculation:

- Typical source areas and grid of points at which the hazard is to be computed.
- Statistical analysis of seismicity data and typical attenuation curves.
- Cumulative conditional probability distribution of acceleration.
- The extreme probability $F_{\max, t}(a)$ for various accelerations and exposure times (T).

fault ruptures, or areas of diffuse seismicity; 2) finite rupture length (i.e., line sources); or (3) a mixed source. The boundaries of a source zone are defined based on historic seismicity and the interpretation of available geologic and tectonic evidence where possible.

Once the source zone has been delineated, the magnitude recurrence relationships are defined, using the form:

$$\log N = a - b M$$

for each source zone, where N is the number of earthquakes in a predetermined magnitude range, M , per unit time with a and b being regression constants (Figure 16B). The spacial occurrence of future activity is assumed to be uniform within a given source zone. Thus, if the source zone is divided into n subzones and the number of occurrences for a given magnitude range is N , the number of earthquakes likely to occur in each subdivision, n , for the given magnitude range is

$$\frac{N}{n}$$

After determining the distribution of earthquakes likely to occur in each subdivision of the source zone or line source, the ground motion at a number of sites, usually on a regular grid spacing, is calculated. This is accomplished by attenuating the ground motions resulting from each subdivision, utilizing attenuation relationships such as those presented in Figure 16B.

The influence of the different source zones produces a distribution of ground motion at each grid point. This information can then be used to directly determine the number of

times a specific amplitude of ground motion may be expected to occur for a given period of time, at a specific location, for a given probability of occurrence. The process is briefly explained in the following development.

First, the cumulative conditional probability distribution, $F(a)$, of the desired ground motion parameter, such as acceleration, is calculated (Figure 16C).

$$F(a) = P [A \leq a / M \geq M_{\min}]$$

or

$$F(a) = \frac{\text{expected number of occurrences with } A \leq a \text{ and } M \geq M_{\min}}{\text{total expected number of occurrences } [M \geq M_{\min}]}$$

where a equals the maximum value, and A is equal to the observed value. M_{\min} is some predetermined minimum magnitude.

The peak ground motion corresponding to some extreme probability, $F_{\max,t}(a)$, is calculated for different exposure times (Figure 16D). The extreme probability function $F_{\max,t}(a)$ is defined as:

$$F_{\max,t}(a) = e^{-\hat{U}t[1-F(a)]}$$

where \hat{U} = the mean rate of occurrence

t = the exposure time

$F(a)$ = cumulative probability function

A table of ground motion vs $F_{\max,t}(a)$ is then constructed for the exposure times of interest, such as in Figure 16D. The value of ground motion for a given extreme probability, such as $F_{\max,t}(a) = .90$ can then be determined at each location.

The extreme probability may also be defined as:

$$F_{\max,t}(a) = e^{-t/Ry(a)}$$

where $Ry(a)$ is equal to the return period in years and can be defined as

$$Ry(a) = \frac{1}{[1-F(a)][\text{Expected number of events per year } (M > M_{\min})]}$$

solving for $Ry(a)$,

$$Ry(a) = -\frac{t}{\ln[F_{\max,t}(a)]}$$

As an example, for an extreme probability of 0.90, and an exposure time of 10 years,

$$Ry(a) = -\frac{10}{-.1054} = 94.9 \text{ years}$$

Thus, for an extreme probability of 0.90 and an exposure time of 10 years, the average return period is approximately 95 years. Similarly, for the same extreme probability with exposure times of 50 and 250 years the average return periods are 474 and 2372 years respectively.

As a point of interest it might be valuable to calculate the probability of exceedence when the exposure time is equal to the return period,

$$t = Ry(a)$$

$$F_{\max,t}(a) = e^{-1} = 0.37$$

the probability of exceedence is equal to

$$1 - F_{\max,t}(a) = 1 - 0.37 = 0.63$$

Thus a ground motion has a 63% probability of exceedence over an exposure time equal to the return period.

Once the $F_{\max,t}(a)$ function has been defined at each grid point for the exposure periods of interest, ground motion values for the desired extreme probability and exposure time may be calculated. The ground motion values are then contoured, producing isoseismal lines.

Seismic Zonation Maps Applicable to Washington State

Prior to evaluating the applicability of specific seismic zonation studies to the present investigation, the problems associated with seismic zonation in Washington State require some discussion. Both seismicity and population in Washington is concentrated within the Puget Sound region. As a result, the majority of seismic zonation studies have concentrated on this area.

A number of difficulties exist in the description of ground motion resulting from earthquake activity in the Puget Sound Region. Problems include: 1) delineation of seismic source zones; 2) definition of attenuation relationships; and 3) describing the effects of overlying soil deposits on bedrock motion. The inability to solve these problems is partially due to the natural scatter in ground motion data produced by earthquakes, but is amplified by the relative lack of ground motion data and surface faulting in the Puget Sound region.

In California, the higher rate of seismicity and greater concentration of strong motion recording devices have produced a large number of earthquake records. These records can usually be associated with specific faults, making the definition of seismic

sources and associated attenuation relationships easier to define.

Strong motion data for the Puget Sound region is limited to recordings from the 1949 and 1965 earthquakes (3 recording sites each). Additionally, the deep focus of the events increase the impact of subsurface geology on attenuation. The horst-graben structure underlying the region is believed to produce focusing of seismic waves [33]. Focusing may amplify ground motions far beyond normal site effects. With only limited data, the determination of an attenuation relationship for surface ground motions is extremely difficult and for bedrock motion is nearly impossible.

These problems are evidenced in the accelerogram recordings from the 1965 Puget Sound earthquake. Table 1 lists the peak acceleration values and epicentral distances from the earthquake for the three local accelerograph sites. Peak acceleration of the Tacoma site was approximately 2 times greater than the next highest value, even though it was over twice as far from the epicenter. This discrepancy cannot be explained by a simple attenuation relationship.

Due to the difficulty of developing an attenuation relationship based on the limited and contradictory strong motion data available for the Puget Sound, most attenuation relationships specific to the area are based on intensity data [15,58,76]. In all cases scatter of several intensity units are present for a given epicentral distance. Thus, a great deal of

TABLE 1
PEAK ACCELERATIONS AND EPICENTRAL DISTANCES FOR THREE PUGET SOUND
STRONG MOTION RECORDERS DURING THE APRIL 1965 EARTHQUAKE [37]

| <u>Location</u> | <u>Epicentral Distance (mi)</u> | <u>Peak Acceleration (cm/s²)</u> |
|-----------------|---------------------------------|---|
| Olympia | 43 | 194.3 |
| Tacoma | 11 | 55.9 |
| Seattle | 14 | 104.0 |

judgment is required in selecting a design intensity value for any distance from the source.

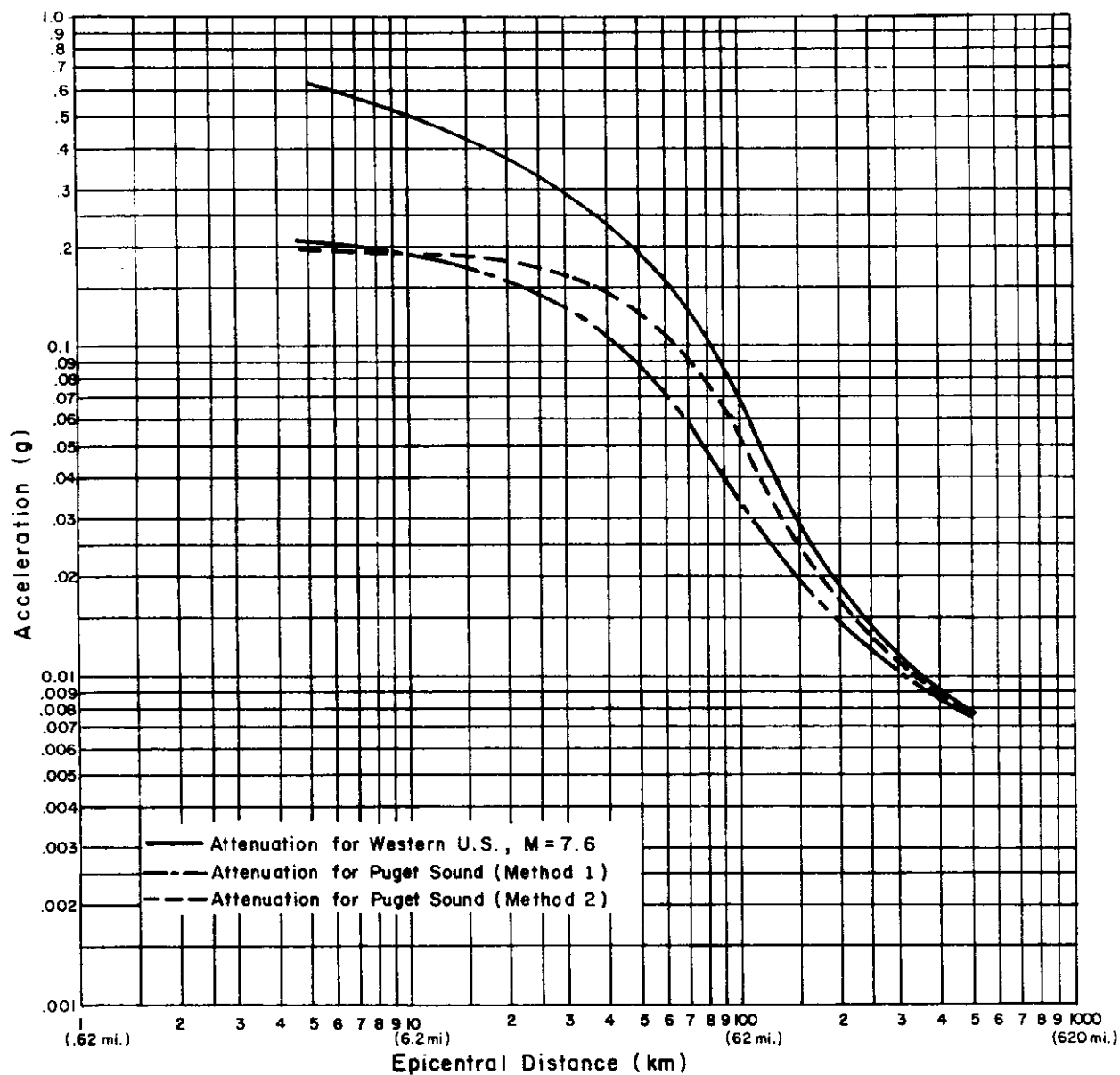
Another problem associated with the use of intensity in defining ground motion relates to how the ground motion values are used in analysis. In order to utilize the basic design procedure set forth in the ATC guidelines, acceleration and/or velocity on bedrock or firm ground is required. Although a number of relationships have been developed between intensity and acceleration, it is questionable how direct a relationship actually exists. Modified Mercalli Intensity in the range of ground motion important for engineering purposes is primarily based on building response to ground shaking. Thus, it is probably more closely related to spectral acceleration (or velocity) than ground acceleration, at least for structures with periods greater than 0.1 second.

Since attenuation relationships based on Puget Sound data is tenuous at best, many investigators have used modified relationships from California [3,5,6,9,65]. Modification is usually limited to a reduction in acceleration based on the difference in focal depth between California and Puget Sound earthquakes. Focal depths for California earthquakes are typically between 3 and 9 mi while the depth of focus for the Puget Sound events of interest range between 25 and 44 mi.

Figure 17 illustrates two methods of modifying an attenuation curve based on California earthquakes. In the first method the mean depth of focus for California and Puget Sound earthquakes are assumed to be 6 and 31 mi respectively, yielding

Figure 17

Attenuation Curve development for the Puget Sound Region



a difference of 25 mi. The peak acceleration at the epicenter of a Puget Sound event is assumed to be equal to peak acceleration at a distance of 25 mi from a California event. Peak acceleration at distance is determined from the California attenuation curve as the peak acceleration at the desired distance plus 25 mi, e.g., peak acceleration at an epicentral distance of 25 mi in the Puget Sound would be equal to a peak acceleration at 50 mi from California.

The second method uses an equivalent hypocentral distance to determine peak acceleration. Again, an average depth of focus is assumed for California and Puget Sound events. Acceleration attenuation for the Puget Sound area is then calculated by setting the hypocentral distances equal. In the second method the same focal depths were used as in method I, 6 and 31 mi for California and the Puget Sound events respectively. As an example, for an epicentral distance of 37 mi in the Puget Sound region, the peak acceleration value from the California curve would be taken at a distance of:

$$\sqrt{37^2 + 31^2 - 6^2} = 47.8 \text{ mi}$$

and so on.

As the figure demonstrates, a great deal of discrepancy is evident close to the epicenter, but the curves converge with distance from the source. Due to the lack of data it is difficult to determine which method provides the most accurate answer. However, an equivalent hypocentral distance seems more intuitively correct.

Rasmussen and others (1975)

The first concerted effort to evaluate the seismic hazard of the Puget Sound area was made in 1975 [58]. The result cannot be considered a seismic zonation map due to the format used in the study. However, it does allow for the consideration of site conditions, probability of occurrence (return rate), and ground motion. The study was based on the records of 12 earthquakes originating in the Puget Sound area. Relationships were developed for intensity attenuation, acceleration versus intensity, intensity versus magnitude, earthquake frequency, and site conditions. Although 12 earthquakes are not considered a sufficient sampling for most forms of statistical analysis, the author's felt the events used provided the most reliable data.

Intensity attenuation relationships were developed for both shallow (12-25 mi) and deep (25-37 mi) focus events. Relationships were developed for different magnitudes in each depth range, $M = 5.5, 6.0,$ and 6.5 for shallow earthquakes and $M = 6.5, 7.0,$ and 7.5 for deeper events. Attenuation was presented in the form of upper and lower bounds for each magnitude. Figure 18 presents the attenuation curves for deep focus events. Notice the large variation in intensity for any given epicentral distance and magnitude.

In order to define a single intensity value at a given distance from the epicenter a weighting factor, termed the Average Intensity Function, F , was defined as:

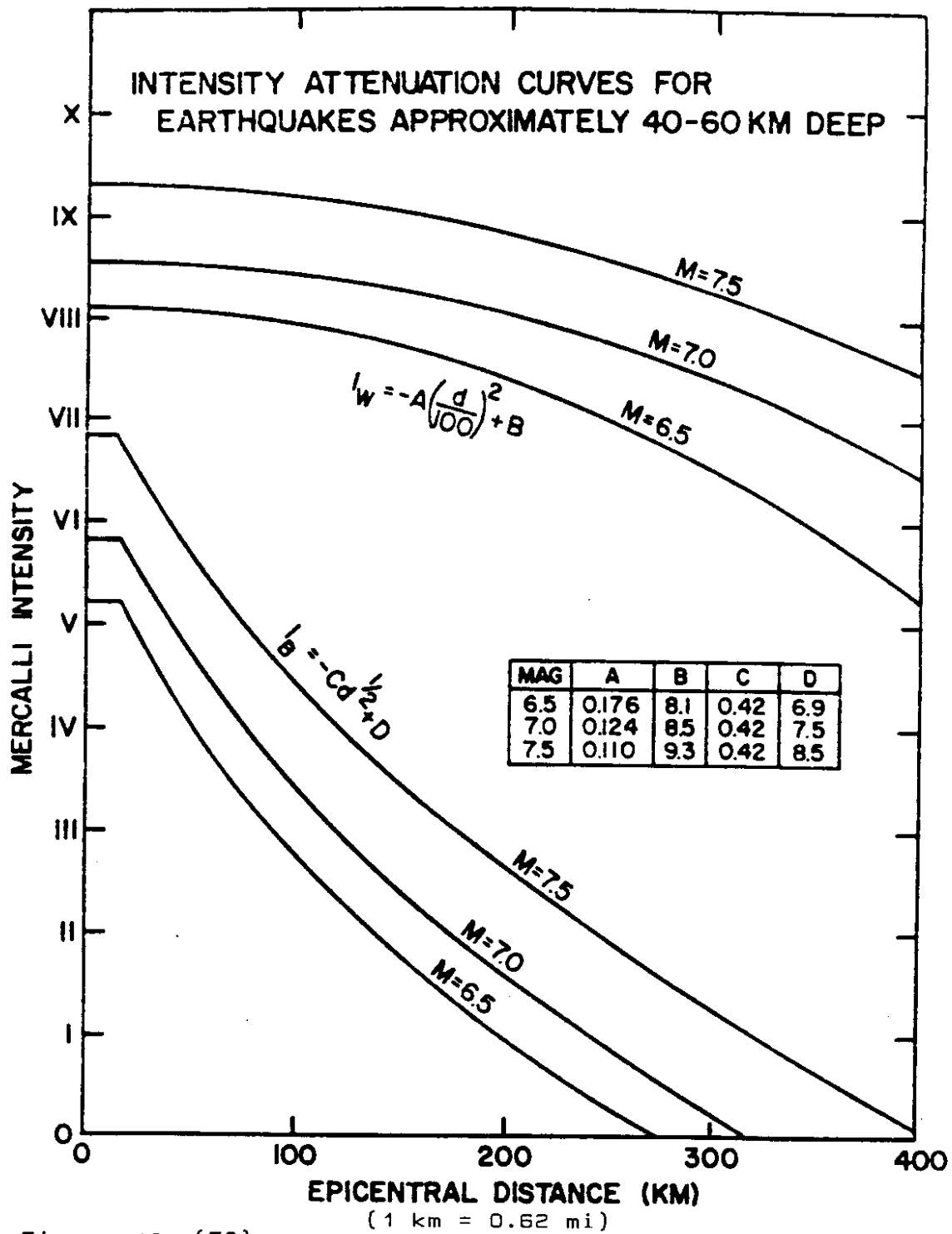


Figure 18. (58)

$$F = \frac{I - I_B}{I_w - I_B}$$

where

I = site intensity

I_B = lower bound intensity

I_w = upper bound intensity

and was assumed to be directly related to the site geology. All soils in the study area were then placed in three groups based on county soil maps and assigned F values. Soils were grouped as follows:

Unit I: compact to moderately compact glacial tills,
(F = 0.55)

Unit II: well drained to moderately well drained
alluvium and outwash (F = 0.65)

Unit III: poorly drained to impervious alluvium and
organic soils which are saturated most of the
year, artificial fill is included in this
group (F = 0.80)

The method used to determine F for the different soil units was not specified.

The equation can be rewritten $I = I_B + F[I_w - I_B]$. Thus, given the earthquake magnitude, distance from the epicenter, and soil type, a site intensity can be determined. The intensity can be converted to acceleration using the relationship provided by the authors.

The author's compared observed intensities from the 1965 earthquake to calculated intensities using the above method. Eighty-six percent of the calculated intensities were within one intensity unit of the observed values. Although the method seems to provide a reasonable approximation of intensity once a source has been chosen, it presents some problems with regard to the design procedure under consideration and the scale of their study.

First, the study only considers the Puget Sound region. Even if this study could be adapted to the AASHTO design procedure, another seismic zonation map would be required for the rest of the state. Use of this procedure should only be considered if it presents a substantial improvement over seismic zonation maps that address seismicity over the entire state.

The primary difficulty in applying the Rasmussen and other's [58] approach is how well the resulting ground motion parameter conforms to the acceleration coefficient utilized in the AASHTO guidelines. Although an argument can be made against the use of intensity data to estimate acceleration, the main problem relates to the probabilistic nature of the AASHTO coefficients and the inability to produce similar values using Rasmussen and other's [58] approach.

The AASHTO guidelines utilized a probabilistic analysis similar to the presented in the preceding section. Each seismic source zone is divided into subzones. Probabilistic ground motions are then determined over a number of grid points, based

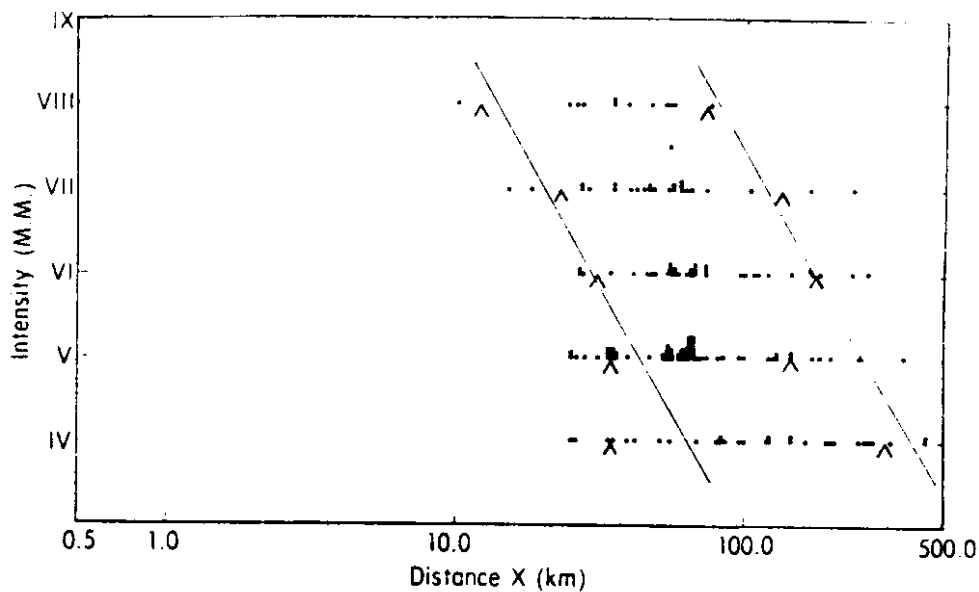
on the relative influence of each subzone, for a given exposure period and probability of exceedence.

Rasmussen and other's [58] method requires the user to define the earthquake's location and then determine site intensity based on attenuation and site conditions. It does not address the probabilistic aspects of the assumption that an earthquake is equally likely to occur anywhere within the seismic source zone. Nor does it consider any possible influence from other source zones outside the study area.

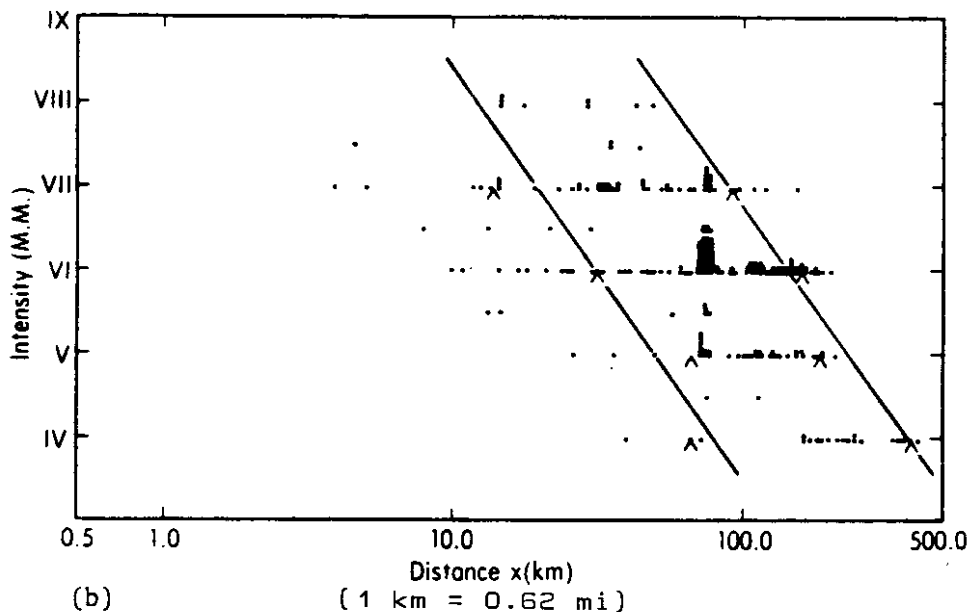
U.S.G.S. Open-File Report 75-375 (1975)

In 1975 the U.S. Geological Survey published a study of earthquake losses in the Puget Sound region based on two hypothetical earthquakes. Both events were assumed to have a magnitude of 7.5 and focal depth of 50 Km. One event was assigned an epicentral location identical to the 1949 earthquake. The other event was located just east of downtown Seattle.

The maps display areas of equal intensity based on attenuation from the source and local soil conditions. Geologic units were grouped into four divisions: 1) alluvium over 15 m deep; 2) overconsolidated material; 3) bedrock; and 4) normally consolidated material. Geologic maps were used to place each geologic unit into one of the above groupings for the area of interest. Attenuation curves were then developed for each group based on intensity data from previous earthquakes. Figure 20 shows intensity attenuation for two of the geologic groupings.



(a)



(b)

Figure 19. Attenuation of intensity with epicentral distance. Each dot represents a reported intensity (a) on overconsolidated material for the April 13, 1949 earthquake or (b) on normally consolidated material for the April 29, 1965 earthquake. Clumps of dots appear where there were numerous reports, as from a large city. Eighty percent of the dots on a line lie between the pointers, and 10 percent on either side. (76)

Due to the large data scatter, 10% pointers were used to bound the majority of data points. Intensity attenuation was calculated using the average distance between pointers.

Since magnitudes were not the same for the earthquakes of record as for the hypothetical events the intensity values had to be modified to account for the disparity. Modification was accomplished using a magnitude vs intensity relationship developed from past Puget Sound events. The attenuation curves based on the real earthquakes were raised by the change in intensity caused by the increased magnitude of the hypothetical events. The attenuation curves based on the 1949 earthquake were used for the hypothetical event placed at the same epicentral location while attenuation curves generated from the 1965 Seattle event were used to calculate intensities for the near-Seattle hypothetical earthquake.

Maps were produced that displayed intensity over the whole study area. Additionally, more detailed maps for some of the higher population areas were constructed. Figures 20, 21 and 22 are provided as examples.

Although the study has to be considered an improvement over the previous investigation [58] since a seismic zonation map was produced, it suffers from many of the same drawbacks with regard to probabilistic analysis. Since each map displays intensities resulting from a single event, the ground motion values do not represent a probability of occurrence compatible with the AASHTO guidelines. Such a map would require a moving epicenter and a probabilistic analysis of the resulting ground motions for

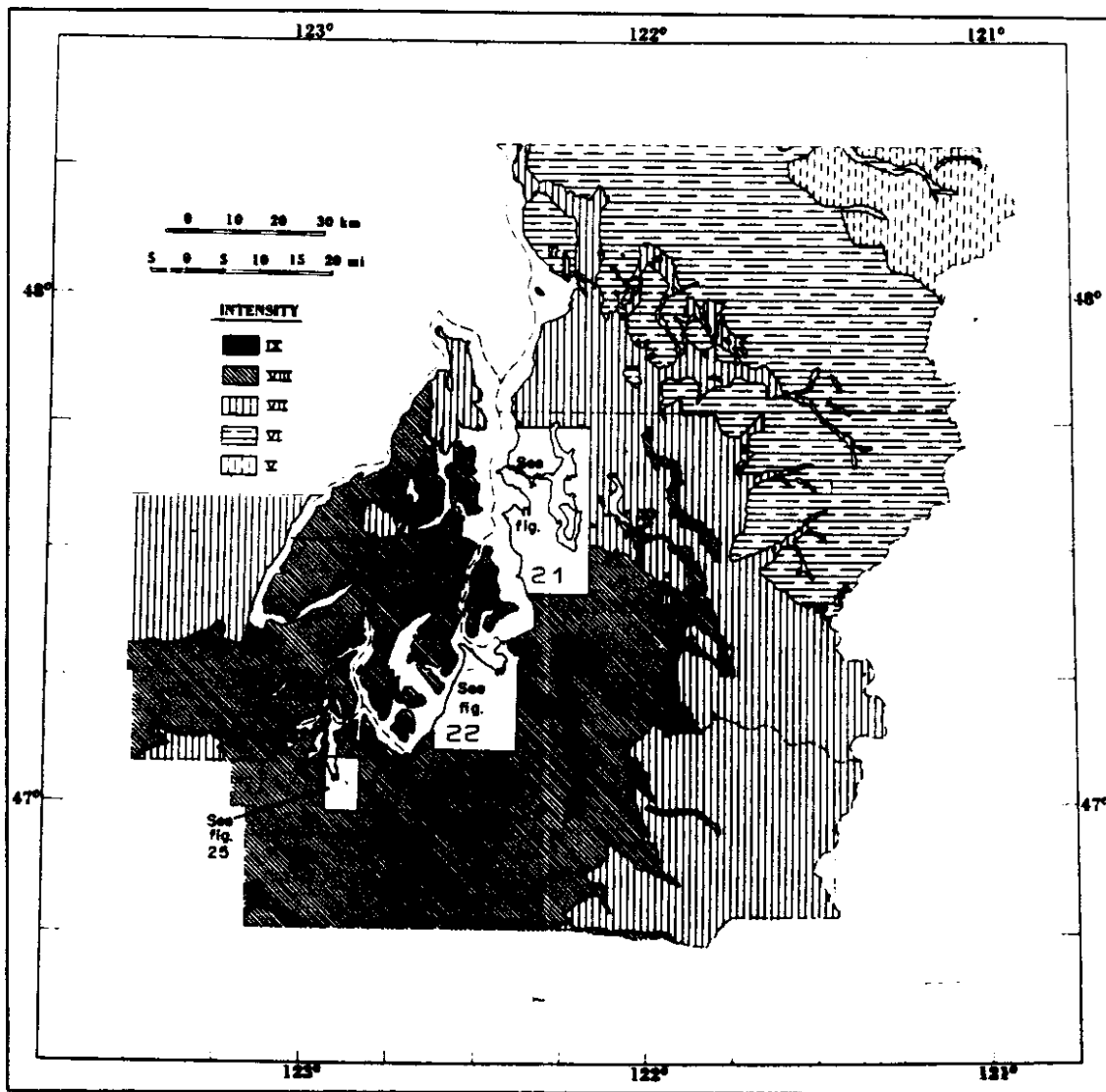


Figure 20.--Map showing estimated Modified Mercalli intensity distribution in Snohomish, King, Pierce, Thurston, Mason, and Kitsap counties for a projected earthquake of magnitude 7.5 located at 47°06' N, 122° 42' W, 50 km (31 mi) deep. (76)

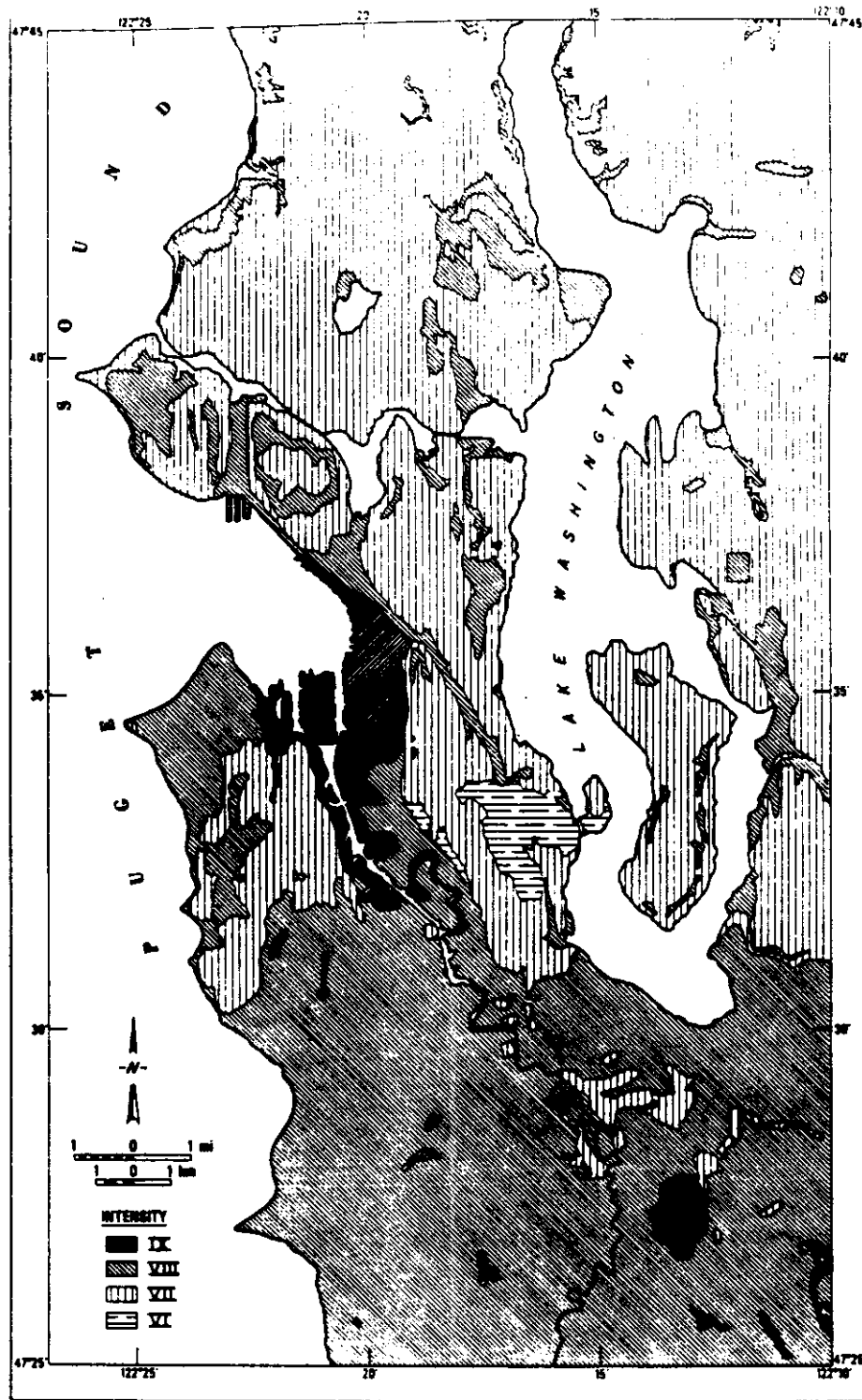


Figure 21. Map showing estimated Modified Mercalli intensity distribution in Seattle for a projected earthquake of magnitude 7.5 located at $47^{\circ}06' N$, $122^{\circ}42' W$, 50 km (31 mi) deep. (76)

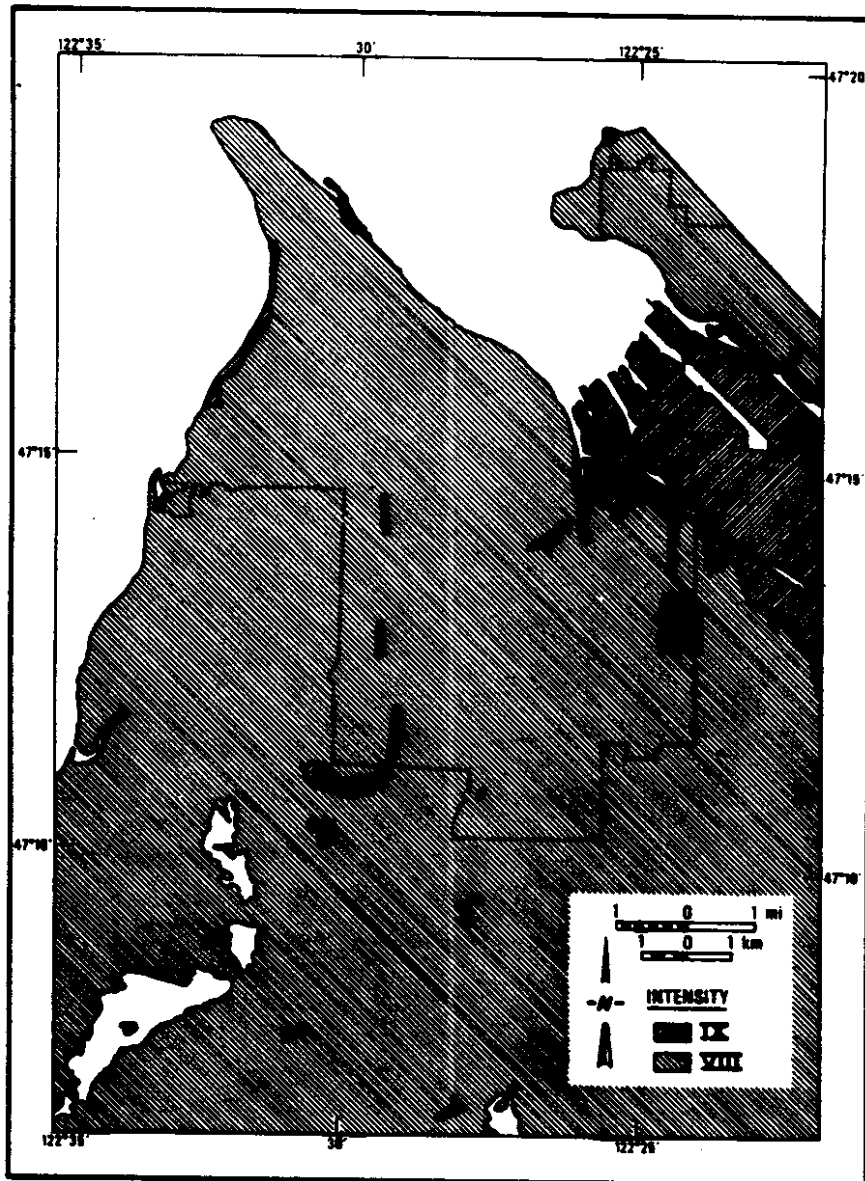


Figure 22 --Map showing estimated Modified Mercalli intensity distribution in Tacoma for a projected earthquake of magnitude 7.5 located at 47°06' N, 122°42' W, 50 km (31 mi) deep. (76)

different earthquake locations throughout the study area. The attenuation relationships are based on single events, which probably provides the most accurate approach for an event with a similar hypocenter and magnitude. However, it does not consider the magnitude dependence of attenuation or the natural variation in ground motion for similar source mechanisms. Since earthquake data for the Puget Sound is limited, it is difficult to accurately define the magnitude dependence, although data from other local events could be used to produce an average regional attenuation value.

The scale of the investigation presents the same problem as the previous study in that a separate map would be required for ground motions outside the study area and the influence from other seismic source zones is not considered.

Algermissen and Perkins, 1976

The 1976 Algermissen and Perkins study [3] generated the first national seismic zonation map that applied the probabilistic concepts outlined in the previous section. The map has been superseded by the more detailed 1982 version [5]. However, it laid the foundation for the 1982 version and was a major influence on the development of the ATC and AASHTO maps, and therefore will be discussed here.

Seismicity in the contiguous United States was defined by 71 seismic source zones. Although an effort was made to incorporate geologic data into the delineation of source zones, historic seismicity was the primary zonation criteria. Source zones for

the western U.S. are displayed in Figure 23. Attenuation for the western U.S. was based on curves by Schnabel and Seed [61]. An exception to this was the Puget Sound region where separate attenuation curves were developed to account for the deeper focal depth [4]. Separate attenuation curves were also used for the Eastern United States, reflecting lower attenuation in that part of the country.

The probabilistic analysis followed the methodology briefly described previously. A single seismic zonation map was published that displayed peak acceleration in rock. The probability of nonexceedence was 90% for an exposure period of 50 years, or a return period of approximately 500 years. The seismic hazard map is presented in Figure 24.

This effort was quite an improvement over previous attempts at national seismic zonation mapping. It provided peak acceleration values for an equal probability of occurrence throughout the U.S., something that had not been attempted previously. Ground motion was presented in terms of acceleration, which could be used more directly in design calculations, making its use more desirable to design engineers than maps depicting ground motion in terms of intensity.

Although the map was a large improvement over previous attempts, it was perceived to have three major shortcomings [5]: 1) lack of sufficient geologic input in the delineation of seismic source zones; 2) presented in terms of only one level of probability; and 3) the seismic hazard presented only in terms of one ground motion parameter, acceleration. As will be seen when

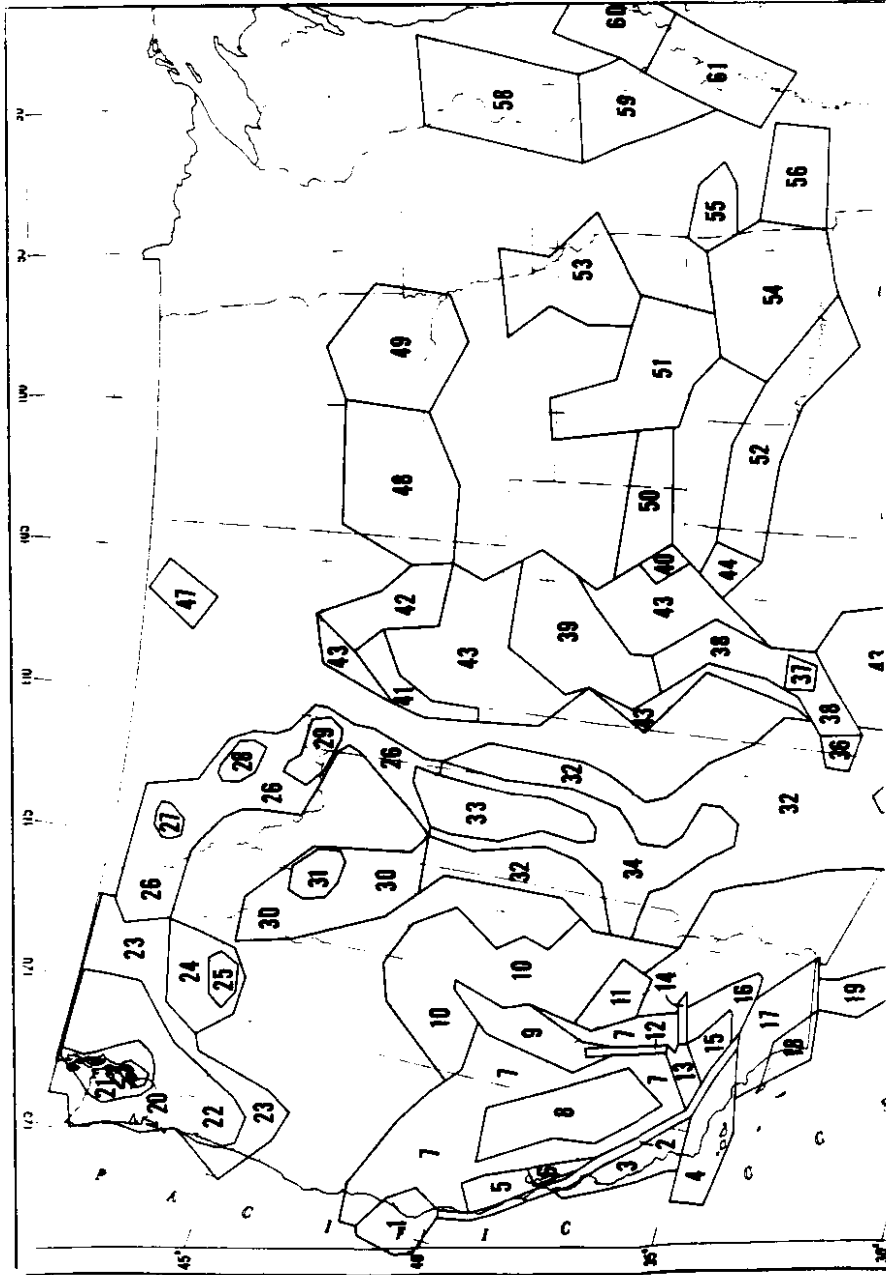


Figure 23. Seismic source areas for the western part of the United States. (3)

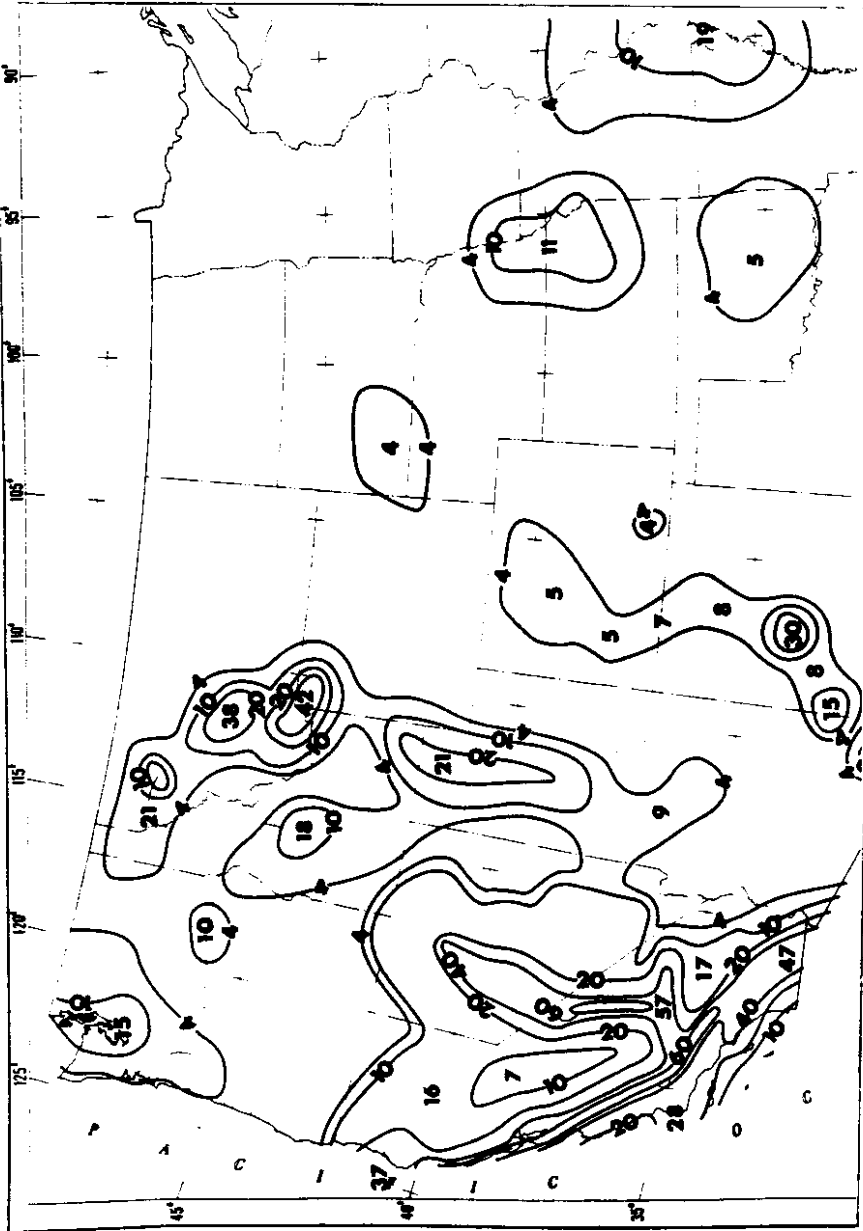


Figure 24. Preliminary map of horizontal acceleration (expressed as percent of gravity) in rock with 90 percent probability of not being exceeded in 50 years. (3)

discussing more recent seismic zonation maps, these problems were addressed and at least partially solved in subsequent efforts [5,56].

ATC Tentative Guidelines for the
Seismic Design of Buildings, 1978

In 1978 the Applied Technology Council (ATC) published tentative guidelines for the seismic designing of buildings [9]. A simplified version of these guidelines was adopted in 1983 by AASHTO for the design of highway bridges [6]. The AASHTO guidelines are presently being employed by WSDOT and thus the original work deserves careful consideration.

The ATC guide specifications for the seismic design of buildings addresses both the geotechnical and structural aspects of seismic design. However, only the geotechnical considerations may be addressed within the scope of the present investigation. They include: (1) the selection of ground motion, (2) the effects of soil site conditions, and (3) the calculation of the spectral design acceleration coefficient.

Selection of Ground Motion Parameters

Two parameters were used to describe ground motion, Effective Peak Acceleration (EPA) and Effective Peak Velocity (EPV). These parameters do not have a direct physical relationship to actual ground motion, but are related to spectral

response [49]. The values are back calculated from a smoothed response spectra assuming a constant of proportionality for ground and spectral acceleration between periods of 0.1 and 0.5 seconds, and for ground and spectral velocities at a period of approximately 1 second. In both cases the constant is assumed to be 2.5 (at 5% damping) i.e.,

$$\text{EPA} = \frac{S_a}{2.5}$$

and

$$\text{EPV} = \frac{S_v}{2.5}$$

where

S_a = spectral acceleration

S_v = spectral velocity

The method of obtaining EPA and EPV from a response spectrum is illustrated in Figure 25.

The EPA and EPV values are related to, but not necessarily equal or even proportional to, peak acceleration and velocity. The EPA and EPV may be either greater or less than peak acceleration or velocity, but generally EPA is smaller than peak acceleration while EPV is usually larger than peak velocity.

The map produced of EPA (shown later) is primarily based on the map developed by Algermissen and Perkins [3]. With the exception of the difference between EPA and peak acceleration, the primary conceptual difference between the two maps is the Algermissen-Perkins map displays acceleration on rock while the ATC map is for EPA on "firm ground." Firm ground includes

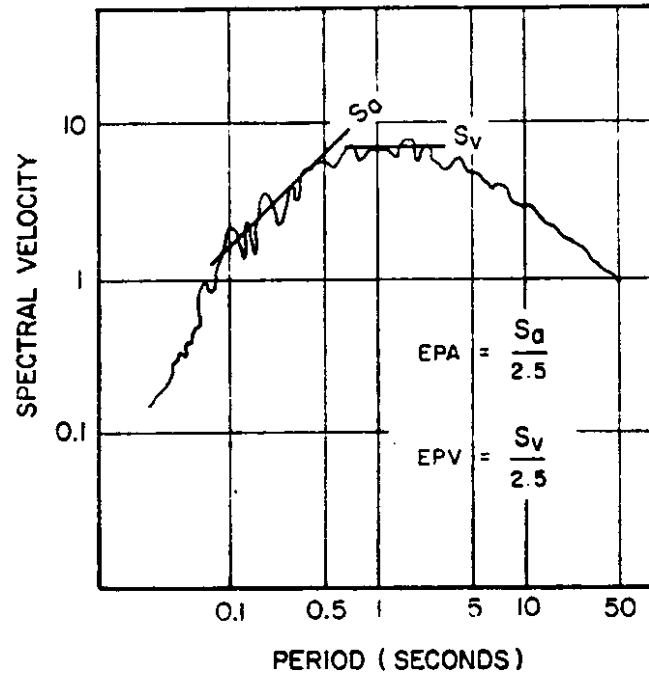


Figure 25.
 SCHEMATIC REPRESENTATION
 SHOWING HOW EFFECTIVE PEAK ACCELERATION
 AND EFFECTIVE PEAK VELOCITY
 ARE OBTAINED FROM A RESPONSE SPECTRUM (9)

shallow, stiff soils in addition to rock. Acceleration contours from the Algermissen-Perkins map were adjusted to account for these differences in concept by a committee of experts. Construction by committee produced contours of EPA that do not attain the same degree of consistency with respect to seismic source zones as the Algermissen-Perkins map. However, the committee felt it provided the best estimate of EPA possible given the available information.

The development of EPV is not as straight forward as EPA. At the time of development, a national map of peak velocity was not available. As a result, EPV is based on EPA, or more precisely the EPV is required to construct the smoothed elastic response spectrum for a given EPA. For example, if $EPA = 0.4g$ then $EPV = 12 \text{ in/s}$ is required.

The above method was used to calculate the maximum EPV from the highest EPA contour in an area. The EPV was then attenuated based on an empirical relationship developed by McGuire [39] for earthquakes in California. He found that EPV decreased by a factor of 2 at approximately 80 miles from the source. Thus, a contour of $EPV = 1/2 EPV_{\max}$ was placed 80 miles from the highest EPV contour in a given region. This velocity attenuation relationship is based on data valid to approximately 100 miles. However, the same attenuation rate was used for greater distances based on intensity attenuation data [9].

In order to utilize EPV in the design equations (yet to be presented) it had to be expressed in terms of a dimensionless acceleration coefficient, A_v , referred to as the "velocity-

related acceleration coefficient." The acceleration coefficient was calculated assuming a ratio of $EPV(\text{in/s})/A_v(\text{g}) = 30$. Thus, for $EPV = 12 \text{ in/s}$, $A_v = 0.4 \text{ g}$, a reasonable ratio when compared to v/a ratios from other sources [32,40,69].

The national maps for EPA, also referred to as A_a , and A_v are presented in Figures 26 and 27. If the two maps are compared the construction method utilized for A_v is easily visualized. The highest contours of A_a and A_v in an area are identical. Subsequent contours are generally more distant from the source for A_v than A_a . In no cases do A_v contours fall within the companion A_a contours. Again, this reflects the slower attenuation rate of velocity.

Conceptually, the construction of A_v based on A_a results in a reasonable approximation. However, a couple of problems exist with the method. First, the v/a ratio is magnitude and distance dependent [32], a factor not considered during development. Secondly, in areas of multiple sources it is not a simple matter to determine which seismic source zone is controlling the location of contours. Consequently, the method used to attenuate velocity is not as easy to apply as it would appear. An acceleration contour may be the result of a smaller magnitude event in an area of relatively low seismicity, rather than the attenuation of a larger event from a higher seismicity area. The location of A_v should not be the same for both instances.

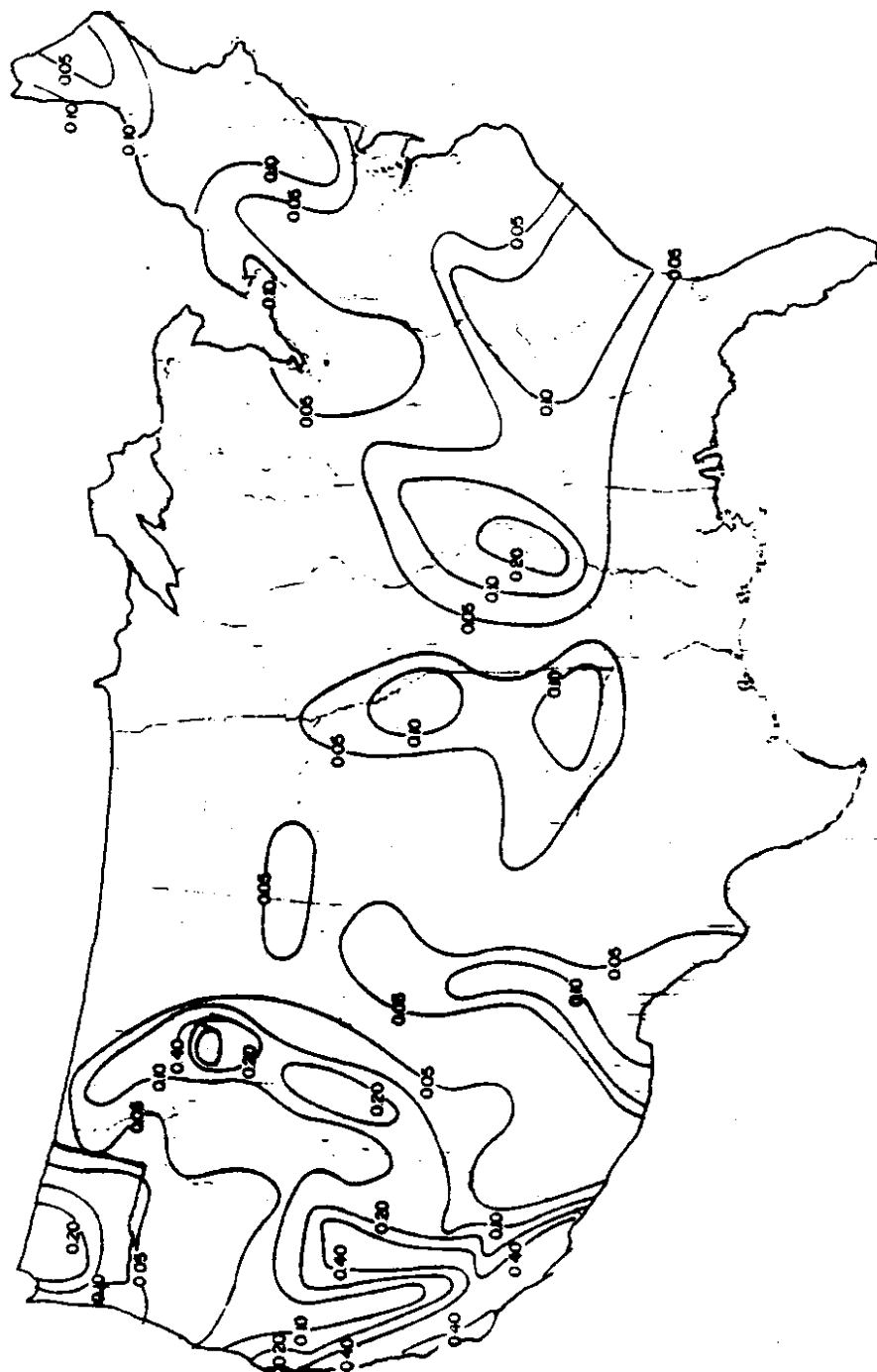


Figure 26. CONTOUR MAP FOR EFFECTIVE PEAK ACCELERATION, EPA (9)

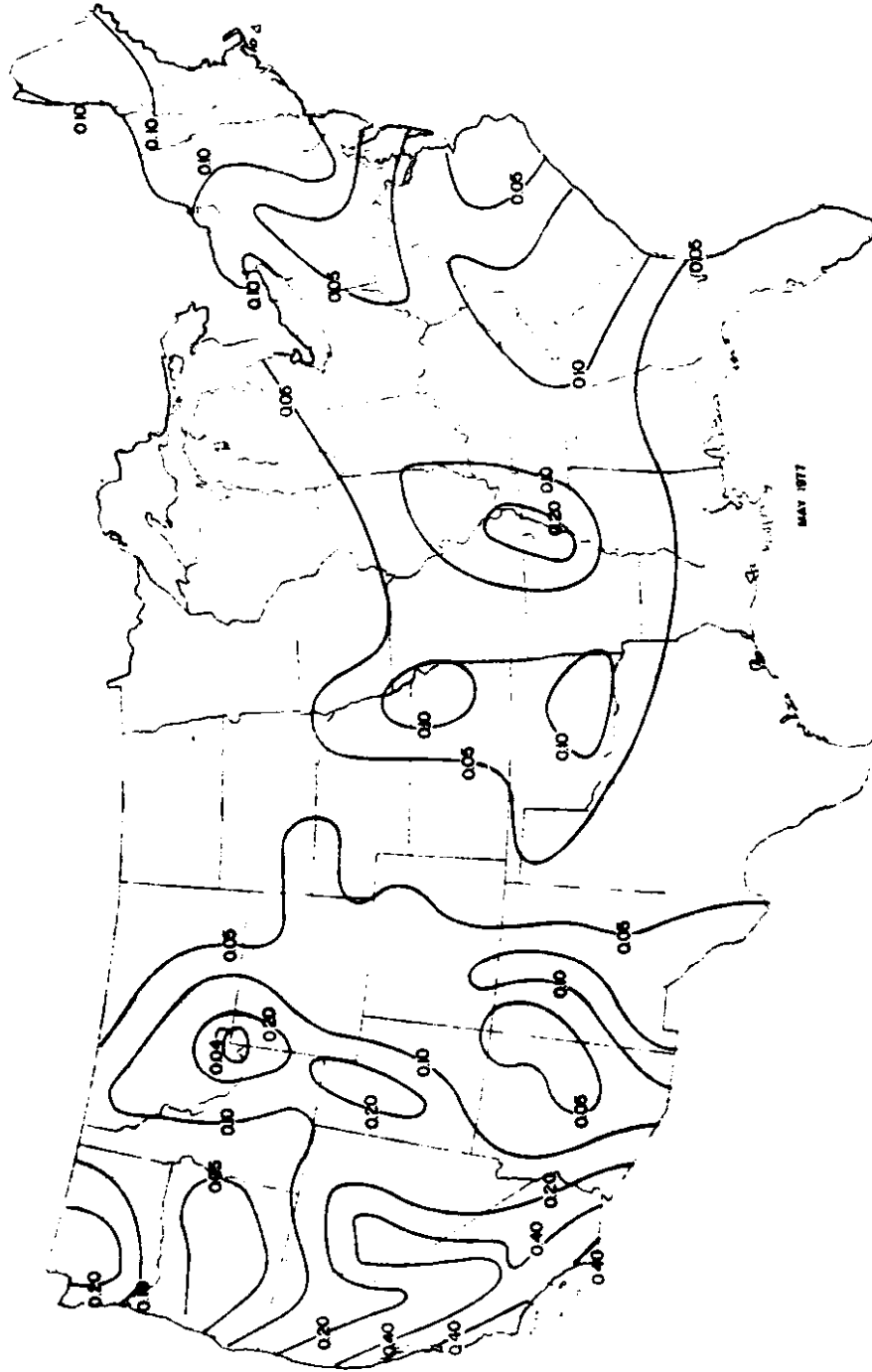


Figure 27. CONTOUR MAP FOR EFFECTIVE PEAK VELOCITY-RELATED
ACCELERATION COEFFICIENT, EPA_v (9)

Design Elastic Response Spectra

A number of factors are known to influence ground shaking and the associated response spectra. Included are:

1. The characteristics of the site soil deposits
2. The magnitude of the design earthquake
3. The earthquake source mechanism
4. Site-Source distance and travel path geology.

Of these, site conditions and distance from the source were the only factors that could be incorporated into the ATC design procedure with any degree of confidence. Spectral studies had shown that site and distance effects could be reasonably approximated using EPA and EPV values [11,43,48].

It has long been recognized that site soil conditions greatly influence ground motions and associated response spectrum. Both the character and degree of spectral influence is at least partially dictated by the dynamic properties of a soil. Thus, characteristic spectral envelopes have been developed for different soil types by a number of investigators [11,28,43,48,64]. Perhaps the most widely recognized study was that by Seed and others [64], which designated the four site classifications depicted in Figure 14. The ATC council simplified the family of curves by combining rock and stiff soil conditions into one soil type while maintaining the other two classifications proposed by Seed and others. The resulting three site profiles were defined as:

- S_1 : Rock of any characteristic (shear wave velocity greater than 2500 ft/sec), or stiff soil conditions less than

200 feet deep. Soil overlying rock must be stable deposits of sands, gravels, or stiff clays.

S_2 : Deep cohesionless or stiff clay soil conditions, including sites where soil depth exceeds 200 ft depth and consists of stable deposits of sands, gravels, or stiff clays.

S_3 : Soft to medium stiff clays and sands characterized by 30 ft or more of soft to medium stiff clay with or without intervening layers of sand or other cohesionless soils.

Normalized smooth response spectra were developed based on the studies previously mentioned and are presented in Figure 28. Spectral acceleration for 5% damping are obtained by multiplying the normalized spectra by A_v . If site conditions are categorized as S_3 and $A_a \geq 0.3$ g the resulting spectral acceleration is multiplied by 0.8 to account for the inelastic attenuation produced by soft soils at high accelerations. When EPV is greater than EPA the portion of the response spectra controlled by velocity should be increased proportionally, as illustrated in Figure 29. Spectra for 2% damping may be obtained by multiplying the ordinates in Figure 28 by 1.25 [11,48].

When designing based on the equivalent lateral force method it is advantageous to express the design coefficient as simply as possible. The lateral design force coefficient, C_s , is defined as follows:

$$C_s = \frac{1.2A_v S}{RT^{2/3}}$$

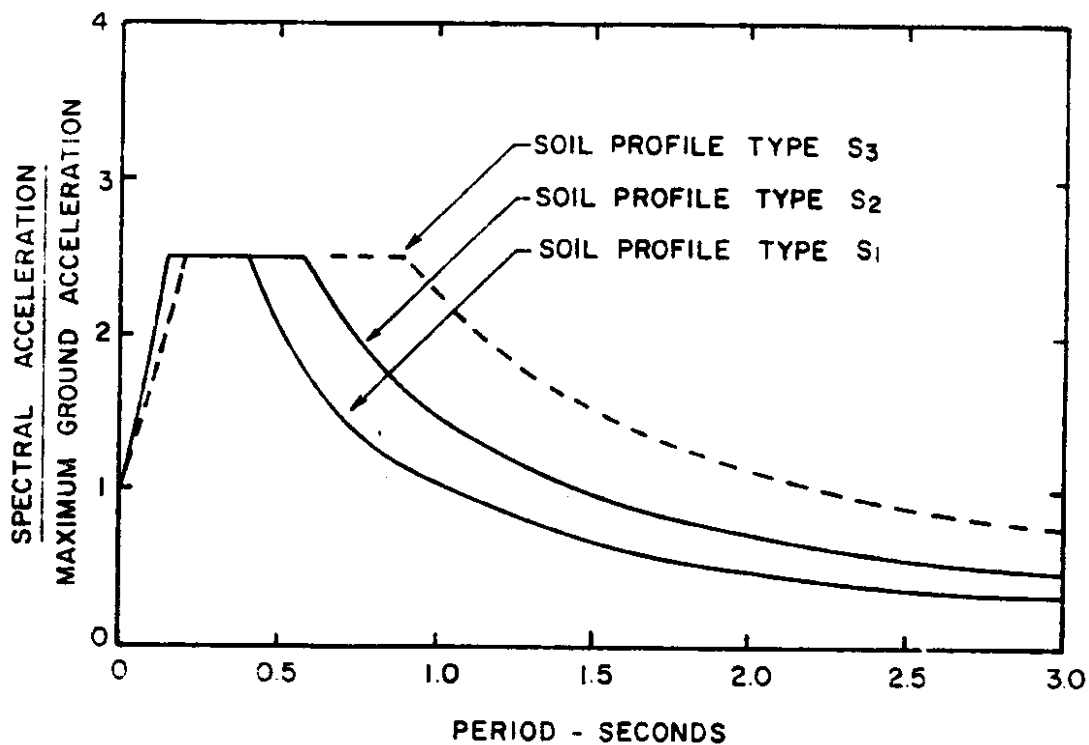


Figure 28. Normalized response spectra recommended for use in building code. (9)

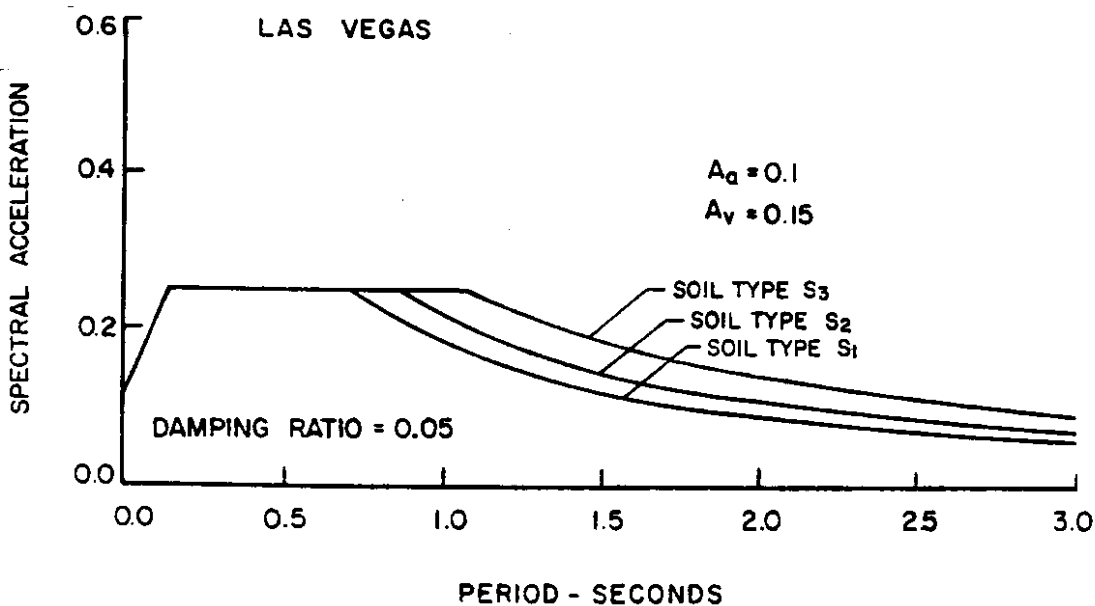
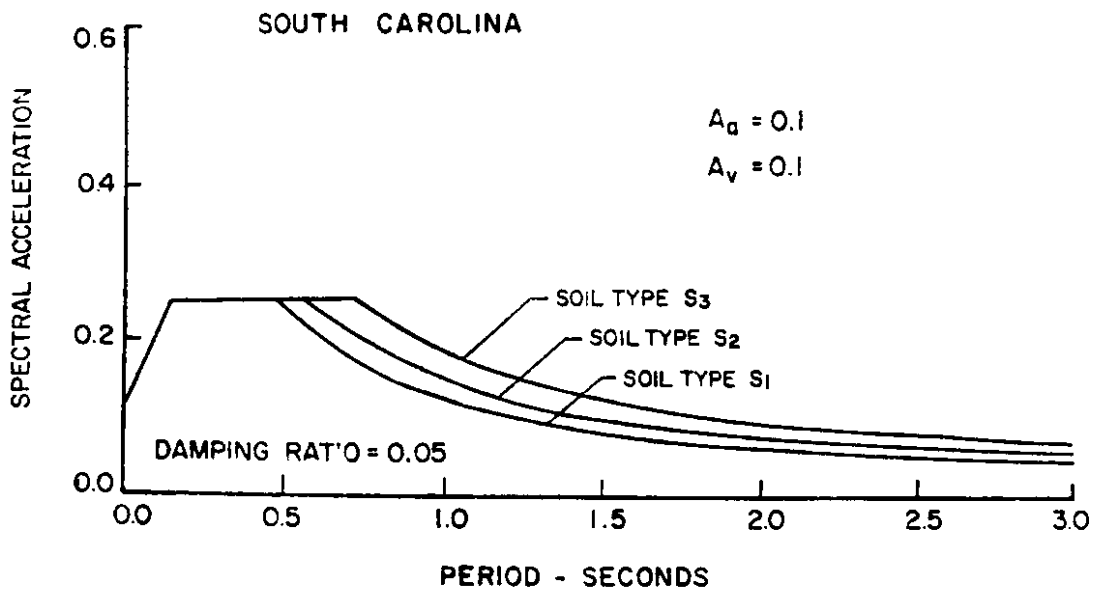


Figure 29. Examples showing variation of ground motion spectra in different tectonic regions. (9)

where

A_v = the velocity-related acceleration coefficient

T = building period

R = seismic response modification coefficient

s = soil profile coefficient: $S_1 = 1.0$, $S_2 = 1.2$, $S_3 = 1.5$

The value of C_s is not to exceed $2.5 A_a/R$ for all soil types.

For S_3 soils when A_a is greater than or equal to 0.3, C_s should not exceed $2A_a/R$.

The equation for C_s was developed such that the lateral force coefficient would be 50% greater than direct use of the response spectra at a period of 2 seconds. The soil profile coefficient, S , was proposed to eliminate the need for estimating the predominant period of the soil deposit and the calculation of a soil factor based on site and building periods. A comparison between C_s and the free field ground motion is presented in Figure 30.

AASHTO Guide Specifications for Seismic Design of Highway Bridges

The AASHTO guide specifications for the seismic design of bridges [6] is presently being used by WSDOT and is based on the ATC 3-06 specification for buildings just discussed [9]. The only difference in design approach related to the present investigation is the selection of the acceleration coefficient.

It was decided to simplify the design procedure for bridges by only utilizing the velocity-related acceleration coefficient A_v , redefined simply, A . The maximum value of C_s was again set

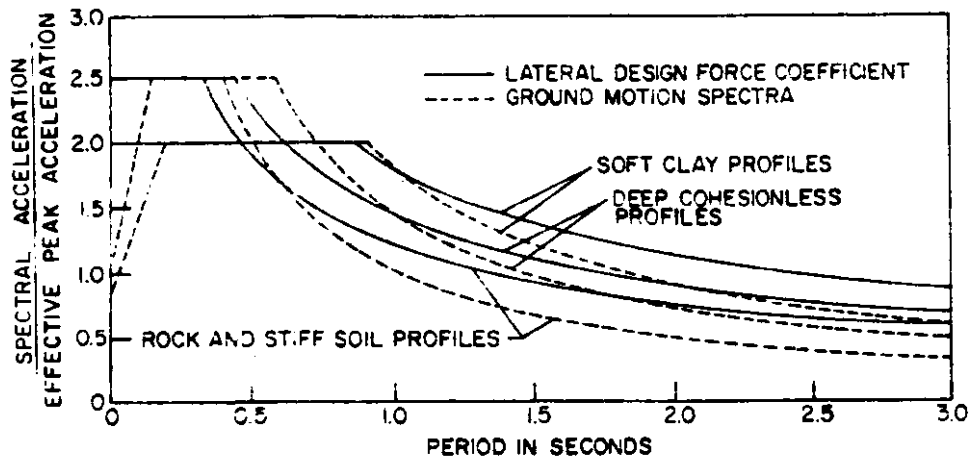


Figure 30. Comparison of free field ground motion spectra and lateral design force coefficients. (9)

at 2.5A for soil types S_1 , S_2 , and S_3 , or 2.0A if $A \geq 0.3$, for soil S_3 . Since A_v is always greater than or equal to A_a , the maximum C_s value for bridges will be at least as large if not larger than buildings, and thus more conservative. The added conservatism was probably considered an equitable tradeoff with the design simplification.

The only other modification relates to how the map(s) are presented. The building guidelines present A_a and A_v as color coded values subdivided along county lines. The bridge guidelines are presented in the more traditional form of isoseismal contours. The rationale for the building guidelines was that county building codes had to be addressed and having contours transcending county lines could cause confusion and be subject to interpretation. Since most bridges are state or federal projects this was not a consideration in the bridge guidelines.

The rest of the design procedure is essentially the same as that for buildings. Thus, it is not necessary to discuss the specifics again.

Evaluation of AASHTO Guidelines

The AASHTO seismic design guidelines for buildings represent a large improvement over previous building code criteria for earthquake loading. The AASHTO guidelines are a straight forward design procedure, based on the best available knowledge and developed by some of the top researchers and practitioners in the field of seismic design. The guidelines are set forth so that

civil engineers not specializing in seismic analysis can understand and apply the design procedure.

Perkins, D.M. and others, 1980

In 1980 Perkins and others [56] published a report and associated maps of peak acceleration and velocity on rock for the Pacific Northwest. The study was a regional seismic zonation project subsequently incorporated into a publication superseding the 1976 Algermissen-Perkins national zonation map [3,5]. The objective was to incorporate more geologic data into the delineation of seismic source zones, determine peak ground motions for more than one exposure period, and express ground motion in terms of velocity as well as acceleration.

The 1976 map displayed peak accelerations for a return period of approximately 500 years based on six seismic source zones in the Pacific Northwest [3]. The 1980 regional zonation maps displayed peak accelerations and velocities for return periods of 100, 500, and 2500 years based on 19 seismic source zones [56]. The map delineating the seismic source zones for the Northwest is presented in Figure 31.

Due to the relatively low rate of seismicity in the Pacific Northwest it was not statistically valid to calculate recurrence intervals for each source zone. As a result all the seismogenic zones were combined into five groups to define recurrence relationships. Groupings were made as follows: 1) zones 1 and 2; 2) zones 3, 18, and 19; 3) zones 4 through 7; 4) zones 8, 14,

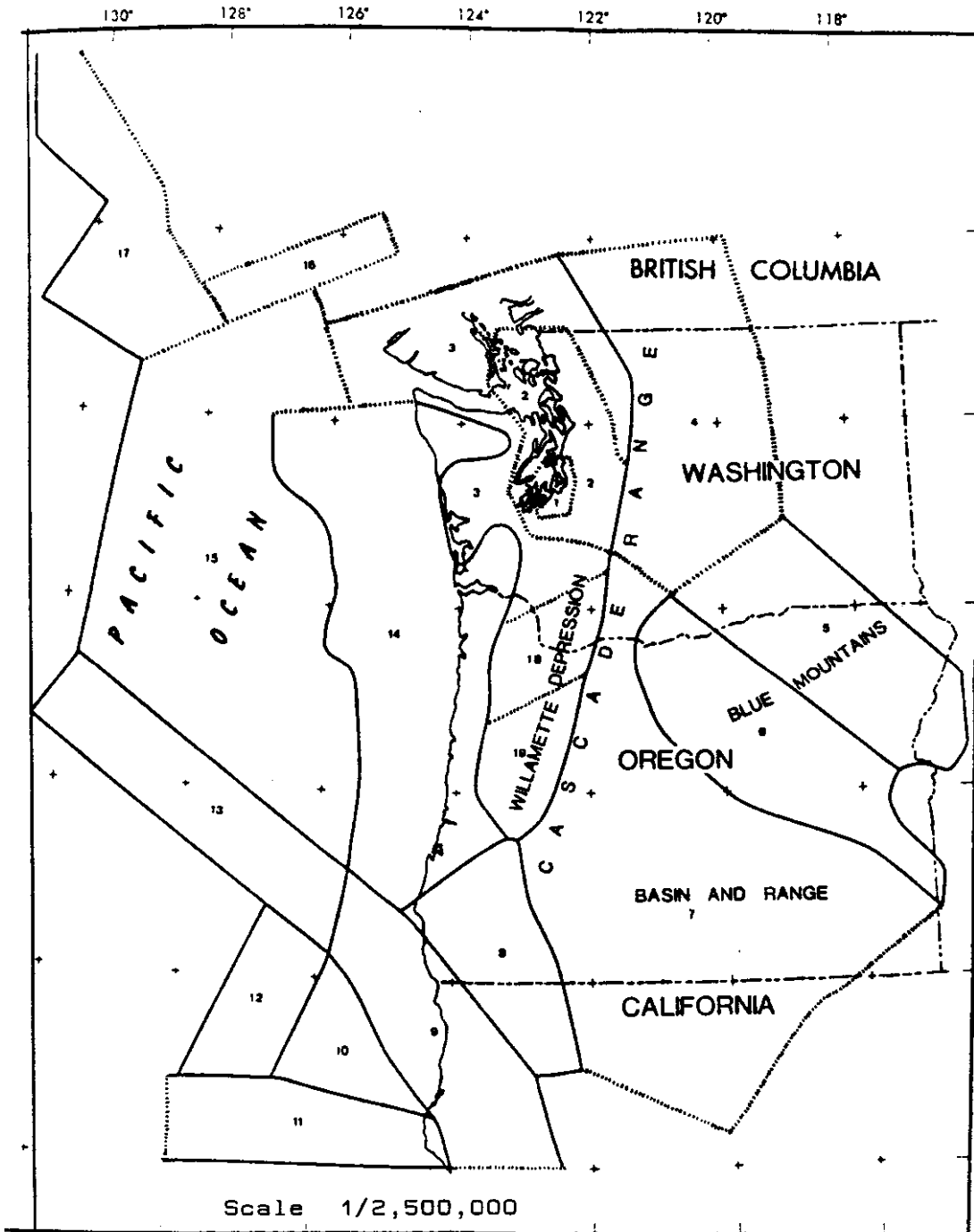


Figure 31. Seismogenic zones for the Pacific Northwest and adjacent outer continental shelf. Dashed lines-boundaries based on seismicity only; Solid lines- boundaries based on geological and geophysical information and historical seismicity. (56)

15, and 16; and 5) zones 9 through 13 and 17. Recurrence rates were then calculated for each group based on the relationship

$$\log N = a + bM_S$$

where N is the annual occurrence rate, M_S is surface wave magnitude, and a and b are regression constants. Epicentral intensities were converted to magnitude using the relationship

$$M_S = 0.6 I_0 + 1.3$$

The smoothed annual rates were then back allocated to the original source zones based on the proportion contributed by each zone. Annual occurrence rates for the zones are presented in Table 2.

Acceleration attenuation curves based on those developed by Schnabel and Seed [61] were used. In the Puget Sound region, the deep events were assumed to have a focal depth of 31 mi. Accelerations were then calculated using an equivalent hypocentral distance as described in a previous section.

The velocity attenuation curves were developed in a manner similar to the acceleration attenuation curves of Schnabel and Seed [61]. They were developed to satisfy three requirements: 1) have magnitude dependent attenuation shapes; 2) the magnitude dependence be specified in terms of M_L for $M < 6.75$ and M_S for greater magnitudes; and 3) the velocity attenuation curves be compatible with the Schnabel and Seed acceleration attenuation curves [55].

A maximum magnitude of 7.3 was assumed for all zones except those in group 5. The zones in group 5 were assigned a maximum magnitude of 7.9.

Table 2.-- Annual earthquake occurrence rates of the Pacific Northwest and the adjacent Outer Continental Shelf (56)

| Zone | b-value | Magnitude levels (Ms) | | | | | | | | | |
|------|---------|-----------------------|------------------|------------------|------------------|------------------|------------------|------------------|--|--|--|
| | | 4.0<M<4.6 4.3 | 4.6<M<5.2 4.9 | 5.2<M<5.8 5.5 | 5.8<M<6.4 6.1 | 6.4<M<7.0 6.7 | 7.0<M<7.6 7.3 | 7.6<M<8.2 7.9 | | | |
| 1 | -0.66 | 0.110 | 0.0442 | 0.0178 | 0.0714 | 0.0288 | 0.00116 | ----- | | | |
| 2 | -.65 | .435 | .175 | .0702 | .0282 | .0114 | .00457 | ----- | | | |
| 3 | -.90 | .124 | .0359 | .0104 | .00296 | .00082 | .00027 | ----- | | | |
| 4 | -1.04 | .348 | .0828 | .0197 | .0046 | .0012 | .0003 | ----- | | | |
| 5 | -1.04 | .124 | .0294 | .0070 | .0016 | .0004 | .0001 | ----- | | | |
| 6 | -1.04 | .0283 | .00673 | .00161 | .00038 | .00009 | .00002 | ----- | | | |
| 7 | -1.04 | .118 | .0280 | .00669 | .00158 | .00039 | .00011 | ----- | | | |
| 8 | -.70 | .0164 | .0062 | .0024 | .0009 | .0003 | .0001 | ----- | | | |
| 9 | -.47 | .208 | .109 | .0569 | .0297 | .0155 | .0081 | 0.0042 | | | |
| 10 | -.47 | .452 | .236 | .123 | .0644 | .0337 | .0176 | .0092 | | | |
| 11 | -.47 | .964 | .503 | .262 | .137 | .0717 | .0375 | .0195 | | | |
| 12 | -.47 | .371 | .194 | .101 | .0529 | .0276 | .0144 | .0075 | | | |
| 13 | -.47 | .690 | .361 | .180 | .0984 | .0514 | .0269 | .0140 | | | |
| 14 | -.70 | .109 | .0417 | .0159 | .0060 | .0023 | .0008 | ----- | | | |
| 15 | -.70 | .345 | .131 | .0500 | .0190 | .0072 | .0026 | ----- | | | |
| 16 | -.70 | .0493 | .0188 | .0071 | .0027 | .0010 | .0004 | ----- | | | |
| 17 | -.47 | .879 | .459 | .240 | .125 | .0654 | .0342 | .0178 | | | |
| 18 | -.90 | .188 | .0543 | .0157 | .00450 | .00126 | .00041 | ----- | | | |
| 19 | -.90 | .0409 | .0118 | .00342 | .00098 | .00027 | .00008 | ----- | | | |

The maps of peak acceleration and velocity for a 50 year exposure period are presented in Figures 32 and 33 respectively. Peak acceleration values are approximately twice as high in Figure 32 as those in the 1976 investigation. Although the increase is not specifically addressed it is probably due to the additional emphasis placed on geologic-tectonic factors in the more recent version.

The data base and resulting ground motions from the investigation were used verbatim in the 1982 Algermissen and others [5] maps of peak acceleration and velocity. Consequently that study will not be addressed separately.

Given the data limitations in the Pacific Northwest, it is felt the authors have seismically zoned the region to the greatest detail practical with regard to peak ground motions on rock. The only possible exception is the Puget Sound region, where an argument for microzonation can be made. The most recent attempt at microzonation in the Puget Sound area will be discussed next.

Ihnen and Hadley, 1984

In 1984 a model study was performed for the Puget Sound region that attempted to synthesize the April, 1965 Seattle earthquake. Although this was not a seismic zonation study, the results were subsequently incorporated into a seismic risk investigation that produced seismic hazard maps for the Puget Sound region. Thus, the methodology and results merit discussion.

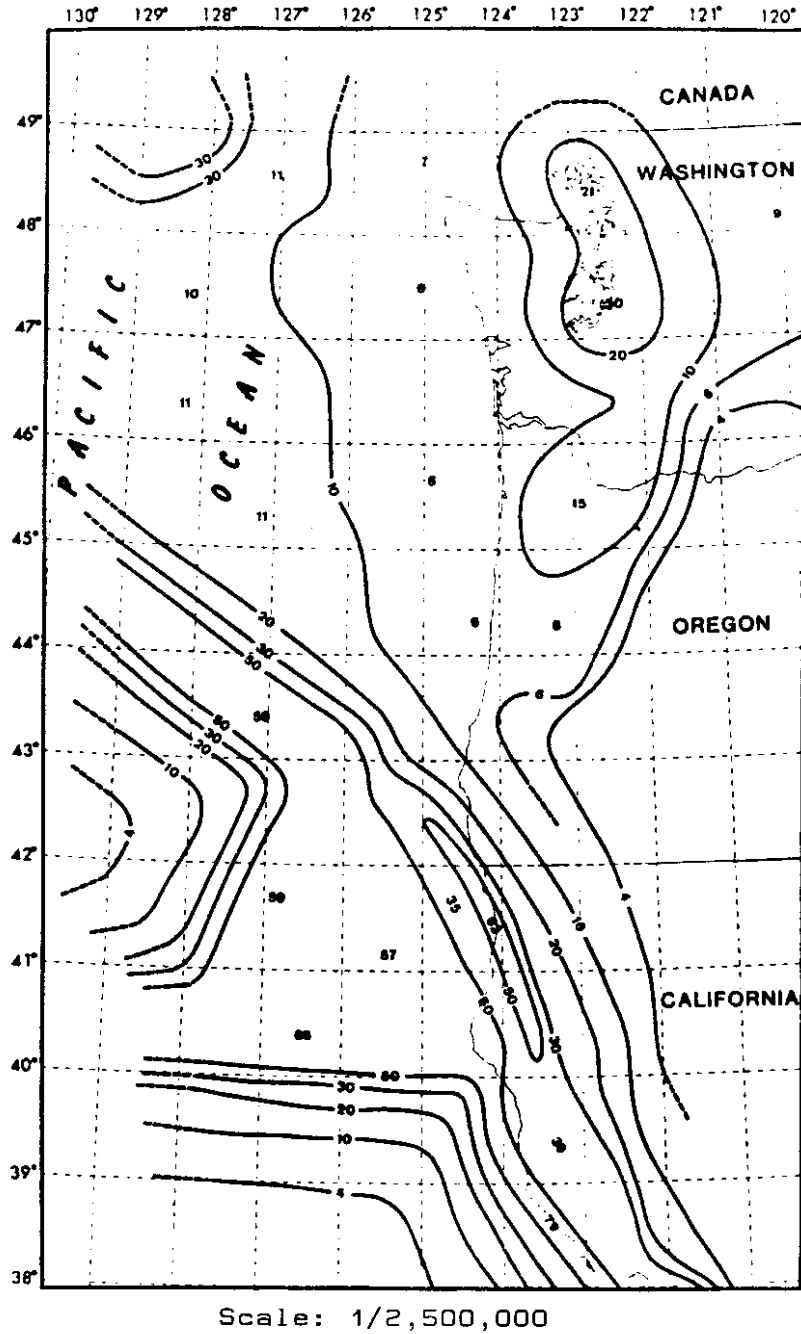


Figure 32. 500 -year return period acceleration on rock (90 % probability of not being exceeded in 50 years). (56)

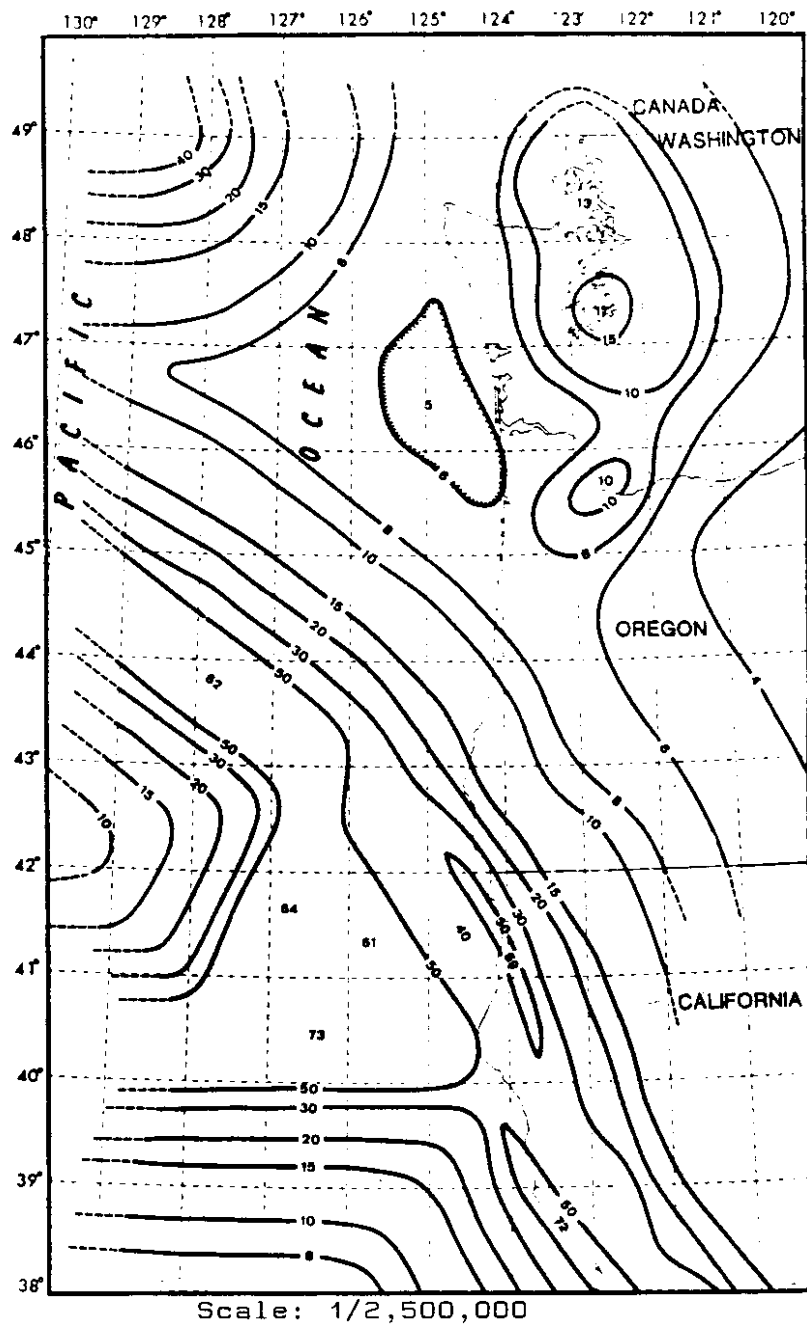


Figure 33. Map of 500-year return period velocity on rock (90 % probability of not being exceeded in 50 years). (56)

Past investigators [2,44] observed that building damage in Seattle, Washington resulting from the April, 1965 earthquake was very irregular and transcended soil boundaries. The author's felt that this was at least partially due to focusing of seismic waves. It is hypothesized that curved bedrock-glacial sediment interfaces tend to focus seismic waves, causing increased ground motion at overlying focal points.

The authors used a three-dimensional raytracing program coupled with a velocity model of the Puget Sound region's subsurface to synthesize the 1965 event. Raytracing is a method of theoretically following a seismic wave from a source (an earthquake focus), through a medium (the earth's crust), to the surface. It is possible to reproduce the reflection, refraction and phase changes experienced by a seismic wave as it travels through the subsurface, provided the subsurface geology is known.

In order to set up a raytracing model the subsurface geology between the source and the area of interest must be defined. Geologic units are defined in terms of seismic velocity (S and P-wave), density, and an elastic attenuation constant (quality factors, Q). Both density and attenuation are typically defined in terms of shear and compressional wave velocity. For the study under discussion they were defined as follows:

$$\rho = 1.74 \alpha^{0.25}$$

$$Q_{\beta} = 30 \beta^{1.25}$$

$$Q_{\alpha} = 3/4 Q_{\beta} (\alpha/\beta)^2$$

where

$$\rho = \text{density [g/cm}^3\text{]}$$

α = P-wave velocity (km/s)

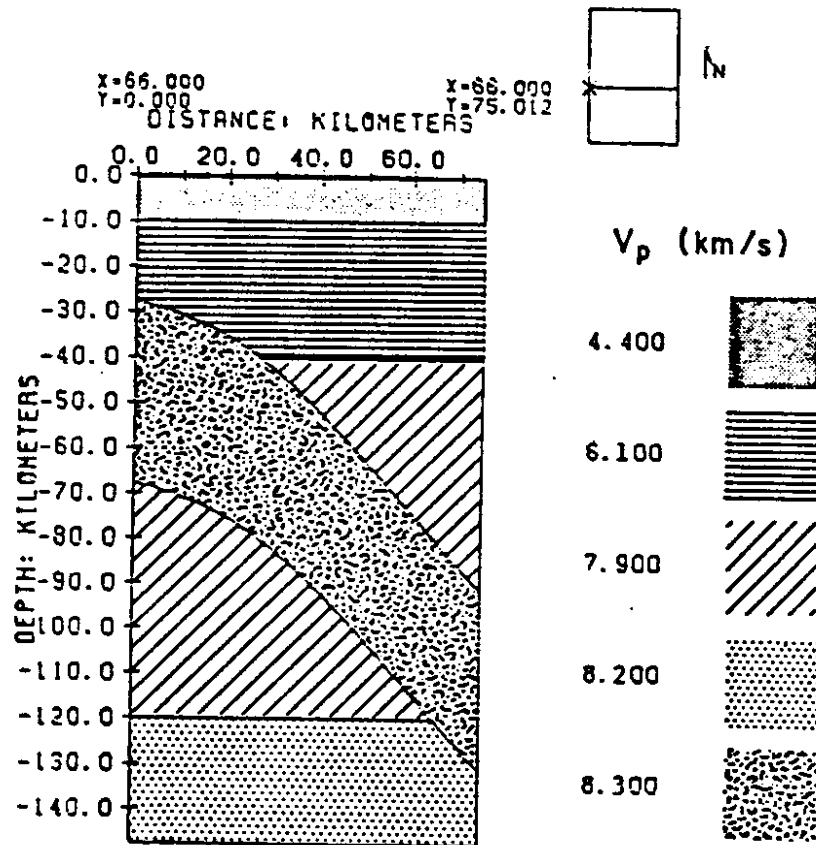
β = S-wave velocity [km/s]

Q_α = P-wave quality factor (attenuation)

Q_β = S-wave quality factor (attenuation)

Once the velocity model has been numerically constructed a source is spacially defined within the model and a set of synthetic receivers is placed on the surface. The computer program then shoots a number of working rays out from the source that terminate on the free surface. A ray capture algorithm is used to find all rays that connect the source with the various receivers. The raytrace output from each receiver is then processed and organized in the form of a synthetic seismogram. From that point different parameters such as peak acceleration may be examined.

The velocity model developed for the 1965 Seattle earthquake study consisted of seven units: (1) a water layer, (2) near surface unconsolidated units, (3 & 4) upper- and lower-crustal layers, (5 & 6) top and bottom of the subducted Juan de Fuca plate, and (7) the upper mantle. Figure 34 illustrates a cross-section through the model. Material velocities above the basement horizon were considered laterally variable with V_s ranging between 490 and 4000 ft/s (150 and 1220 m/s). Velocities at each grid point were defined based on surface geology. Velocities were assigned using known velocities from consolidated sediments with lithologic description similar to those in the study area. Shear wave velocities outside King County were set



1 km = 0.62 mi
1 km/s = 3,281 ft/s

Figure 34. Vertical cross section through velocity model at latitude of 1965 event. Uppermost layers are too thin to be seen in the detail at top of figure. (33)

at a uniform 2360 ft/s (720 m/s) due to the lack of reliable geologic information.

The source for the raytracing study was placed at the hypocenter of the 1965 event. The synthetic receivers were placed in a 48x33 array for a total of 1584 receivers. Due to the extensive computer time required to run the program (0.75 CPU hours on a Prime 750 computer) a sensitivity study was performed to determine which, if any, ray instructions could be discounted without substantial effect on accuracy. It was found that neither P-waves, nor the water layer significantly influenced results. Thus, they were eliminated from consideration.

The results of the simulation are expressed in terms of "peak ground acceleration" (PGA). In this case PGA is defined as the square root of the sum of the squares of the N-S and E-W acceleration time histories. Thus, it is really an average peak acceleration rather than an absolute peak acceleration. Results in terms of log PGA are shown in Figure 35.

In order to separate soil amplification from focusing, the program was run with horizontally layered bedrock (Figure 36) and horizontally layered near surface deposits (Figure 37) to provide a basis of comparison. It was found that soil amplification increased surface accelerations by as much as a factor of two while focusing increased accelerations by up to a factor of five.

The authors also plotted peak horizontal acceleration as a function of distance, generating an attenuation curve for the Puget Sound region. The data and associated attenuation curve is

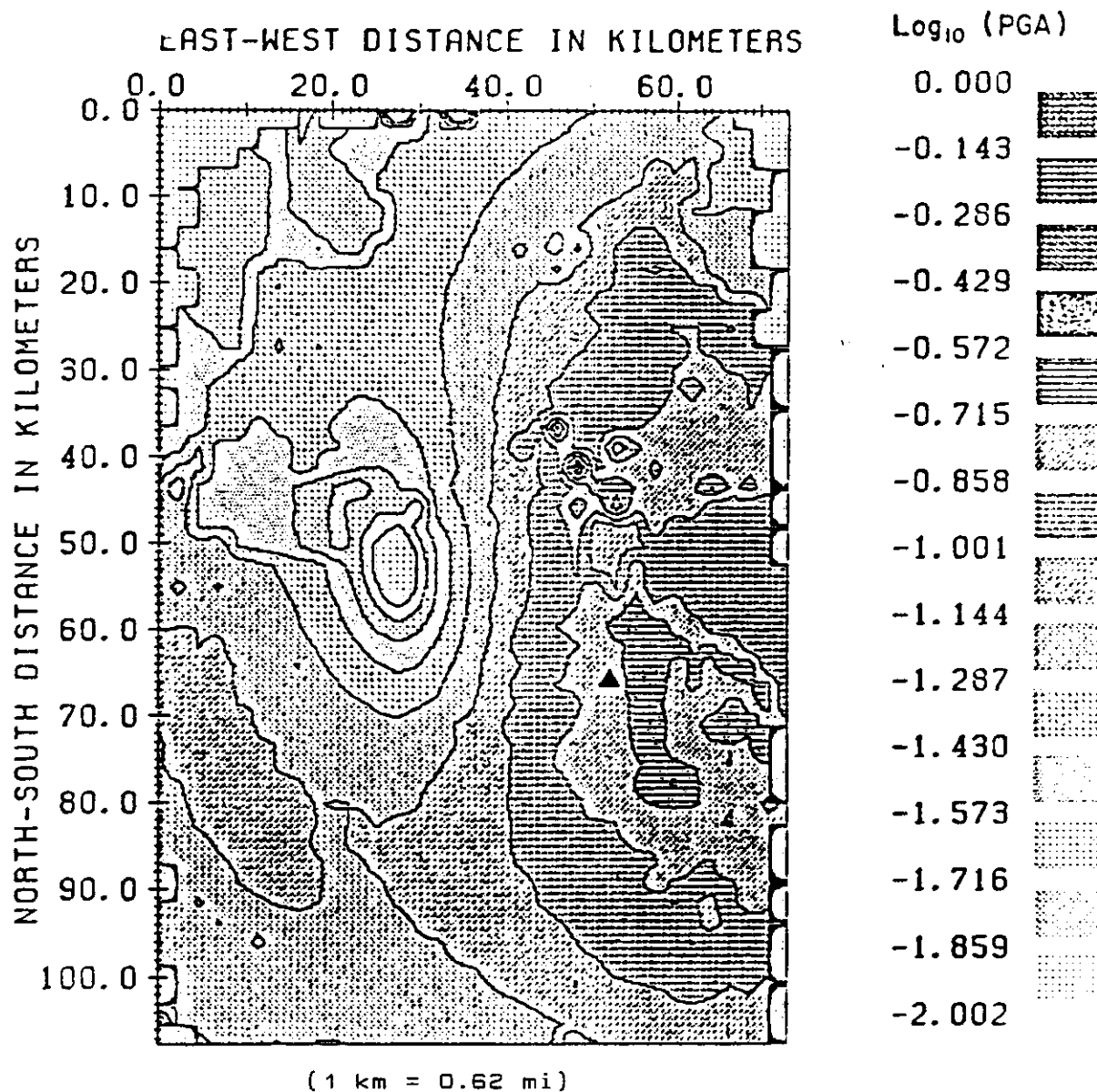


Figure 35. Contoured peak horizontal accelerations, 1965 earthquake, ISC epicenter. Note that the quantity contoured is the base ten log of acceleration, expressed as a fraction of g. Every change of 0.33 units is crudely equivalent to one seismic intensity unit (Richter, (1958), p. 140). Low values of acceleration within 2-4 km of the edge of the model are artifacts of the modeling procedure and should be ignored. Triangle is epicenter of 1965 earthquake. (33)

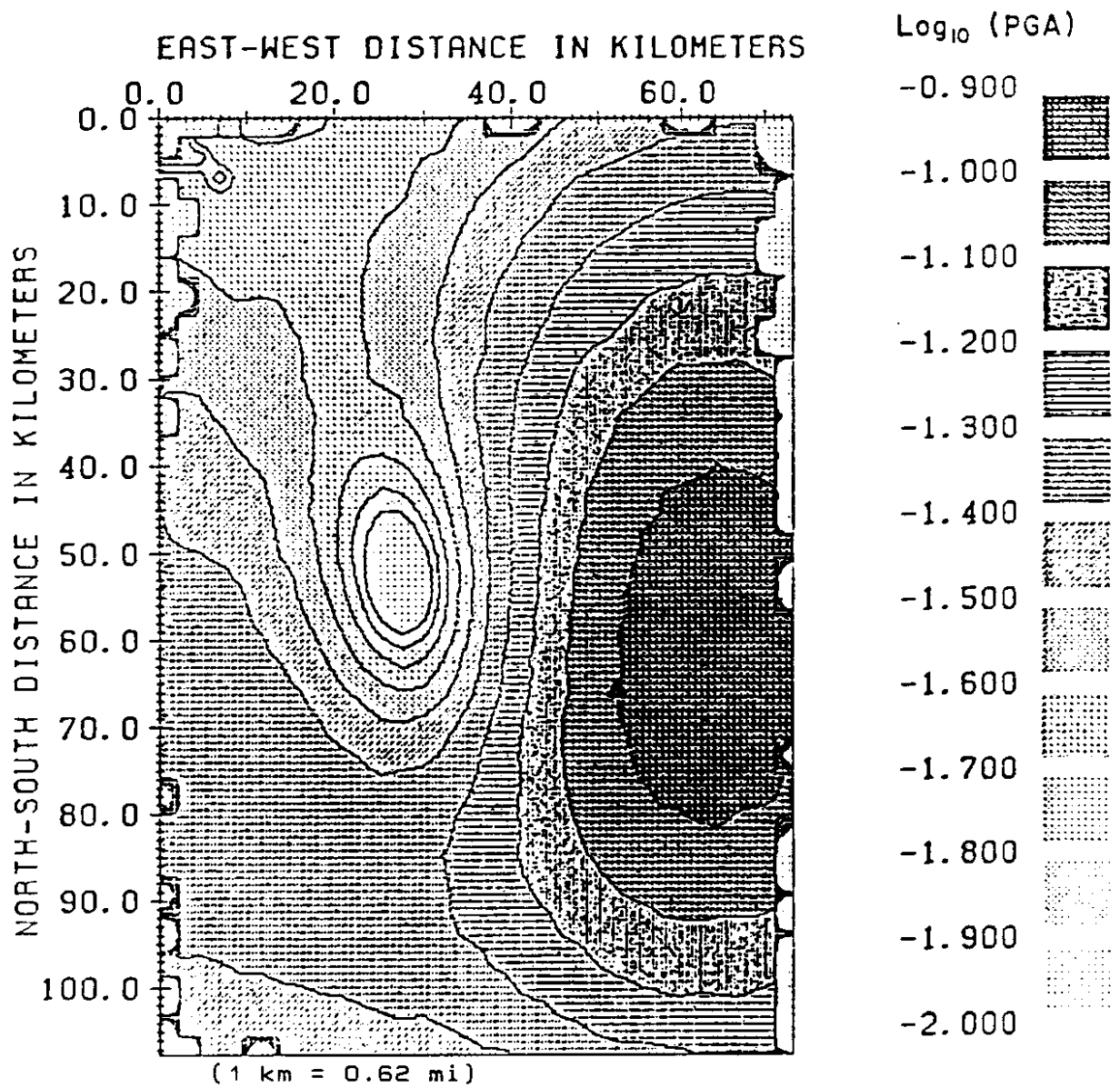


Figure 36. Contoured peak horizontal acceleration for the case of uniform bedrock at surface. Triangle is epicenter of 1965 event. (33)

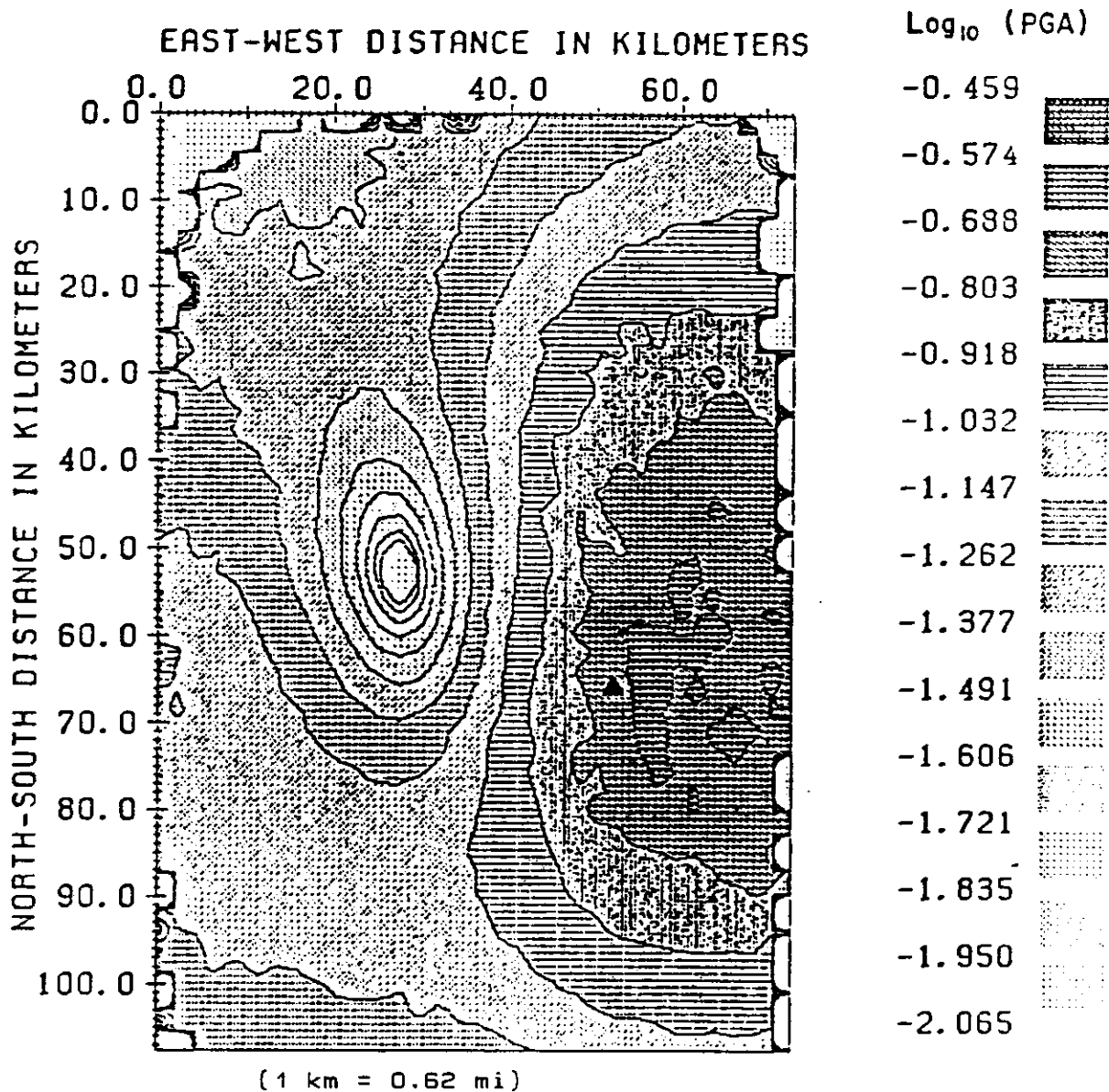


Figure 37. Contoured peak horizontal acceleration for model with a layer of laterally varying velocity but uniform thickness near the surface. Triangle is epicenter of 1965 event. (33)

plotted in Figure 38 and exhibits the degree of scatter typical of actual data.

The model compared well with the accelerogram recording from Seattle, but was unsuccessful in matching the Olympia recording. Table 3 compares actual to predicted values for the three sites. It should be noted that the peak acceleration value for Seattle, as listed by CIT, is 7.75% g rather than the 11% g used by the authors. Additionally the CIT peak value for Olympia is 19.4% g instead of the 16% g indicated. The 11% g value used by the authors is a corrected value used in a previous study [37]. The origin of the 15% g listed for the Olympia recording is unknown.

The raytracing approach to estimating ground motions generated by a seismic event is the most theoretically rigorous method yet attempted. Additionally, it appears to approximate ground motions in the Seattle area fairly well based on the limited data available for comparison. However, it does suffer from some shortcomings.

The primary problem is the lack of detailed knowledge of the subsurface underlying the Puget Sound region. The model is highly dependent on the subsurface geometry and physical properties, neither of which are well defined. Since the raytrace results were scaled to the Tacoma accelerogram only two model calibration points were available, Seattle and Olympia. The Seattle results compare either excellent or fair, depending on which recorded value is used, the Olympia values are off by a factor of 4.4 to 5.6, again depending on which recorded value is used. Even though the anomalous recording at Olympia may be due

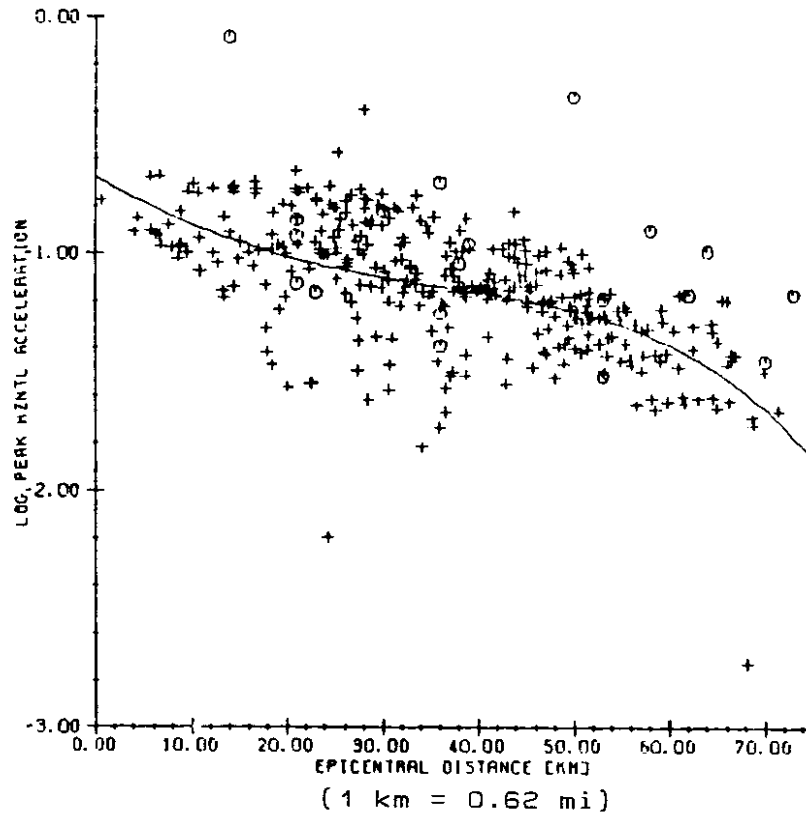


Figure 38. Plot of logarithm of peak ground acceleration (as fraction of g) vs. epicentral distance. Pluses (+) are predicted values from raytrace simulation of 1965 event. Circles are data from Japanese earthquakes. (33)

Table 3

COMPARISON OF RECORDED AND PREDICTED PEAK ACCELERATION VALUES FOR
THE 1965 SEATTLE EARTHQUAKE

| Site | Peak Acceleration (%g) | |
|---------|------------------------|----------|
| | Predicted | Recorded |
| Seattle | 10.6 | 11 |
| Tacoma | 6.7* | 6.7 |
| Olympia | 3.6 | 16.0 |

*raytrace results were scaled to Tacoma accelerogram
recording.

to an unknown subsurface structure as hypothesized by the authors, a model cannot be validated based on the comparison of one data point. Particularly in this case, since a similar peak acceleration at Seattle could be generated by a number of different velocity models using various geometries and material properties.

This is not to say that the method is invalid, or does not present a reasonable approximation to ground motion in the Seattle or Tacoma area. The model does appear to generate accelerations consistent with intensity reports, particularly in the Duwamish River Valley.

Ihnen and Hadley, 1986

In 1986 seismic risk maps were published as an extension of the raytracing project previously discussed [34]. The maps expressed PGA with a 95% chance of nonexceedence in 50 years, or a return period of 975 years. The final map incorporates the effects of local soil conditions and subsurface focusing into the peak acceleration values.

The authors used the SEISMIC.EXPOSURE risk assessment computer program [46] to generate the "base risk" map for their study. Although the program differs somewhat from that used by Algermissen and others [3,5], the approach is similar and does not merit a separate discussion. The authors chose the constrained form of the relationship developed by Campbell [16] to describe attenuation:

$$PGA = [0.0185e^{(1.28M)}] [(R+0.147e^{(0.732M)})^{1.75}]$$

where

PGA = peak ground acceleration, expressed as a decimal
fraction of g

M = Magnitude = M_L if $M < 6.0$
= M_S if $M \geq 6.0$

R = distance from fault rupture zone [Km] (taken as
hypocentral distance in study)

The Puget Sound region was divided into three source zones, two shallow and one deep. One of the shallow zones covered the whole study area (Zone 1) while the second covers only the central portion of the study area and represents higher earthquake activity in the central Puget Sound region (Zone 2). The deeper zone (Focus ≥ 25 mi) lies on the subducted plate (Zone 3). All three zones are illustrated in Figure 39.

Recurrence relationships were defined as follows:

Zone 1: $\log N = 4.53 - 1.02 M$

Zone 2: $\log N = 4.79 - 1.02 M$

Zone 3: $\log N = 3.67 - 0.73 M$

where N is the annual number of events and M is magnitude.

The SEISMIC.EXPOSURE program [46] was used to generate separate "base risk" maps for each group, as well as the combined map illustrated in Figure 40. Although it reflects the seismicity of the two shallow zones, acceleration values are dominated by zone three. Accelerations are higher in the northwest where the slab is 19 mi deep and decrease to the southeast where the slab is approximately 56 mi deep. The

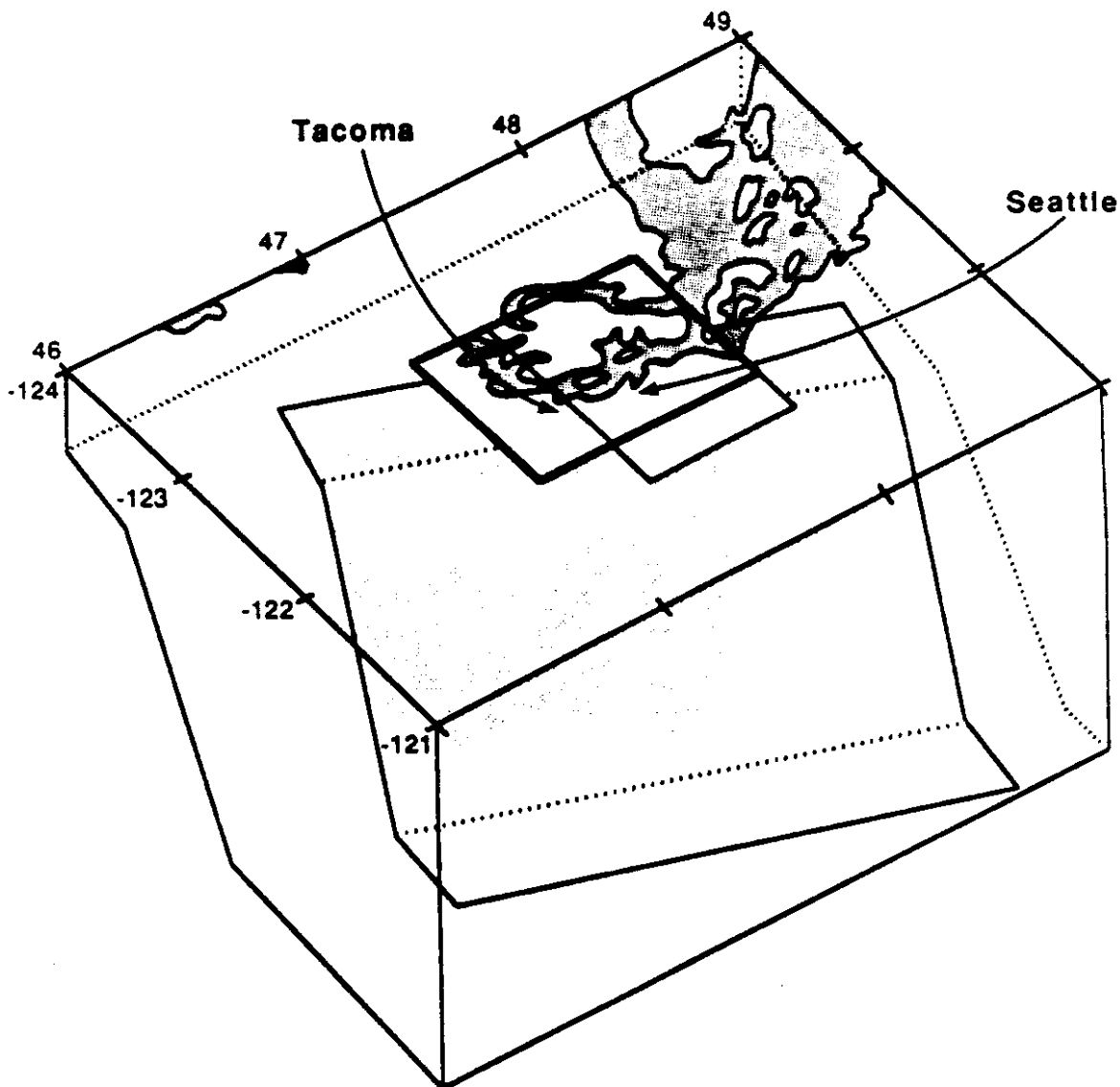


FIGURE 39. Perspective plot of the Puget Sound area and the subducted Juan De Fuca plate, showing the three seismic source zones used in this study. The study area is contained within the area from 47 to 49 N and 122 to 123 W (darkly outlined box). Source Zone I extends over the entire 3 degree by 3 degree area shown, Zone II is outlined by the E-W oriented lightly outlined box and Zone III lies on the subducted plate. (34)

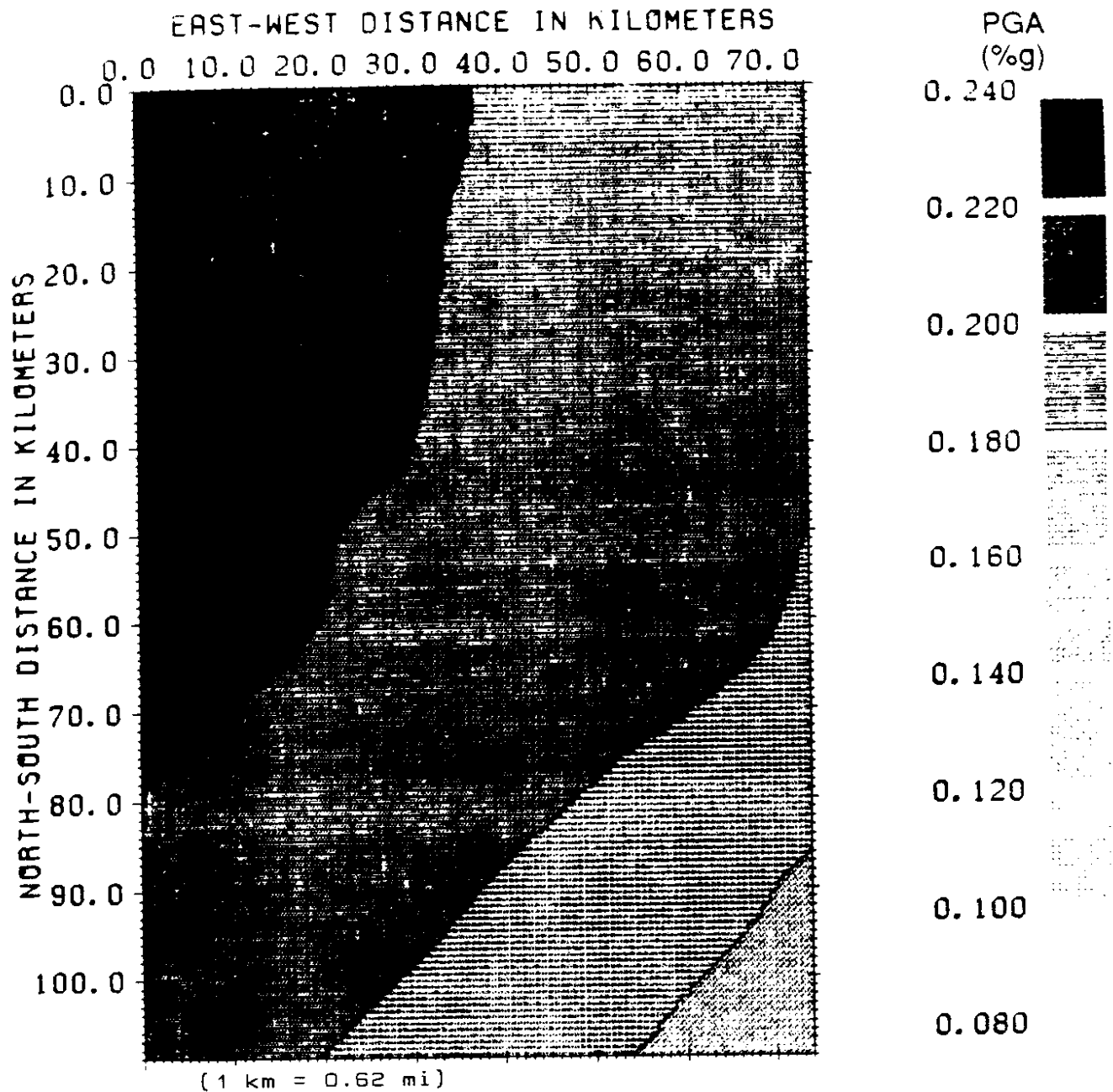


Figure 40. "Base risk map" for Puget Sound earthquakes including all three seismic zones. (34)

highest acceleration value is about 0.22 g, in the northwest corner.

Once the "base risk" map was established the effects of soil type and focusing were superimposed. The effects of soil type on ground acceleration were addressed using a theoretical study relating shear wave velocity to soil amplification [8]. The authors felt this method eliminated some of the variables such as earthquake mechanism, directivity, and recording details, associated with empirical studies. Figure 41 is the amplification curve used to estimate soil response.

Shear wave velocities were assigned to the mapped geologic unit as described in the previous section. The lithologic description of each unit was matched to a unit of known velocity and assigned an appropriate value. Amplification factors were then applied to each unit using the relationship illustrated in Figure 41. The amplification effects were then superimposed on the "base risk" map as shown in Figure 42.

To accurately estimate the effects of focusing, a raytrace simulation at each subzone within seismic Zone 3 would be required. The amount of computer time required for such an undertaking would be prohibitive. Thus, the authors simplified the analysis to two raytrace simulations, recognizing this would only provide a first-order estimate of focusing effects.

Both simulations placed the source at great depth, although neither depth nor location were specified. In the first simulation the sediment-basement was modeled to reflect actual subsurface topography, and for the second simulation the

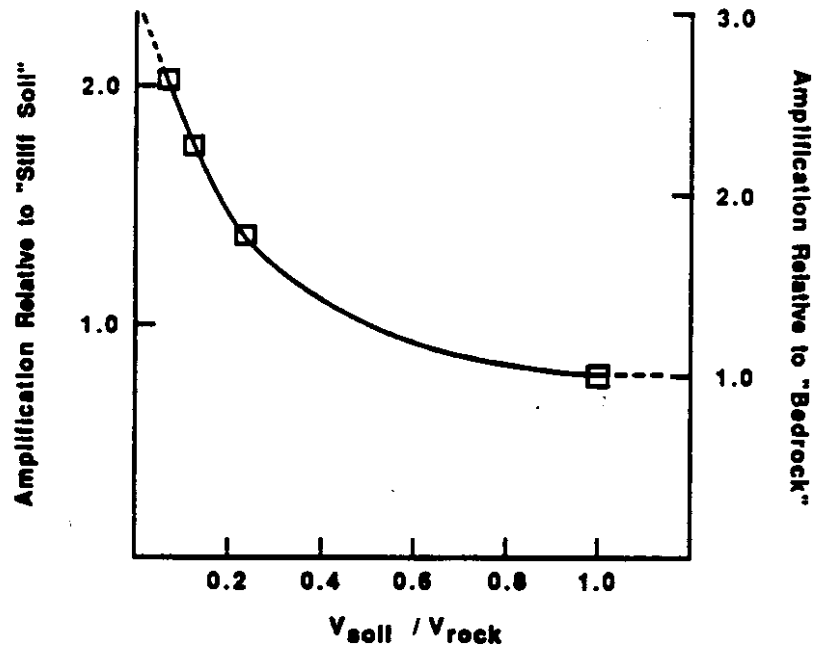


Figure 41. Amplification of PGA as a function of site shear-wave velocity. Scale on the left shows amplification relative to bedrock, scale on the right shows amplification relative to $V_s = 1.2$ km/s (3,937 ft/s) "average" soil conditions. (34)

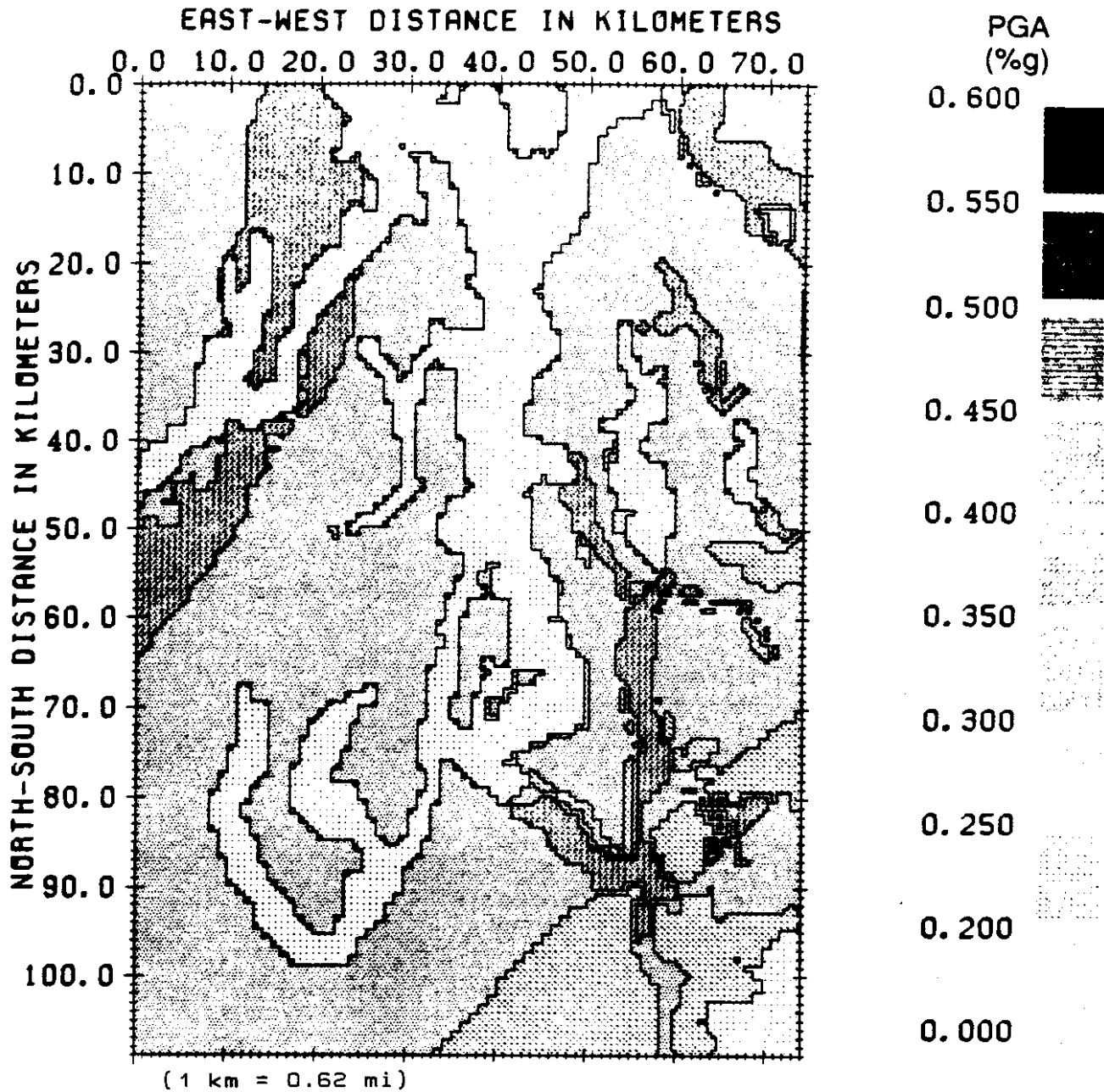


Figure 42. Seismic risk map for Puget Sound, including the "base risk" map of Figure 40 and corrections for soil type at each site as described in the text. Contours are PGA for which there is a 5% chance of exceedance in 50 years time. Areas covered by water are assigned zero risk for plotting purposes. (34)

sediment-basement contact was a flat layer at 820 ft depth. It was felt that the ratio of simulation 1 to simulation 2 would provide a reasonable approximation of site amplification due to focusing. The highest amplification resulting from focusing was slightly greater than 2 and was concentrated around the two sediment basins underlying the Puget Sound region. Figure 43 is the seismic risk map, including "base risk," soil amplification, and focusing.

The authors state that site accelerations obtained from the map should only be used as a general guide to expected acceleration levels, not a statement of maximum PGA. It must be realized that the methods used to estimate amplification due to site soil conditions and focusing are approximate and speculative.

Although the use of shear wave velocity to estimate the dynamic properties of soils is an accepted approach, it is not without problems. First, it is most accurate on a site-specific basis when shear wave velocity, site geometry, and soil properties are well defined. The authors used approximate methods in defining velocity and must have made a number of simplifying assumptions regarding soil deposit geometry and strength properties. The strain dependency of the shear modulus and internal damping of a soil also presents a problem when using velocity to define soil amplification. Shear wave velocity is measured at much lower strain levels than those experienced during a seismic event. Thus, the shear modulus will be higher and damping ratio lower when estimated using shear wave velocity

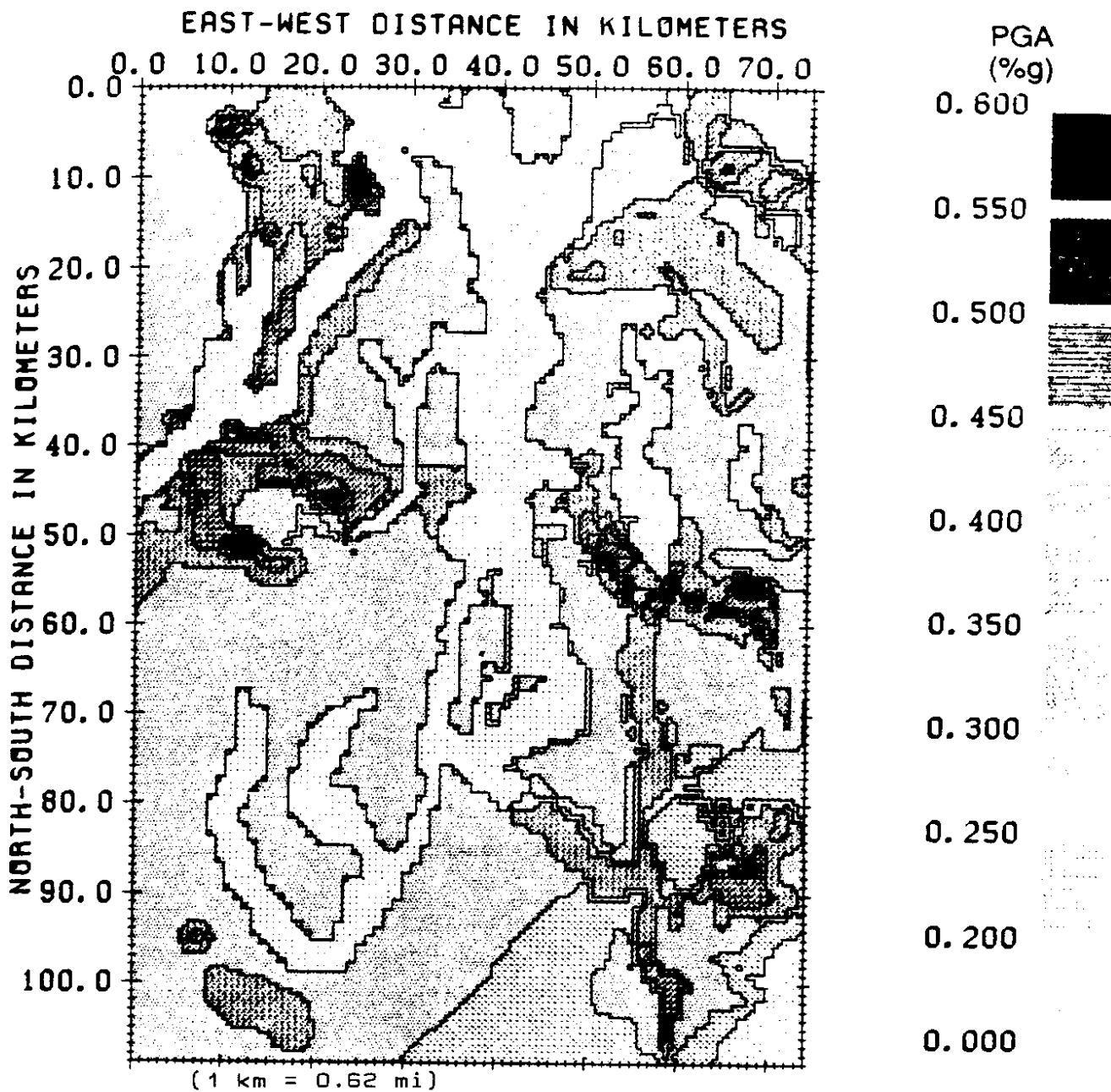


Figure 43. Map of risk from seismic ground motion in Puget Sound, Washington, including "base risk", corrections for soil type and estimated amplification from focusing by near-surface structure. Contours are of peak horizontal ground acceleration for which there is a 5% chance of exceedance in 50 years. (34)

than what might be expected in an earthquake. Although values can be approximated using strain related reduction curves, it is not a method that lends itself well to such a large scale project.

As stated by the authors, the focusing portion of the study is only a first-order approximation and should be recognized as such. It provides the reader with an indication of areas where focusing may be a problem. However, a great deal of significance should not be assigned to the specific amplification values.

It would appear that the most benefit can be derived from the map(s) when used as a planning tool. The map(s) do provide a good approximation of relative ground motion. However, it is questionable whether the actual acceleration values should be used for design. Special care should be taken if the map incorporating focusing is used, since that aspect of the study is the most speculative.

IV. RECOMMENDATIONS FOR THE MODIFICATION OF WSDOT
SEISMIC DESIGN PROCEDURES

Selection of Seismic Design Coefficients

When considering the use of a seismic zonation map other than that developed within the AASHTO guidelines two questions must be answered: (1) Was the new map developed in a manner consistent with AASHTO design procedures? and (2) Will the new map provide design coefficients of greater accuracy than those presently being used?

With regard to the first question, the main concern is whether the prospective map was developed using a statistical procedure comparable to that used for the ATC map and that the probability of exceedence, or return period, is similar. Another requirement is that the ground motion parameter be of a similar nature, if not exactly the same, as the velocity-related acceleration coefficient used in the AASHTO procedure.

The second question regarding improved accuracy is more subjective. It is a matter of judgment as to which, if any, of the available seismic zonation studies offer a marked improvement over the original AASHTO map. This is particularly true for the Pacific Northwest where the paucity of data requires considering whether the accuracy of a given map exceeds the accuracy of the data used to generate that map.

An examination of the methods used in generating the zonation maps or procedures described in the previous section quickly eliminates two of the available studies. The work done

by Rasmussen and others [58] provides a reasonable approximation of ground motion, given a source location. The authors' method provided a fairly good correlation to measured intensities for the 1965 Seattle earthquake. However, the definition of ground response is not consistent with that used in the AASHTO guidelines. In order to express ground motion at a given location that is statistically valid, the motion due to events from all subzones within all applicable source zones must be considered. This approach is not possible unless the results from their investigation is used as input parameters for a new zonation study.

Additionally, the study is in terms of intensity. Although it is possible to estimate acceleration from intensity data, estimation of velocity, or a velocity-related acceleration is not as well documented. Although the need for a velocity term in the central portion of the study area may not be necessary, velocity effects should be considered with distance from the source. Also, the method could only be used for the central Puget Sound area requiring a different map for other locations within the state.

The USGS study [76] suffers from many of the same drawbacks as the work by Rasmussen and others [58]. The maps were generated using individual events rather than a statistical sampling of ground motion, they do not provide ground motions easily related to velocity, and they only address a limited area. Thus, this study was not considered a valid replacement or companion to the AASHTO map.

This leaves two possible maps for consideration: (1) the Perkins and others [56]/Algermissen and others [5] maps; and (2) the Ihnen and Hadley [34] map. The Ihnen and Hadley map expresses acceleration in terms of a 95% probability of nonexceedence in 50 years. Although not the same probability of exceedence as the AASHTO map (90% probability in 50 years), a statistically similar method of generating the "base risk" map was used. Empirical methods are available to modify the ground motions to an equal probability of non-exceedence.

However, questions must be raised as to whether the accuracy of the techniques used to produce the maps exceeds the accuracy of the data available. The amplification due to focusing should be discounted for two reasons: 1) the model is validated based on very limited data; and 2) the focusing portion was not generated in a manner statistically consistent with the rest of the study.

The methodology used to generate site soil response must also be questioned. The authors feel that the use of theoretical amplification factors based on shear wave velocity eliminate some of the uncertainties associated with empirical studies. Although this method is undoubtedly easier to incorporate into a computer generated risk map, it is doubtful that it does more than exchange one set of uncertainties for another. This is particularly true when applied on such a large scale with so little site-specific information.

There are also two of the same problems found in the previously discussed studies. The scale of the investigation

would necessitate a separate map for areas outside the original study area, and there is not an accurate method available for expressing the results in terms of a velocity-related coefficient.

However, it should be stressed that the study does have definite applications for planning. The comparison of acceleration values for different sites should provide a good indication of which site is more seismically stable. However, the absolute value of acceleration is too speculative for bridge design.

This leaves what is essentially an improvement of the 1976 Algermissen Perkins map [3] as a candidate for replacement of the AASHTO map. The study appears in two forms, the original 1980 study of Northwest seismicity [56], and the 1982 national maps [5]. The study provides a number of advantages over the previously discussed possibilities. First, the AASHTO map relied heavily on the original 1976 Algermissen and Perkins study [3]. Thus, if the 1982 study is an improvement over the original 1976 effort, it might be assumed it also is an improvement over the AASHTO map. Additionally, maps are presented that express velocity in the same probabilistic terms as acceleration, making it possible to develop a velocity-related acceleration coefficient. Since the velocity values used in the AASHTO guidelines were based on the construction of smoothed response spectra and simplified velocity attenuation relationships, the Algermissen-Perkins velocity maps should provide greater accuracy.

Another possible advantage is that Algermissen-Perkins published maps of ground motion for different exposure periods. Thus, if it were desired to design noncritical bridges for a shorter return period it would be relatively simple. The AASHTO guidelines allow consideration of the importance of a structure through their seismic performance categories (SPC). However, a variation in design procedure based on importance of the structure is only made for acceleration coefficient values exceeding 0.29g. An alternative approach could be taken. In cases where a structure is not considered essential and a certain risk of failure is acceptable, a lower design ground motion based on a shorter return period may be a preferable approach.

Considering the increase in seismic source zones from six to nineteen, the incorporation of additional geologic information, and improvements in statistical analysis, the work by Perkins and others [56] should be considered as an improvement over the 1976 national map [5], for the northwest. The primary question is how feasible it would be to modify the map(s) to conform to the AASHTO input motion guidelines.

Two primary differences exist between the Perkins and AASHTO maps. First, the Perkins maps are expressed in terms of ground motions on rock while the AASHTO values are on "firm ground", firm ground being a combination of rock and stiff soil. The second difference is the form of the ground motion parameter. The AASHTO guidelines utilize the velocity-related acceleration coefficient previously defined. The Perkins study expresses ground motion in terms of acceleration and velocity.

The feasibility of developing a velocity-related acceleration coefficient based on the work of Perkins and others will be examined first. Recall that the purpose of the velocity-related acceleration coefficient was to 1) account for the slower attenuation of velocity than acceleration with distance from the source; and 2) consider the influence of velocity on the damage of long period buildings located at a distance from the source. Recall further that the AASHTO peak velocity values were developed based on the smoothed response spectra construction procedures rather than actual measured or recorded velocity values. Additionally, velocity was attenuated using a simple relationship developed by McGuire [39] stating that EPV decreased by a factor of 2 at 80 miles from the source. This relationship was then extended to greater distance, halving EPV values every 80 miles.

With the AASHTO objectives and methodology in mind, it seems reasonable that a map of A_v could be developed based on the work of Perkins and others, and such a map would provide greater accuracy than the existing AASHTO version. Ideally, the map would be generated by attenuating acceleration, using velocity attenuation curves, as a part of the original zonation mapping process. However, the time and expense required to accomplish such a task is beyond the scope of the present investigation.

An alternate method of developing A_v based on the existing acceleration and velocity maps developed by Perkins and others is proposed. The method is simple, but requires a large amount of judgment on the part of the individual performing the work.

The A_v contours can be constructed based on the velocity contours as follows. The ratio of a/v at a source is determined, and then multiplied by the velocity contour value located at some distance from the source, generating an acceleration coefficient attenuated at the same rate as velocity, i.e., a velocity-related acceleration coefficient.

This would be a simple endeavor provided only one seismic source zone was being considered. However, with multiple source zones the modification procedure is not straight forward. Not only are both acceleration and velocity attenuation dependent on magnitude, but the v/a ratio also varies with magnitude. Thus, the a/v ratio used to transform the velocity contours to A_v contours will vary with the statistical parameters of the seismic source zone influencing the contour at a particular location. If a velocity contour is influenced by more than one seismic source zone and the influencing zones have different statistical parameters, the v/a ratio applied to the contour will vary. In most cases this will require a shift in the contour location.

Prior to modifying the existing map it is necessary to examine the spacial variations of certain parameters. By doing so it is possible to determine which seismic source zone is controlling the location of the velocity contour for a particular area. As discussed previously the v/a ratio is one of the most useful parameters commonly available and will be used for analysis herein.

First, the variation of v/a with magnitude and distance should be examined to obtain an understanding of how the ratio

will vary between source zones with different statistical characteristics. Table 4 lists a , v and v/a at various distances from the source for magnitudes of 5.6, 6.6, and 7.6. These values were obtained directly from the velocity and attenuation curves used in the two related studies [5,56].

Examination of the table reveals that at a given distance from the source, v/a increases from low magnitude to high magnitude. For a given magnitude, v/a increases with distance from the source. Both of these trends are consistent with other studies [32]. It should be noted that the v/a ratio became unstable at distances less than 6 mi and peak accelerations less than 0.01 g. However, this was not considered a problem within the context of the present analysis.

Once a general understanding of how v/a varies with magnitude and distance had been developed, the variation through specific cross sections within the state should be examined. As will be seen this provides a reasonable estimate of the area of influence of each source zone encountered along the cross section. Two cross sections were chosen for examination. The first (section A-A') runs east-west through the center of the Puget Sound region. The second (section B-B') trends north-south approximately along the centerline of the Puget/Willamette trough. It was felt that the combination of these two sections would transect the majority of important source zones in the state, providing the information required to develop a statewide map of Av .

Table 4
 VARIATION OF a, v, AND v/a AT DISTANCE FROM THE SOURCE
 Magnitude

| Distance (mi) | Acceleration (a/v) | | | Velocity (cm/s) | | | v/a (cm·g/s·a) | | |
|------------------|--------------------|-------|-------|-----------------|-----|-----|----------------|-----|-----|
| | 5.6 | 6.6 | 7.6 | 5.6 | 6.6 | 7.6 | 5.6 | 6.6 | 7.6 |
| 6.2 | 0.27 | 0.42 | 0.50 | 12 | 32 | 50 | 44 | 76 | 100 |
| 12.4 | 0.15 | 0.27 | 0.37 | 6.9 | 21 | 41 | 46 | 78 | 110 |
| 31.1 | 0.050 | 0.10 | 0.19 | 2.7 | 8.7 | 22 | 56 | 87 | 120 |
| 62 | 0.013 | 0.073 | 0.027 | 1.1 | 3.8 | 11 | 85 | 141 | 150 |
| 124 | - | - | 0.016 | -- | -- | 2.9 | -- | -- | 180 |

The location of cross sections A and B is shown in Figure 44. The data for A-A' was obtained from the Algermissen and others study [5] because it displays contours to the eastern border of Washington. The Perkins and others [56] maps were used for B-B' due to the greater detail.

Figures 45 and 46 plot a , v and v/a along cross sections A and B respectively. The maps exhibiting 90% probability of nonexceedence in 50 years were used since this is the same statistical risk allowed in the AASHTO map. As Figure 45 illustrates, both a and v peak in the Puget trough and decay to the east and west, indicating the Puget Sound region is the dominant source zone along the cross-section. The v/a ratio demonstrates the same general trend but provides more insight into the influence of lesser source zones. The most obvious characteristic is the minimum located in the Puget Sound region, indicating a major source zone. The slight change in slope between 140 and 200 miles reflects the influence of the Lake Chelan source zone. At approximately 300 miles v/a starts decreasing due to the influence of a source zone in northeastern Montana.

The plots of a , v , and v/a for cross section B-B' are presented in Figure 46. Similar to A-A', source zones are characterized by peaks of a and v coinciding with low v/a ratios. In this case two distinct source zones are present. The major influence is again from the Puget Sound region. A lower amplitude source is located within the Willamette depression, centered near Vancouver, WA. Approximately 106 mi south of B a

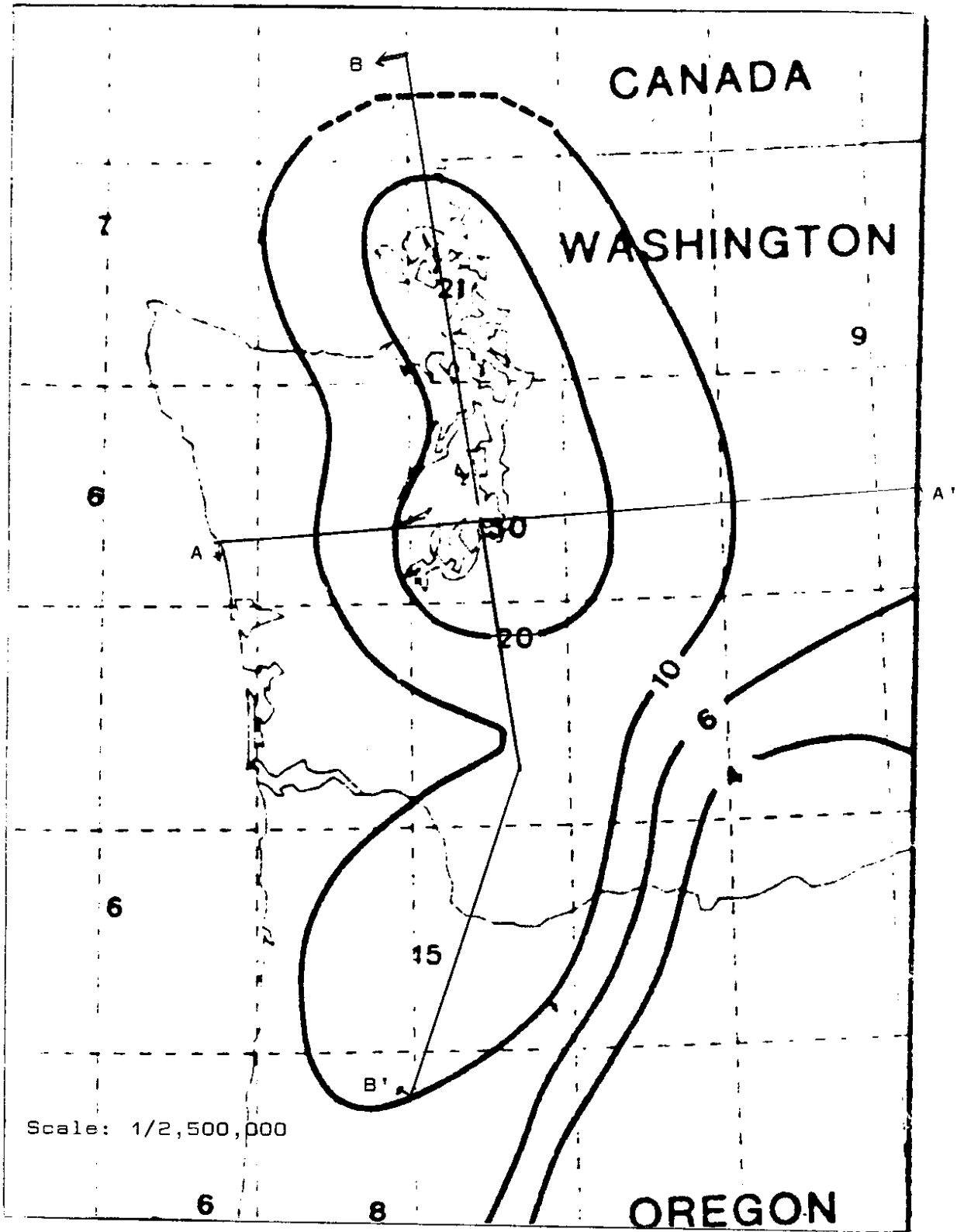


Figure 44. Locations of cross sections A and B.

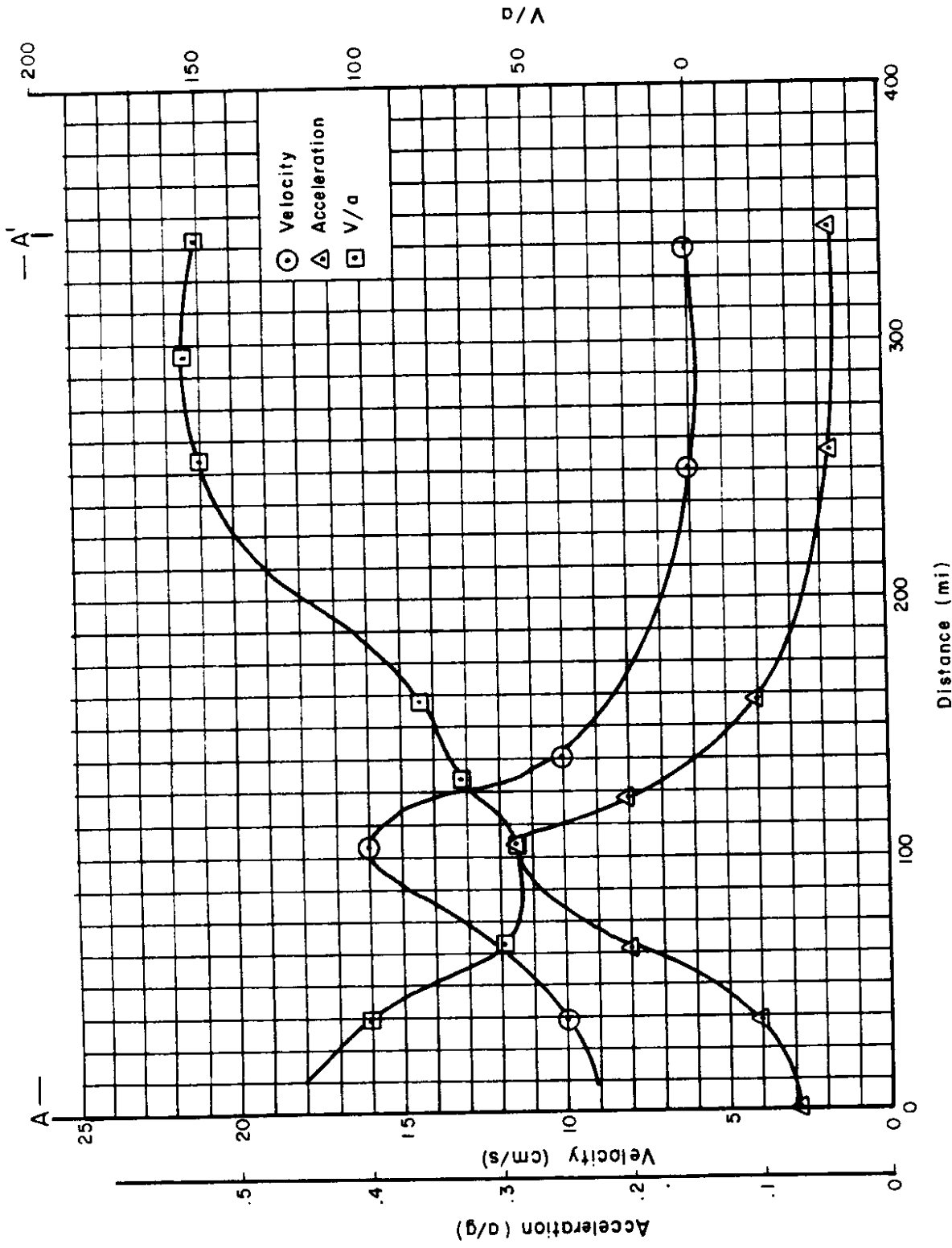


Figure 45. Variation of a, v, and v/a for cross section A-A' (475-year return period).

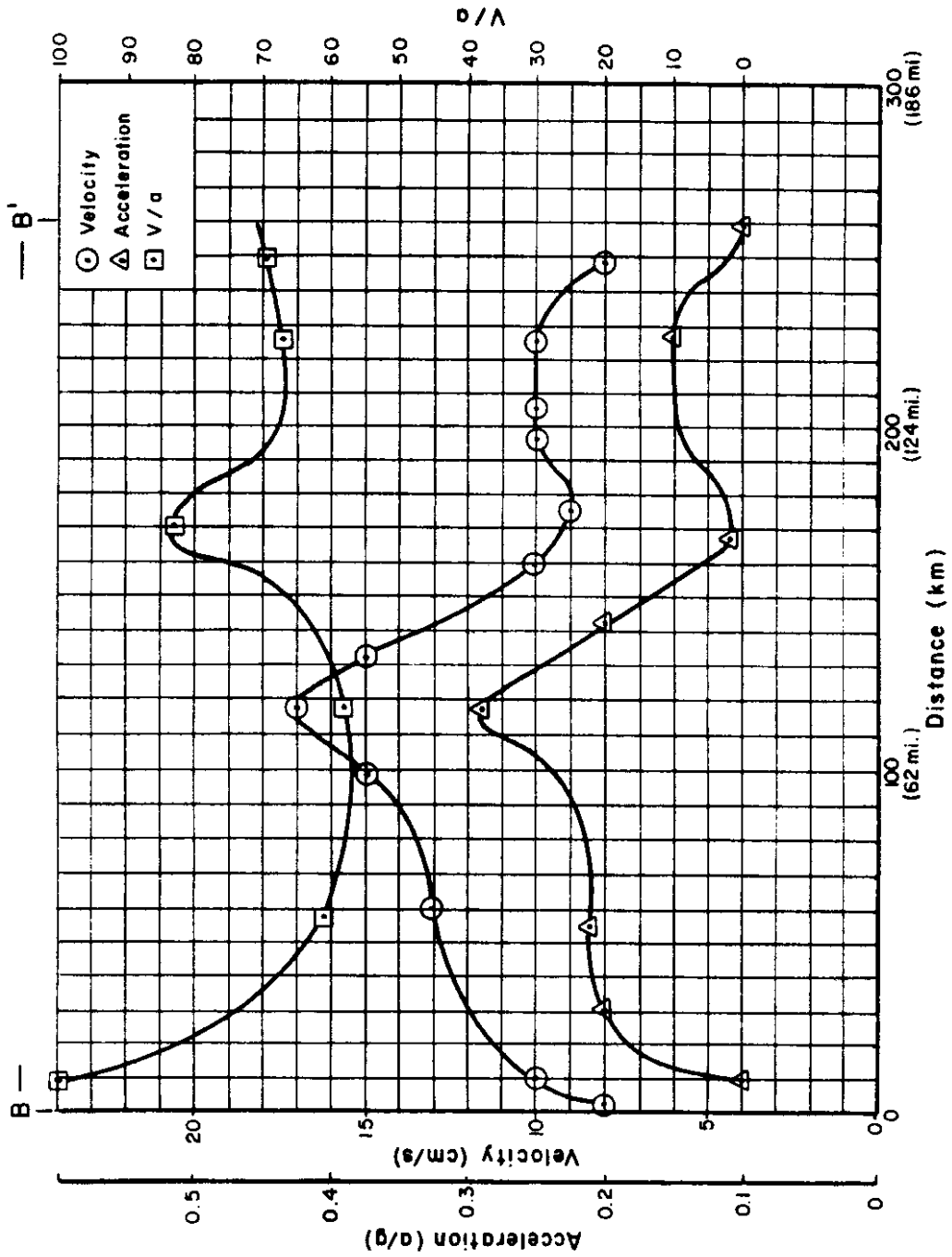


Figure 46. Variation of a, v, and v/a for cross section B-B' (475-year return period).

minimum of a and v and a maximum of v/a are present. This juncture indicates a change in source zone controlling ground motions, from the Puget Sound zone in the north to the Willamette zone in the south.

The preceding plots of v/a are extremely helpful in determining the influence of different source zones on the isoseismal contours. However, emphasis should not be placed on the absolute values. With the exception of locations where both v and a values are displayed, v/a ratios are the result of interpolation and thus subject to error.

Fortunately, v and a tend to coincide spatially at the center of most source zones where the ratio is of the greatest importance for the development of an Av map.

Development of a Velocity-Related Acceleration Map Based on Acceleration and Velocity Maps

The basic methodology for generating a map of Av based on the work of Perkins and others [56] and Algermissen and others [5] has been outlined in the previous section. However, some of the assumptions and construction specifics should be detailed. The Av values are calculated along the velocity contours by taking the a/v ratio from the center of the seismic source zone(s) and multiplying it by the velocity contour value, i.e.,

$$\frac{a}{v} \cdot V = Av.$$

This produces an acceleration value attenuated at approximately the rate of velocity attenuation.

In cases where a velocity contour is the result of more than one source zone the source v/a ratio is applied to the portion of the contour considered to be influenced by that particular source zone. Since v/a ratios will generally be different for different sources, a discontinuous contour results. The discontinuity is eliminated by interpolation and smoothing with the higher value placed closer to the source. A high degree of judgment is required on the part of the investigator.

Contours generated in such a manner will not exhibit typical contour values such as 0.05, 0.15, 0.20g. For ease of use, contours have been shifted slightly so that typical contour values may be obtained. Adjustment was performed by a combination of judgment and interpolation using the velocity attenuation curves developed by Perkins and others [56]. As in the development of the AASHTO map, Av contours were never placed nearer to the source than the acceleration contour of equal value. The proposed contour map of Av for Washington State is presented in Figure 47.

When considering the impact of changing the definition of the acceleration coefficient from acceleration on firm ground and rock to acceleration on rock, two factors must be considered: 1) the change in ground acceleration, and 2) the change in spectral acceleration. As previously noted acceleration is the ground motion parameter least affected by site conditions. For peak accelerations above about 0.15 g peak accelerations tend to be slightly greater in rock than stiff soil sites. Conversely, at accelerations below 0.1 g peak accelerations on rock sites are

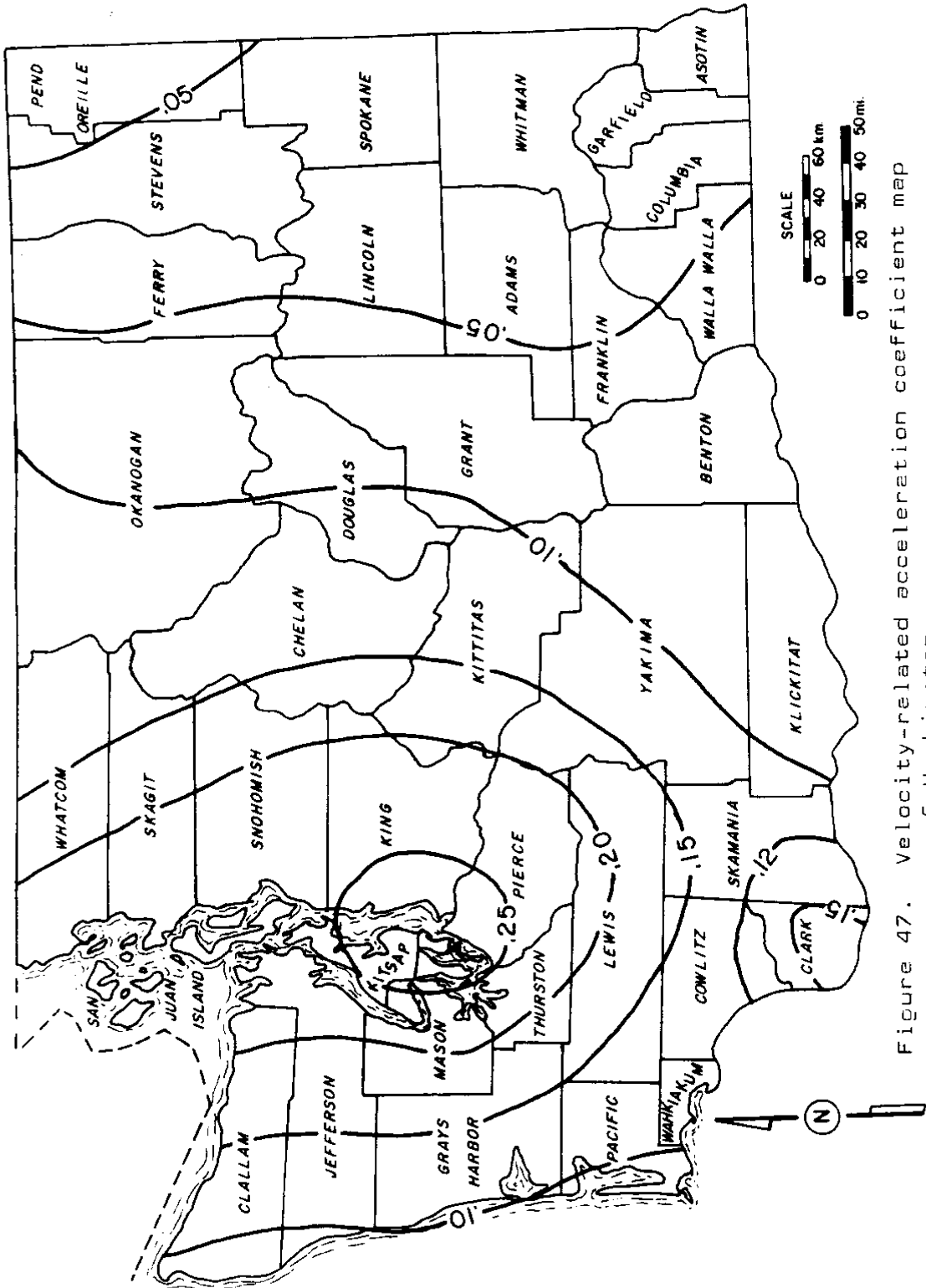


Figure 47. Velocity-related acceleration coefficient map of Washington.

typically lower than on stiff soil sites. The maximum difference in peak acceleration between the two site conditions is only about 10% in the range of accelerations important for engineering purposes. Figure 13 shows the difference in attenuation between rock and stiff soil sites.

The difference in spectral response between rock and stiff soil was illustrated in Figure 14. As the figure demonstrates, stiff soils exhibit greater spectral amplification than rock sites. This does not necessarily mean spectral accelerations are going to be higher on stiff soil sites. Since accelerations tend to be higher on rock for values greater than 0.15 g, spectral acceleration may be higher on rock for fairly strong ground motions, even if spectral amplification is greater on firm ground.

A comparison of the AASHTO design coefficient, C_s for soil type I to the acceleration spectra for rock and stiff soil in the original ATC-3 publication shows that C_s for soil type I approximates the average acceleration spectra for stiff soil sites. Thus, C_s for type I soil is applicable to stiff soil conditions and probably slightly over conservative for rock sites. Acceleration on stiff soil usually exceeds that on rock when acceleration is less than 0.15 g. However, since amplification is only about 10% at most, and the greatest amplification occurs at lower levels of acceleration, it is questionable whether such a small increase in ground motion requires consideration.

Three options are available to address this problem: 1) consider the difference between accelerations on rock and "firm ground" insignificant and use the same soil modification factors (I, II, III); 2) empirically modify the map to account for the difference; and 3) create a new soil modification factor, for firm ground conditions. The first option, ignoring the difference, is considered reasonable since the spectral response curve for type I conditions more closely resembles the stiff soil spectra than the rock spectra.

Evaluation of Model Soil Profiles

The AASHTO approach for consideration of soil effects on ground motion uses representative ground motion spectral shapes modified in ATC-3 to determine corresponding values of effective peak ground acceleration and smoothed spectral shapes for three typical site conditions. These modifications were based on a study of ground motions recorded at locations with different site conditions and the exercise of experienced judgment in extrapolating beyond the data base. Coefficients were developed for each of three typical conditions (soil types I, II, III) [6,9].

An alternative approach to evaluating soil effects on ground motion is using the computer program SHAKE to develop soil amplification factors for the design criteria. The program analyzes a one-dimensional soil column for shear wave motions propagating from the rock level to the top of the soil column. This approach has some limitations because only vertically

propagating one-dimensional soil effects are considered while surface waves, oblique transmission of waves through the soil, and reflection and refraction phenomena are not considered.

However, it was proposed in this study to develop model soil profiles representing typical Washington bridge sites and to analyze their response using SHAKE. The objective was to use two earthquakes (1949 and 1965 Washington earthquakes) and to compare the spectral response of the model soil profiles with the response spectra used for the AASHTO soil types. Although two earthquakes are insufficient to develop response spectra for use in design, they do provide sufficient data to determine if the AASHTO approach to evaluating soil effects on ground motion is appropriate for Washington soils.

Model soil profiles used for this study are shown in Figure 48 and were provided by the WSDOT geotechnical staff. Each profile shows a variation of thickness and properties. In order to evaluate maximum and minimum response, each profile was divided into two profiles (soft properties and thick, stiff properties and thin) and each was analyzed for both earthquakes for some variety of frequency characteristics. Table 5 is a comparison of the normalized response spectra for the model soil profiles and the equivalent AASHTO type soils. The table illustrates the fact that the highest normalized response for the model soil profiles falls within the range of response spectra of the AASHTO type soils. This suggests that the AASHTO approach is a conservative design guide for Washington soils.

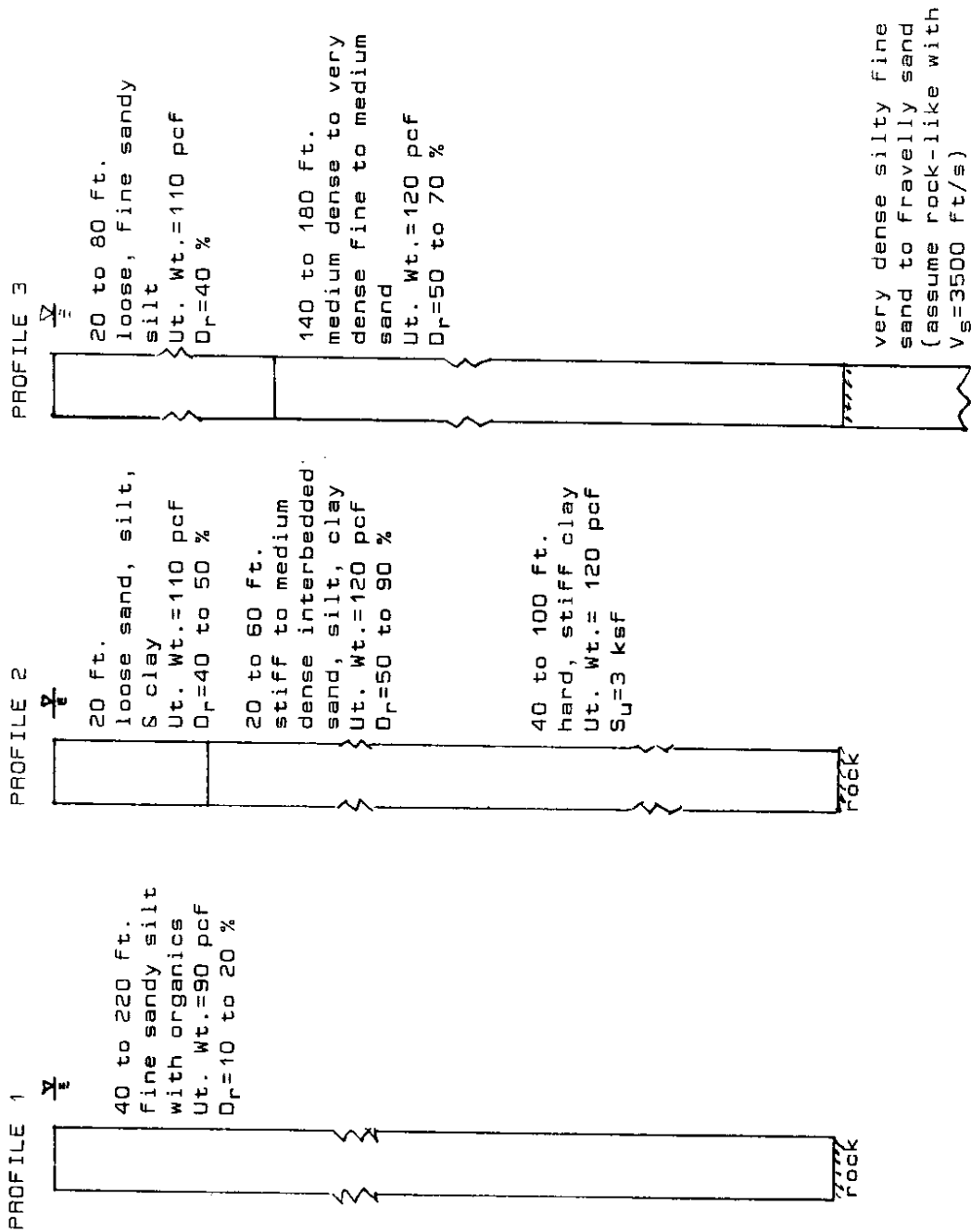


Figure 48. Model soil profiles for Washington.

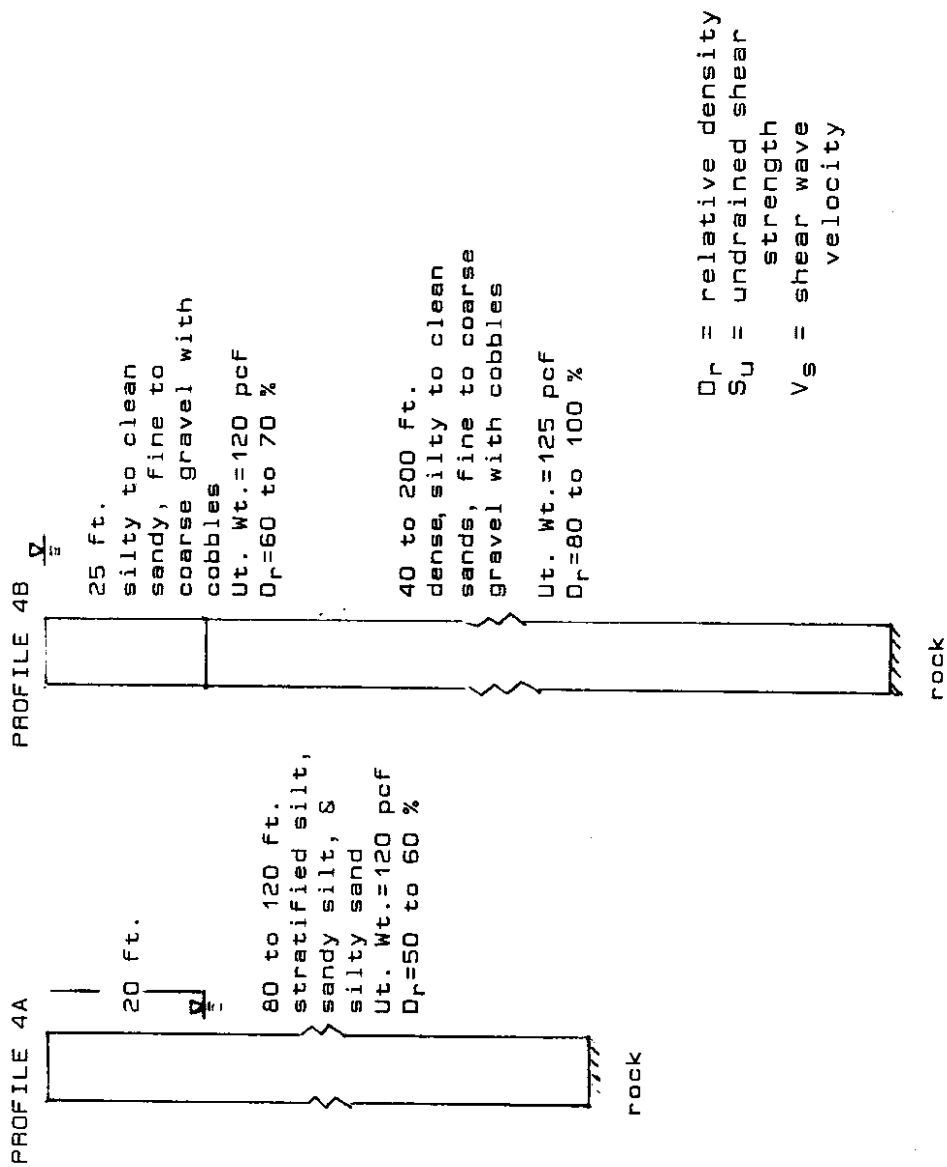


Figure 48. (Continued)

Table 5

COMPARISON OF NORMALIZED RESPONSE SPECTRA FOR MODEL SOIL PROFILES AND AASHTO SOIL PROFILE TYPES I, II, III. COMPARISON IS DONE FOR SPECTRAL RESPONSE BETWEEN PERIODS OF 1 AND 2 SECONDS. NORMALIZED RESPONSE SPECTRA = SPECTRAL ACCELERATION/MAX GROUND ACCELERATION.

| Profile | Soil Properties | SHAKE | AASHTO |
|---------|-----------------|---------|---------|
| 1* | soft & thick | no data | 1.2-2.3 |
| 1* | stiff & thin | no data | 1.2-2.3 |
| 2 | soft & thick | 0.5-1.9 | 1.2-2.3 |
| 2 | stiff & thin | 0.7-1.3 | 0.8-1.5 |
| 3 | soft & thick | 1-1.8 | 1.2-2.3 |
| 3 | stiff & thin | 0.5-2.0 | 1.2-2.3 |
| 4A | soft & thick | 0.3-0.9 | 0.5-1.1 |
| 4A | stiff & thin | 0.3-0.8 | 0.5-1.1 |
| 4B | soft & thick | 0.6-1.4 | 0.8-1.5 |

*No dynamic data available for high organic silts.

It appears that there may be two approaches to improving the AASHTO design method for site coefficient selection. One approach is an extensive SHAKE analysis and the second approach is development of synthetic response spectra. The SHAKE approach would require analysis of model soil profiles with several appropriately chosen earthquakes (site conditions, accelerations, frequency characteristics, etc.). The results could be used to develop averaged response spectra and soil amplification factors for all model profiles. Hence, the bridge designer could choose an amplification factor for the period of the structure.

The second approach is being studied by TRAC investigators at Washington State University. The end product should be similar to the first approach; however, their method may not be subject to the limitations of SHAKE mentioned above.

REFERENCES

1. Algermissen, S.T., 1969, Seismic Risk Studies in the United States, 4th World Conf. of Earthquake Engr., Santiago, Chile, p. 1-27.
2. Algermissen, S.T., and Harding, S.T., 1965, Preliminary Seismological Report, in, The Puget Sound Washington Earthquake of April 29, 1965, U.S. Dept. Commerce/U.S. Coast and Geodetic Survey, pp. 1-26.
3. Algermissen, S.T., and Perkins, D.M., 1976, A Probabilistic Estimate of Maximum Acceleration in Rock in the Contiguous United States, U.S.G.S., O.F.R. 76-416, 45p.
4. Algermissen, S.T., and Perkins, D.M., 1976, Seismic Risk Evaluation at the Balkan Region, UNESCO, p. 18-19.
5. Algermissen, S.T., Perkins, D.M., Thenhaus, P.C., Hanson, S.L. and Bender, B.L., 1982, Probabilistic Estimates of Maximum Acceleration and Velocity in Rock in the Contiguous United States, U.S.G.S., O.F.R. 82-1033, 99p, 3 plates.
6. AASHTO, 1983, Guide Specifications for Seismic Design of Highway Bridges, ATC-6, 105p.
7. Ando, M. and Balazs, E.I., 1979, Geodetic Evidence for a Seismic Subduction of the Juan de Fuca Plate, J. Geophys. Res., V84, p. 3023-3028.
8. Apsel, R.S., Hadley, D.M., and Hart, R.S., 1983, Effects of Earthquake Rupture Shallowness and Local

- Soil Conditions on Simulated Ground Motions,
U.S.N.R.C., ICR-3102/UCRL-15495.
9. ATC, 1978, Tentative Provisions for the Development of Seismic Regulations for Buildings, ATC-3-06, Nat. Bus. of Stds., Spec. Publ. 510.
 10. Atwater, T., 1970, Implications of Plate Tectonics for the Cenozoic Tectonic Evolution of Western North America, GSA Bull, V. 81, pt. 4, p. 3513-3535.
 11. Blume, J.A. and Associates, 1973, Recommendations for Shape of Earthquake Response Spectra, Prepared for Directorate of Licensing, U.S. Atomic Energy Commission, Contract No. AT(49-5)-3011.
 12. Boore, D.M. and Joyner, W.B., 1982, The Empirical Prediction of Ground Motion, Bull. Seis. Soc. of Amer. V 72, No. 6, pp. 543-560.
 13. Boore, D.M., Joyner, W.B., Oliver, A.A. III, and Page, R.A., 1980, Peak Acceleration, Velocity, and Displacement from Strong-Motion Records, Bull. Seis. Soc. of Amer., V 70, No. 1, pp. 305-321.
 14. Bor, Sheng-Sheang, 1977, Scaling for Seismic Source Spectra and Energy Attenuation in the Chelan Area, Eastern Washington, M.S. Thesis, Unpublished, University of Washington, Seattle, 76p.
 15. Brazee, R.J., 1976, An Analysis of Earthquake Intensities with Respect to Attenuation, Magnitude, and Rate of Recurrence (Revised Ed.), NOAA Environmental

- Data Service, NOAA Technical Memorandum EDS NGSDC-2, Aug, 103p.
16. Campbell, K.W., 1981, Near-Source Attenuation of Peak Horizontal Acceleration, Bull. Seis. Soc. of Amer., V 71, No. 6, pp. 2039-2070.
 17. Converse Consultants, 1980, Report on Earthquake Motions for Reservoir Seismic Stability Analyses, Seattle, WA, Conducted for City of Seattle Engineering Dept., 19p.
 18. Coombs, H.A., Milne, W.G., Nuttli, O.W., and Slemmons, D.B., Report of the Review Panel on the December 14, 1872 Earthquake, Preliminary Safety Analysis Report, WPPSS #1, V 12A, Appendix 2RA.
 19. Crosson, R.S., 1972, Small Earthquakes, Structure, and Tectonics of the Puget Sound Region, Seis. Soc. of Am. Bull., V 62, No. 5, pp. 1133-1171.
 20. Crosson, R.S., 1983, Review of Seismicity in the Puget Sound Region from 1970 through 1978, Proceedings Workshop XIV, Earthquake Hazards of the Puget Sound Region, WA, U.S.G.S., O.F.R. 83-19, p. 6-18.
 21. Crosson, R.S., 1986, Review of Seismicity and Tectonics in Western Washington, Symposium on the Mexico City Earthquake, Struc. Engrs. Assoc. of Wash., Jan 25.
 22. Danes, Z.F., Bonno, M.M., Brau, E., Gilham, W.D., Hoffman, T.F., Johansen, D., Jones, M.H., Malfait, B., Masten, J., and Teague, G.O., 1965, Geophysical Investigation of the Southern Puget Sound Area,

- Washington, Jour. Geophys. Research, V 70, No. 22, pp. 5573-5580.
23. Donovan, N.C., 1973, A Statistical Evaluation of Strong Motion Data Including the February 9, 1971 San Fernando Earthquake, Proc. 5th World Conf. of Earthquake Engr., Rome, V.I., pp. 1252-1261.
 24. Donovan, N.C., 1982, Strong Motion Attenuation Equations--A Critique, Third International Earthquake Microzonation Conference Proc., V I, pp. 377-388.
 25. Easterbrook, D.J., 1969, Pleistocene Chronology of the Puget Lowland and San Juan Islands, Washington, Geol. Soc. of Amer. Bull., V 80, p. 2273-2286.
 26. Hall, J.B. and Othberg, K.L., 1974, Thickness of Unconsolidated Sediments, Puget Lowland, Washington, Washington D.N.R., Div. of Geol and Earth Resources, GM-12.
 27. Hawkins, N.M. and Crosson, R.S., 1975, Causes, Characteristics and Effects of Puget Sound Earthquakes, University of Washington, July.
 28. Hayashi, S., Tsuchida, H. and Kurata, E., 1970, Acceleration Response Spectra on Various Site Conditions, Proceedings, 3rd Japan Earthquake Symposium, Tokyo.
 29. Hays, W.W., and Algermissen, S.T., 1982, Problems in the Construction of a Map to Zone, the Earthquake Ground-shaking Hazard, 3rd International Earthquake

- Microzonation Conference Proceedings, Vol. 1, pp. 145-156.
30. Heaton, T.H. and Kanamori, H., 1983, Seismic Potential Associated with Subduction in the Northwestern United States, *Seis. Soc. Bull.*, V. 3, p. 933-941.
 31. Housner, G.W., 1970, Strong Ground Motion, in Wiegel, R.L., *Earthquake Engineering*, Prentice-Hall, pp. 75-91.
 32. Idriss, I.M., 1978, Characteristics of Earthquake Groundmotions, State-of-the-Art Report, Proceedings ASCE Geotech. Engr. Div. Specialty Conference, Pasadena, CA, June 19-21, V 3, pp. 1151-1265.
 33. Ihnen, S. and Hadley, D.M., 1984, Prediction of Strong Motion in the Puget Sound Region: The 1965 Seattle Earthquake, Sierra Geophysics, Annual Technical Report to U.S.G.S., 38p.
 34. Ihnen, S.M. and Hadley, D.M., 1986, Seismic Risk Maps for Puget Sound, Washington, Sierra Geophysics, Inc., Rpt. #SGI-R-86-127, for U.S.G.S., Contract #14-08-0001-21306.
 35. Joyner, W.B. and Boore, D.M., 1981, Peak Horizontal Acceleration and Velocity from Strong-Motion Records Including Records from the 1979 Imperial Valley, California, *Earthquake, Bull. Seis. Soc. of America*, V 71, No. 6, pp. 2011-2038.
 36. Krinitzsky, E.L. and Marcuson, W.F. III, 1983, Principals for Selecting Earthquake Motions in

- Engineering Design, Bull. Assoc. Engr. Geol., VXX, No. 3, pp. 253-265.
37. Langston, C.A., 1981, Calculation of Strong Ground Motion and Local Field-Far Field Relationships for the April 25, 1965, Puget Sound, Washington, Earthquake, U.S.G.S., O.F.R. 81-377.
 38. Langston, C.A. 1983, A Study of Puget Sound Strong Ground Motion, Proceedings of Working XIV: Earthquake Hazards of the Puget Sound Region, Washington, U.S.G.S., O.F.R. 83-19, p. 59-104.
 39. McGuire, R.K., 1975, Seismic Structural Response Risk Analysis, Incorporating Peak Response Progressions on Earthquake Magnitude and Distance, Report R74-51, Dept. Civil Engr., M.I.T., Cambridge, Mass.
 40. McGuire, R.K., 1978, Seismic Ground Motion Parameter Relations, Jour. Geotech. Div. ASCE, V104, No. GT4, April, pp. 481-490.
 41. Michaelson, C.A., 1983, Three-Dimensional Velocity Structure of the Crust and Upper Mantle in Washington and Northern Oregon, M.S. Thesis, University of Washington, 100p.
 42. Milne, W.G., 1956, Seismic Activity in Canada, West of the 113 Meridian, 1841-1951, Publication of the Dominion Observatory, Ottawa, Vol. XVIII, No. 7, Ottawa, California, 1956.

43. Mohraz, B., 1976, A Study of Earthquake Response Spectra for Different Geological Conditions, Bull. Seis. Soc. of America, V 66, No. 3, pp. 915-935.
44. Mullineaux, D.R., Bonilla, M.G., and Schlocker, J., 1967, Relation of Building Damage to Geology in Seattle, Washington During the April, 1965 Earthquake, U.S.G.S. Professional Paper 575-D, pp. D183-D191.
45. Murphy, L.M. and Ulrich, 1951, United States Earthquakes 1949. U.S. Dept. of Commerce, Coast and Geodetic Survey, Serial No. 748, 28p.
46. NOAA, 1982, Development and Initial Application of Software for Seismic Exposure Evaluation, Vol. 1, Software Description.
47. Newmark, N.M., 1968, Problems in Wave Propagation in Soil and Rock, Proc. Symposium on Wave Propagation and Dynamic Properties of Earth Materials, Univ. of New Mexico, Albuquerque, pp. 7-26.
48. Newmark, N.M., 1973, A Study of Vertical and Horizontal Earthquake Spectra, for the Directorate of Licensing, U.S. Atomic Energy Commission, Contract No. AT(49-5)-2667.
49. Newmark, N.M. and Hall, W.J., 1969, Seismic Design Criteria for Nuclear Reactor Facilities, Proc. 4th World Conf. on Earthquake Engr., Santiago, Chile, p. 37-50.
50. Newmark, N.M. and Hall, W.J., 1982, Earthquake Spectra and Design, Earthquake Engr. Research Inst., 103p.

51. Nuttli, O.W., 1979, The Relation of Sustained Maximum Ground Acceleration and Velocity to Earthquake Intensity and Magnitude, State-of-the-Art for Assessing Earthquake Hazards in the United States, U.S. Army Engineer Waterways Experiment Station, Misc. paper 5-73-1, Report 16, 74p.
52. Nuttli, O.W., 1981, Similarities and Differences Between Western and Eastern United States Earthquakes, and their Consequences for Earthquake Engineering, Earthquakes and Earthquake Engineering--Eastern United States, ed. J.E. Beavers, Ann Arbor Science, V. 1, pp. 25-51.
53. Orphal, D.L. and Lahoud, J.A., 1974, Prediction of Peak Ground Motion from Earthquakes, Bull. Seis. Soc. of Amer., V 64, No. 5, pp. 1563-1574.
54. Page, R.A., Boore, D.M., Joyner, W.B., and Coulter, W.H., 1972, Ground Motion Values for Use in the Seismic Design of the Trans-Alaska Pipeline System, U.S.G.S. Circular 672.
55. Perkins, D.M., 1980, Outer Continental Shelf Seismic Risk, in, Summaries of Technical Reports, V. IX: U.S.G.S. Open-File Report 80-6, p. 166-168.
56. Perkins, D.M., Thenhaus, P.C., Hanson, S.L., Ziong, J.I., and Algermissen, S.T., 1980, Probabilistic Estimates of Maximum Seismic Horizontal Ground Motion on Rock in the Pacific Northwest and the Adjacent Outer Continental Shelf, OFR 80-471, USGS, 39p, 7 plates.

57. Rasmussen, N., 1967, Washington State Earthquakes 1840 through 1965, Bull. Seis. Soc. of America, V 57, No. 3, pp. 463-476.
58. Rasmussen, N.H., Millard, R.C., and Smith, S.W., 1975, Earthquake Hazard Evaluation of the Puget Sound Region, Washington State, Contract CPA-WA-10-19-1015, Office of Emergency Preparedness, U.S.G.S., 99p.
59. Rohay, A.C., 1982, Crust and Mantle Structure of the North Cascades Range, Washington, Ph.D. Dissertation, University of Washington, 1982, 163p.
60. Savage, J.C., Lisowski, M., and Prescott, W.H., 1981, Geodetic Strain Measurements in Washington, J. Geophys. Res. V86, p. 4929-4940.
61. Schabel, P.B. and Seed, H.B., 1973, Accelerations in Rock for Earthquakes in the Western United States, Bull. Seis. Soc. Amer., V63, No. 2, pp. 501-516.
62. Seed, H.B., 1986, Presentation on the Geotechnical Aspects of Building Damage Resulting from the 1985 Mexico City Earthquake, Symposium on the Mexico City Earthquake, Jan 25, 1986, No proceedings.
63. Seed, H.B. and Idriss, A.M., 1969, Influence of Soil Conditions on Ground Motions During Earthquakes, ASCE Soil Mech. and Fnd. Engr. Div., V. 95, No. SM1, pp. 99-137.
64. Seed, H.B., Ugas, C. and Lysmer, J., 1976, Site-Dependent Spectra for Earthquake-Resistant Design, Bull. Seis. Soc. Amer., V 66, No. 1, pp. 221-243.

65. Shannon & Wilson, 1980, Geotechnical Engineering Studies, West Seattle Freeway Bridge Replacement, City of Seattle, Vol 1: Engineering Studies and Recommendations, 47p (+ appendix).
66. Steinbrugge, K.V. and Cloud, W.K., 1965, Preliminary Engineering Report, in, The Puget Sound, Washington Earthquake of April 29, 1965, U.S. Dept. Commerce/Coast and Geodetic Survey, pp. 27-51.
67. Taber, J.J., Jr., 1983, Crustal Structure and Seismicity of the Washington Continental Margin, Ph.D. dissertation, University of Washington,
68. Taber, J.J. and Smith, S.W., 1985, Seismicity and Focal Mechanism Associated with the Subduction of the Juan De Fuca Plate Beneath the Olympic Peninsula, WA, Bull. Seis. Soc. Am., V 75, No. 1, pp. 237-249.
69. Trifunac, M.D., 1976, Preliminary Analysis of the Peaks of Strong Earthquake Ground Motion--Dependence of Peaks on Earthquake Magnitude, Epicentral Distance and Recording Site Conditions, Bull. of the Seis. Soc. of Amer., V 66, No. 1, pp. 189-219.
70. Trifunac, M.D. and Brady, A.G., 1975, On the Correlations of Seismic Intensity Scales with the Peaks of Recorded Strong Ground Motion, Bull. Seis. Soc. of Amer., V 65, No. 1, pp. 139-162.
71. Ulrich, F.P., 1948, Zones of Earthquake Probability in the United States, Building Standards Monthly, V 17, No. 3, p. 11-12.

72. U.S. Army Corps of Engineers, 1981, Lower Snake River Dams, McNary and Mill Creek-Geological and Seismological Review, Walla Walla District, C.O.E.
73. U.S. Army Corps of Engineers, 1981, Earthquake Analysis of Chief Joseph Dam, Columbia River, Washington, Supplement 4 to design memo, 42, U.S. Army Corps of Engineers, 81p.
74. U.S. Army Corps of Engineers, 1982, Earthquake Analysis of Chittenden Lock and Dam, Design Memorandum No. 8, Seattle District.
75. U.S. Army Corps of Engineers, 1983, Earthquake Analysis of Mud Mountain Dam, Design memo No. 25, Seattle District, 134p.
76. U.S.G.S, 1975, A Study of Earthquake Losses in the Puget Sound, Washington Area, Open-File Report 75-375, 297p.
77. U.S.G.S., 1979, Earthquake Information Gulletin, V 11, No.5, p. 176.
78. Weaver, C.S. and Smith, S.W., 1983, Regional Tectonic and Earthquake Hazard Implications of a Crustal Fault Zone in Southwestern Washington, Jour. Geophys. Res., V88, No. B12, pp. 10,371-10,383.
79. Weichert, D.H. & Hyndman, R.D., A Comparison of the Rate of Seismic Activity and Several Estimates of Deformation in the Puget Sound Area.
80. Wilson, J.R., 1983 Relationships between Late Quaternary Faults and Earthquakes in the Puget Sound

Washington Area, Proceedings of Workshop XIV:
Earthquake Hazards of the Puget Sound Region, WA,
U.S.G.S., O.F.R. 83-19, p. 165-177.

81. Woodward-Clyde Consultants, 1977, Review of the North Cascade Earthquake of 1872, Preliminary Safety Analysis Report, WPPSS No. 1, V2A, Appendix 2RB.
82. Yount, J.C., Dembroff, G.R. and Barats, G.M., 1985, Map Showing Depth to Bedrock in the Seattle 30 by 60 Quadrangle, Washington, U.S.G.S. Misc. Field Studies Map, MF-1692.

GLOSARY OF SELECTED TERMS

Acceleration coefficient-- A numerical value usually based on the effective peak acceleration or the effective peak velocity. See page 79 of text.

Attenuation curve-- A plot of distance vs acceleration response of the ground for a range of earthquake magnitudes. The curve is based on observation and is generally used to evaluate the severity of ground motion to be expected at some distance from the source of an earthquake.

Exposure period-- As used in this report, the amount of time an area is subject to possible earthquakes, i.e. 50 years, 100 years, etc..

Response spectrum-- A graphical representation of the maximum response of a single-degree-of-freedom damped elastic system to dynamic motion. It is typically presented as a plot of spectral acceleration, velocity, or displacement versus building period or frequency. This represents the maximum value of the parameter of interest (a, v, or d) that will be experienced by a single-degree-of-freedom structure for a given input motion. The period at which a particular motion value is indicated represents the natural period of the structure.

Subduction-- The descent of the downbent edge of a lithospheric plate into the asthenosphere (of the earth) so as to pass beneath the edge of the adjoining plate.